

V

# COLLECTOR FROTHER INTERACTION IN A FLOTATION SYSTEM

By  
VINOD KUMAR BANSAL

ME

1975 TH  
D ME/1975/D  
B227c

BAN

COL



DEPARTMENT OF METALLURGICAL ENGINEERING  
INDIAN INSTITUTE OF TECHNOLOGY KANPUR  
SEPTEMBER, 1975

# COLLECTOR FROTH INTERACTION IN A FLOTATION SYSTEM

A Thesis Submitted  
in partial Fulfilment of the Requirements  
for the Degree of  
DOCTOR OF PHILOSOPHY

By  
VINOD KUMAR BANSAL

to the

DEPARTMENT OF METALLURGICAL ENGINEERING  
INDIAN INSTITUTE OF TECHNOLOGY KANPUR  
SEPTEMBER, 1975



U.S. AIR FORCE  
CENTRAL LIBRARY  
Acc. No. 45527


31 JAN 1976

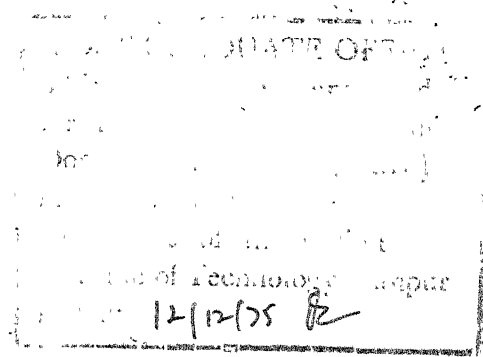
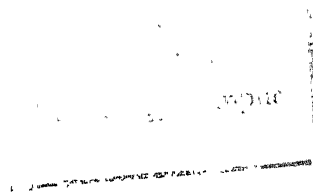
ME-1975-D--BAN-COL

## CERTIFICATE

Certified that this work on 'Collector-Frother Interaction in a Flotation System', has been carried out under our supervision and that it has not been submitted elsewhere for a degree.

(A.K. Biswas)  
Professor  
Dept. of Metallurgical Engg.  
Indian Institute of Tech.,  
Kanpur-208016

  
(D. Balasubramanian)  
Assistant Professor  
Department of Chemistry  
Indian Institute of Technology,  
Kanpur-208016





## ACKNOWLEDGEMENTS

The author expresses his deep gratitude and appreciation to Prof. A.K. Biswas and Prof. D. Balasubramanian under whose guidance this work reached its successful completion. Their lively interest, constructive criticism and sound guidance have been instrumental in shaping this dissertation in its present form. Their constant encouragement and amiable counsel were the sustaining factors throughout the course of these investigations.

Thanks are also due to Dr. T.W. McGee of the Dow Chemical Co., Michigan, USA for providing highly purified nonionic surface active reagents without which this work would not have been possible.

The help rendered by Mr. B.P. Srivastava of C.D.R.I. Lucknow, during the course of NMR studies is gratefully acknowledged.

The author gratefully acknowledges the help rendered by Mr. V.P. Gupta, Dept. of Metallurgical Engineering in the fabrication of the light-scattering filter assembly.

The author expresses his gratitude to all his colleagues in the Department of Metallurgical Engineering and the Department of Chemistry whose love and affection for him had always been overwhelming.

V.K. Bansal  
V.K. Bansal

## CONTENTS

<u>Chapter</u>	<u>Page</u>
LIST OF TABLES	vi
LIST OF FIGURES	ix
SYNOPSIS	xii
I. INTRODUCTION	
I.1 Froth Flotation	1
I.2 Surface Active Reagents and Surface Activity	3
I.3 Hemi-Micelle Concentration	4
I.4 Micellisation	7
I.5 Philosophy of the Problem	13
I.6 Statement of the Problem	14
References	17
II. MATERIALS	
II.1 Minerals	18
II.2 Collectors	19
II.3 Frothers	21
II.4 Other Chemicals	22
III. COLLECTOR-FROTHER INTERACTION AT DIFFERENT INTERFACES IN A FLOTATION SYSTEM	
III.1 Introduction	23
III.2 Interaction at the Liquid-Gas-Interface	25
III.3 Interaction at Liquid-Solid-Air Interfaces	30
III.4 Interaction at the Liquid-Solid Interface	39
III.5 Discussion	47
References	53

<u>Chapter</u>	<u>Page</u>
IV. CONDUCTIVITY MEASUREMENT OF COLLECTOR-FROTHER INTERACTION	
IV.1 Introduction	56
IV.2 Experimental	60
IV.3 Results and Discussion	60
References	74
V. LIGHT-SCATTERING STUDIES ON THE SIZES AND SHAPES OF THE MICELLES OF PPG, AND ON THE INTERACTION BETWEEN PPG AND IONIC SURFACTANTS	
V.1 Introduction	76
V.2 Experimental	86
V.3 Results and Discussion	94
References	125
VI. COLLECTOR-FROTHER INTERACTION IN THE BULK PHASE AS MONITORED BY NUCLEAR MAGNETIC RESONANCE	
VI.1 Introduction	100
VI.2 Experimental	133
VI.3 Results and Discussion	134
References	150
VII. SUMMARY AND CONCLUSIONS	153
APPENDIX EXPERIMENTAL DATA	162

## LIST OF TABLES

<u>Table</u>		<u>Page</u>
3.1	Adsorption of Nonionic Frother on Rutile Surface	46
4.1	Effect of Nonionic (PPG) on $\Lambda_o$ Value of Na-DBS at 35°C	69
5.1	Scattering Function and Radii of Gyration For Various Structures	84
5.2	Molecular Weight, Radius of Gyration and Number of Monomer of Micelles	115
6.1	NMR Spectral Features of Mixtures of Na-DBS and PPG-3	136
6.2	NMR Spectral Features of Mixtures of Na-DBS and PPG-4	137
I.	Surface Tension Values of Sodium Oleate Solutions	163
II.	Surface Tension Values for Pure Low Molecular Weight Nonionic (PPG-3)	164
III.	Surface Tension Values for Pure High Molecular Weight Nonionic (PPG-4)	165
IV.	Effect of Nonionic on Surface Tension of Sodium Oleate Solution	166
V.	Effect of Sodium Oleate on Surface Tension Values of Nonionics	167
VI.	Effect of Collector Concentration on Flotation Recovery of Calcite	168
VII.	Effect of Collector Concentration on Flotation Recovery of Calcite	169
VIII.	Effect of Collector Concentration on Flotation Recovery of Calcite (Nonionic Concentration = $5.14 \times 10^{-5}$ m/l)	169

<u>Table</u>	<u>Page</u>
IX. Effect of Collector Concentration on Flotation Recovery of Calcite (Nonionic Concentration = $2.78 \times 10^{-4}$ m/l)	170
X. Effect of Nonionic (PPG-3) on Flotation Recovery of Calcite (Na-DBS Concentration = $7.45 \times 10^{-5}$ m/l)	171
XI. Effect of Nonionic (PPG-3) on Flotation Recovery of Calcite (Na-DBS Concentration $1.02 \times 10^{-4}$ m/l)	172
XII. Effect of Nonionic (PPG-4) on Contact Angle in the System Rutile-Sodium Oleate-Air	173
XIII. Adsorption of Sodium Oleate on Rutile (Direct Adsorption Method)	174
XIV. Effect of Nonionic (PPG-3) on Adsorption of Sodium Oleate on Rutile (Direct Adsorption Method)	175
XV. Effect of Nonionic (PPG-4) on Adsorption of Sodium Oleate on Rutile (Direct Adsorption Method)	176
XVI. Specific Conductivity Data for Na-DBS Solution Alone And in Presence of Nonionic (PPG-4)	177
XVII. Specific Conductance Values of Na-DBS Solution in Presence of Nonionic (PPG-3) Surfactant	179
XVIII. $HC/\Delta\tau_{\theta}$ Values of PPG-3 Micelles	181
XIX. $HC/\Delta\tau_{\theta}$ Values of PPG-4 Micelles	182
XX. $HC/\Delta\tau_{\theta}$ Values of Sodium Dodecyle Benzene Sulfonate (Na-DBS) Micelles	183
XXI. Effect of Na-DBS (Concentration = $2.55 \times 10^{-5}$ m/l) on $HC/\Delta\tau_{\theta}$ Values of PPG-4 Micelles	184
XXII. Effect of Na-DBS (Concentration = $5 \times 10^{-5}$ m/l) on $HC/\Delta\tau_{\theta}$ Values of PPG-4 Micelles	185
XXIII. Effect of Na-DBS (Concentration = $5 \times 10^{-5}$ m/l) on $HC/\Delta\tau_{\theta}$ Values of PPG-3 Micelles	186

<u>Table</u>	<u>Page</u>
XXIV. Effect of Na-DBS (Concentration = $8.5 \times 10^{-4}$ m/l) on $HC/\Delta\tau_{\theta}$ Values of PPG-3 Micelles	187
XXV. Particle Scattering Factor Values of PPG-3 Micelles	188
XXVI. Particle Scattering Factor Values of PPG-4 Micelles	189
XXVII. Effect of Sodium Oleate (Concentration = $10^{-5}$ m/l) on $HC/\Delta\tau_{\theta}$ Values of PPG-3 Micelles	190
XXVIII. Effect of Sodium Oleate (Concentration = $5 \times 10^{-5}$ m/l) on $HC/\Delta\tau_{\theta}$ Values of PPG-3 Micelles	191
XXIX. Effect of Sodium Oleate (Concentration = $10^{-4}$ m/l) on $HC/\Delta\tau_{\theta}$ Values of PPG-3 Micelles	192
XXX. Effect of Sodium Oleate (Concentration = $10^{-5}$ m/l) on $HC/\Delta\tau_{\theta}$ Values of PPG-4 Micelles	193
XXXI. Effect of Sodium Oleate (Concentration = $5 \times 10^{-5}$ m/l) on $HC/\Delta\tau_{\theta}$ Values of PPG-4 Micelles	194
XXXII. Effect of Sodium Oleate (Concentration = $10^{-4}$ m/l) on $HC/\Delta\tau_{\theta}$ Values of PPG-4 Micelles	195

## LIST OF FIGURES

<u>Figure</u>		<u>Page</u>
1.1	Hemi-Micelle Concentration for Quartz-DNA System	5
1.2	Micelles of Surfactant Molecules	8
1.3	Critical Micelle Concentration of Sodium Dodecyl Sulfate	9
3.1	Effect of Nonionic (PPG) Additives on Surface Tension Values of Sodium Oleate Solution	27
3.2	Effect of Sodium Oleate Additive on Surface Tension Value of Nonionic Solution	28
3.3	Effect of Nonionic (Low Mol. Weight) on Flotation Recovery-Calcite Flotation by Na-DBS	32
3.4	Effect of Low Mol. Weight Nonionic on Flotation Recovery of Calcite	33
3.5	Effect of Nonionic on the Flotation Recovery of Rutile	34
3.6	Effect of High Mol. Weight Nonionic (PPG-4) on Contact Angle System Na-Oleate-Rutile-Air	37
3.7	Effect of Nonionic (PPG) on Adsorption of Sodium Oleate on Rutile	41
3.8	Effect of Nonionic (PPG) on Adsorption of Sodium Oleate (Direct Estimation on Solid Method)	42
3.9	Effect of Concentration of Sodium Oleate and Nonionic (PPG-4) on Zeta-Potential of Rutile	43
4.1	Equivalent Conductivity of Sodium Dodecyl Sulfate in Water As a Function of the Square Root of the Molality	57

<u>Figure</u>		<u>Page</u>
4.2	Effect of Low Mol. Weight Nonionic on Specific Conductance Value of Na-DBS	61
4.3	Effect of Low Mol. Weight Nonionic on Specific Conductance Value of Na-DBS	62
4.4	Effect of Low Mol. Weight Nonionic on Equivalent Conductance of Na-DBS	63
4.5	Effect of High Mol. Weight Nonionic on Specific Conductance Value of Na-DBS	64
4.6	Effect of High Mol. Weight Nonionic on Specific Conductance Value of Na-DBS	66
4.7	Effect of High Mol. Weight Nonionic on Equivalent Conductance of Na-DBS	67
4.8	Specific Conductance Against Concentration for Na-Oleate Alone and Mixed With Nonionic (Low Mol. Weight) at 25°C	70
4.9	Specific Conductance Against Concentration for Na-Oleate Alone and Mixed With Nonionic (High Mol. Weight) at 25°C.	71
5.1	Filter Assembly	89
5.2	Zimm Plot for Pure Nonionic Micelle (PPG-3)	96
5.3	Zimm Plot for Pure Nonionic Micelle (PPG-4)	103
5.4	Zimm Plot for Sodium Dodecyl Benzene Sulfonate Micelle	105
5.5	Zimm Plot for Low Mol. Weight (PPG-3) Nonionic Micelle in Presence of Na-DBS (Concentration = $5 \times 10^{-5}$ m/l)	107
5.6	Zimm Plot for Low Mol. Weight (PPG-3) Nonionic Micelle in Presence of Na-DBS (Concentration = $8.5 \times 10^{-4}$ m/l)	108
5.7	Zimm Plot for High Mol. Weight (PPG-4) Nonionic Micelle in Presence of Na-DBS (Concentration = $2.55 \times 10^{-5}$ m/l)	109



<u>Figure</u>		<u>Page</u>
5.8	Zimm Plot for High Mol. Weight (PPG-4) Nonionic Micelle in Presence of Na-DBS (Concentration = $5.00 \times 10^{-5}$ m/l)	110
5.9	Effect of Na-DBS on the Particle Scattering Factor of Low Mol. Weight Nonionic Micelle	111
5.10	Effect of Na-DBS on the Particle Scattering Factor of High Mol. Weight Nonionic Micelle	112
5.11	Particle Scattering Factor of Micelle vs. $kSR_g$	113
5.12	Zimm Plot for Low Mol. Weight Nonionic (PPG-3) Micelle (Concentration of Sodium Oleate = $10^{-5}$ m/l)	117
5.13	Zimm Plot for Low Mol. Weight Nonionic Micelle in Presence of Sodium Oleate (Concentration = $5 \times 10^{-5}$ m/l)	118
5.14	Zimm Plot for Low Mol. Weight Nonionic Micelle in Presence of Sodium Oleate (Concentration = $10^{-4}$ m/l)	119
5.15	Zimm Plot for High Mol. Weight Nonionic (PPG-4) (Concentration of Sodium Oleate = $10^{-5}$ m/l)	120
5.16	Zimm Plot for High Mol. Weight Nonionic Micelle (PPG-4) in Presence of Sodium Oleate (Concentration = $5 \times 10^{-5}$ m/l)	121
5.17	Zimm Plot for High Mol. Weight Nonionic Micelle in Presence of Sodium Oleate (Concentration = $10^{-4}$ m/l)	122
5.18	Micelle Models	123
6.1	Effect of Na-DBS on Chemical Shift of Propylene Oxide Peak of Nonionic Surfactant	135
6.2	$\Delta V(C + h)$ vs $\Delta V(C)$	144

## SYNOPSIS

Froth flotation is one of the most important processes in the mineral industry. The efficiency of this process is critically dependent on the nature of the collector and frother used in the process. In this study, an attempt has been made to elucidate the nature of the interaction of some specific surfactant frothers and collectors between themselves and its influence on mineral flotability.

In this specific study, we have studied the interaction of ionic collectors sodium oleate and sodium dodecyl benzene sulfonate with the nonionic frothers tripropylene glycol monomethyl ether and tetra propylene glycol monomethyl ether.

To study the nature of the specific interactions of the collectors and frothers at the interfaces in flotation systems, we have carried out specific studies of mineral flotation by various combinations of concentrations of collector and frother, of the adsorption of collector and frother at mineral surfaces and of the contact angle and surface tension of collector-frother solutions. These studies have produced evidence for the presence of mutual interaction between collector and frother as well as the synergistic co-adsorption of collector and frother molecules

at the solid-liquid gas interfaces. These mutual interaction and synergistic co-adsorption increase the efficiency of the flotation process.

The interaction of collectors with frothers in the bulk phase has been examined by conductivity, light-scattering and nuclear magnetic resonances studies. The conductivity studies on sodium dodecyl benzene sulfonate alone and in presence of the non-ionic frothers at various concentrations indicate the presence of pre-micellar aggregates and mixed micelles. These micelles are formed by incorporating frother molecules in collector micelles when the frother concentration alone is below its cmc (critical micelle concentration) and vice versa. Sodium oleate has also been shown to behave in a fashion similar to sodium dodecyl benzene sulfonate.

Light scattering by frothers dispersed in water alone and in presence of the ionic collectors has been studied in order to elucidate the micelle parameters. The frothers, tri and tetra propylene glycol monomethyl ethers were found to form micelles with an aggregation number of the order of  $10^3$  at  $35^\circ\text{C}$ . The shapes of these micelles could not be unequivocally established, but are shown to be either unsymmetrical ellipsoids or Mcbain type boxes. Sodium dodecyl benzene sulfonate is incorporated into these nonionic (frother) micelles to form mixed micelles, whose shapes seem to be essentially similar to those of the pure

nonionic micelles. At low concentrations, sodium oleate shows a similar behavior while at higher concentration, hydrolysis of sodium oleate makes meaningful interpretation of light-scattering data difficult.

Nuclear magnetic resonance studies have been carried out on pure solutions and mixtures of sodium dodecyl benzene sulfonate and the frothers at concentrations above their cmc values. The changes in the chemical shift values and the integration values of the polypropylene protons and collector protons along with other available data have been interpreted in terms of mixed micelle formation with the simultaneous presence of highly fluid mixed micelles of varying compositions.

## CHAPTER I

### INTRODUCTION

#### I.1 FROTH FLOTATION:

Froth flotation is one of the most important and useful separation processes in the mineral industry. In the process of froth flotation, adhesion is obtained between mineral particles and air rising through a pulp. This temporarily buoyant combination rises, forms a froth, and is removed. The crux of the process of flotation is the existence of a selective tendency for some particles to adhere to air and for other particles to adhere to water. This selective tendency of mineral particles is augmented by the use of flotation reagents. The flotation reagents added to the pulp during flotation process are, broadly, of three types -collectors, modifiers and frothers.

##### I.1.a: Collectors:

Collectors are surfactants which preferentially adsorb to the surfaces of specific types of particles, and by so doing render part of the surface sufficiently hydrophobic to cling tenaciously in the air-water interface when the pulp is aerated, until finally removed as part of a mineralised froth.

A collector must adsorb to the selected mineral surface so as to cover it partially with a film which is water-repellent. Success in achieving this specific adsorption is essential if the particles thus modified are to be selectively removed from the pulp as part of the mineralised froth. Some of the most commonly used collectors are (1) Ethyl, propyl, butyl, and amyl xanthates, particularly the ethyl and the amyl xanthate of sodium or potassium, (2) Diethyl and dicyesyl dithiophosphates, and (3) Fatty acids and soaps. Fatty or alkyl chain collectors have the general formula  $\text{CH}_3(\text{CH}_2)_n\text{X}$  where X is usually a carboxy, sulphate or sulphonate group and n usually exceeds 9. The first two groups are usually used for the flotation of sulphide minerals while the third group for non-sulphide minerals.

#### I.1.b Frothers:

A widely held concept of the frothing agent is of a surfactant of low solubility and surface tension, with no collecting power or interaction with collector agents but which stabilises air-liquid or froth interface. Frother molecules are heteropolar, with their hydrophilic groups characteristically nonionic (e.g. OH, COOH, C=O,  $\text{NH}_2$ ), the hydroxyl being the commonest, as in terpineols ( $\text{C}_{10}\text{H}_{17}\text{OH}$ ), cresols ( $\text{CH}_3\text{C}_6\text{H}_4\text{OH}$ ) and alcohols ( $\text{C}_5\text{H}_{11}\text{OH}$ , etc.).

Froth flotation process is essentially dependent on the selection of collector and frother, both of which are surface

active agents. In the past, it was believed that collector action is essentially on the solid-liquid interface and the frother acts at the liquid-gas interface. But the work of Leja (1) showed for the first time that a collector not only acts on the liquid-solid interface but may also affect the frother behavior and similarly frother may affect the collector action. The increase of the flotation recovery of corundum by the addition of n-alcohols observed by D.W. Fuerstenau (2) has been explained by Schubert and Schneider (3) recently in terms of co-adsorption of collector and frother. They also called these additives as secondary collectors and the adsorption of these secondary collectors might be due to the interaction between collector and frother. Recently Lekki and Laskowski (4,5) observed the joint action of frother and collector in flotation. The assumption that collector acts only at the solid-liquid interface and frother acts only at liquid-gas interface is probably oversimplified and needs detailed investigation.

## I.2 SURFACE ACTIVE REAGENTS AND SURFACE ACTIVITY:

Surface activity can be defined as the pronounced tendency of a solute to concentrate at an interface. The reagents having this type of tendency are called surface active reagents. These types of compounds (molecules) are composed of two segregated portions: one which has sufficient affinity for the solvent to bring the entire molecule into solution, and the other portion is relatively incompatible

with the solvent because it has less affinity for the solvent molecules than the solvent molecules have for each other. This kind of solute molecules with dual property will tend to concentrate at an interface. These ~~types~~ of compounds can be broadly divided into three subgroups.

1. Anionic surface active agents: e.g.  $C_{17}H_{33}COO^-/Na^+$ ;
2. Cationic surface active agents: e.g.  $C_{12}H_{25}NH_4^+/Cl^-$ ;
3. Nonionic surface active agents: e.g. Polyoxyethylene monohexadecylother.

In general both collector and frother are surface active reagents; collectors are generally ionic while frothers are nonionic in nature.

### I.3 HEMI-MICELLE CONCENTRATION:

Hemi-micelle concentration is defined as the concentration of the collector at which marked changes in the parameters (contact angle, adsorption density, zeta potential, flotation recovery) occur in a mineral flotation system. The adsorption and flotation behavior can be explained with the help of the hemi-micelle hypothesis. For hemi-micelle formation, ions should be ~~adsorbed~~ individually at low concentration, but at higher concentrations, there should be marked changes in interfacial parameters as the adsorbed collector ions associate into hemi-micelles. Fig. 1.1 presents plots of a number of interfacial parameters for the system quartz-dodecylamine acetate (DAA) at pH 6-7 and at  $20^{\circ}$ - $25^{\circ}$ C (6).



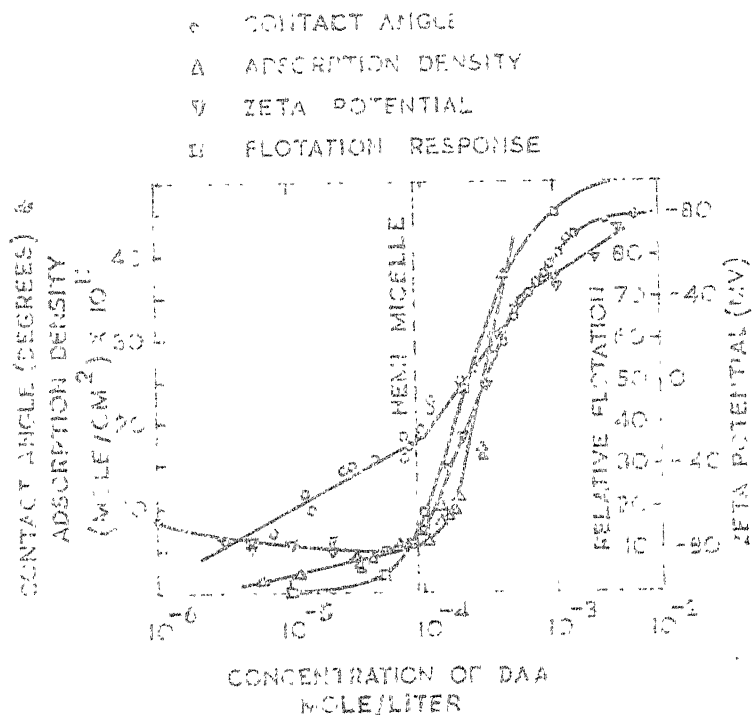


FIG.11 HEMI MICELLE CONCENTRATION  
 FOR QUARTZ - DAA SYSTEM

Ref. D.W. Fuerstenau, T.W. Healy and P. Somasudaran  
 Transactions Society of Mining Engineers p-321,  
 Dec-1964

The following parameters are plotted as a function of the concentration of DAA: (1) Contact angle, (2) Adsorption density, (3) Zeta potential, and (4) Halimond tube flotation recovery for DAA and quartz at neutral pH. Hemi-micelle formation occurs at approximately  $10^{-4}$  M DAA, as shown by the marked changes in the parameters. The theory of hemi-micelle can be approached by expressing the adsorption density within the Stern plane of the electrical double layer in the form;

$$\Gamma_i = 2rC \exp [(-W_e + n\phi')/kT]$$

where,

$W_e$  = Electrostatic free energy term that describes the process of bringing the polar groups together,

$\phi'$  = Cohesive free energy per  $\text{CH}_2$  group,

$\Gamma_i$  = Adsorption density,

$r$  = Radius of organic ion,

$C$  = Equilibrium bulk concentration of the organic ion,

$n$  = Number of  $\text{CH}_2$  group.

If we select the hemi-micelle concentration, that is,

$$C = C_{\text{HM}}$$

Then,

$$C_{\text{HM}} = (\Gamma_i/2r) \exp [(W_e - n\phi')/kT]$$

or 
$$C_{\text{HM}} = A' \exp [(W_e - n\phi')/kT]$$

$$\ln C_{\text{HM}} = W_e + \ln (\Gamma_i/2r) - (\phi'/kT) n$$

The slope of the plot  $\ln C_{HM}$  vs.  $n$  gives us the value of  $\phi'$  in terms of  $kT$ .

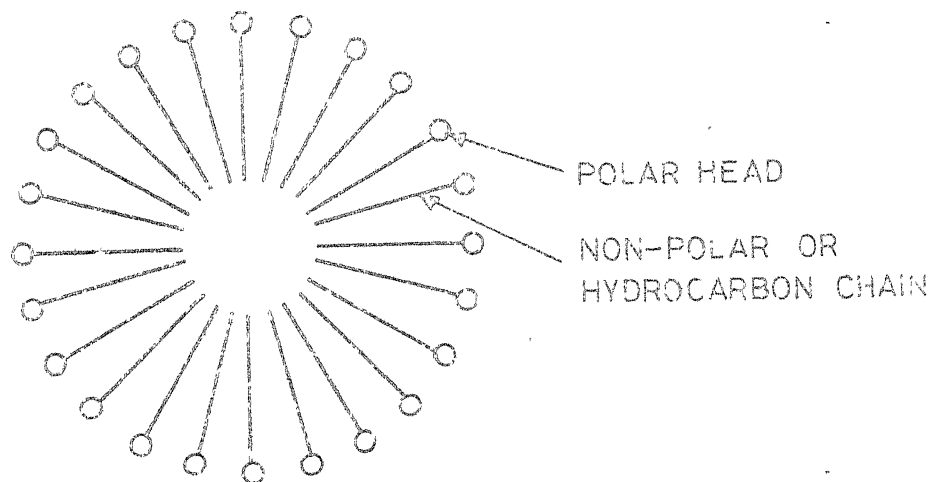
#### I.4 MICELLIZATION:

##### I.4.1: Micelle:

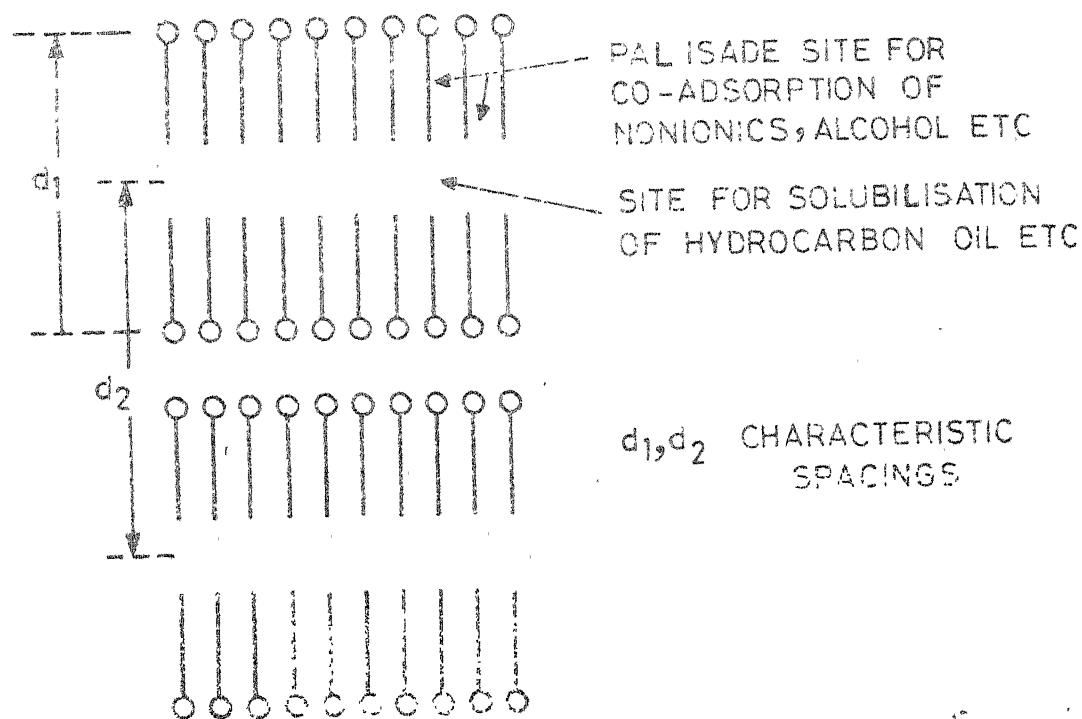
When a surface-active agent is dissolved in water, the condition for the system to exhibit minimum free energy stipulates that there should be minimum contact between the water molecules and the nonpolar hydrocarbon chain of the surfactant molecule. This minimum contact is achieved when surfactant molecules concentrate at the surface and orient with their polar group directed towards the aqueous phase and their hydrocarbon chain directed outwards. In the bulk of the solution, minimum contact between hydrocarbon chains and water molecules is accomplished by the clustering of the surfactant molecules in such a manner that the hydrocarbon chains of many molecules are in contact and are surrounded and hidden by polar groups. This aggregation of surfactant molecules is called a micelle (Fig. 1.2).

##### I.4.2 Critical Micelle Concentration:

Aqueous solutions of surfactants exhibit more or less abrupt changes in their physical properties over a narrow concentration range. This rapid change in properties is generally accepted to be due to the formation of oriented aggregates



SPHERICAL MICELLE  
(HARTLEY)



LAMELLAR MICELLE  
(Mc BAIN)

## MICELLES OF SURFACTANT MOLECULES

FIG.12

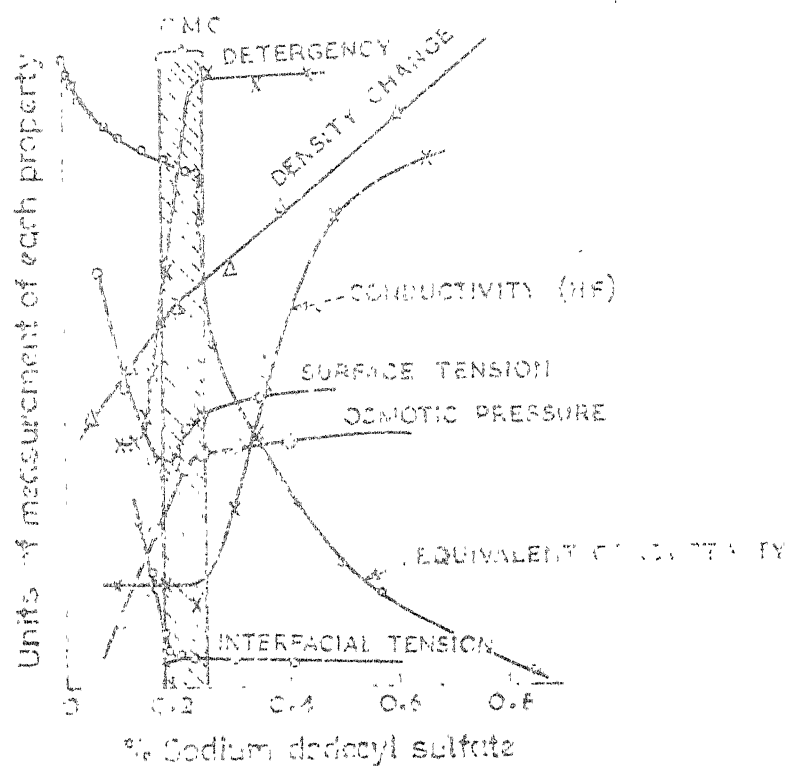


FIG. 13 CRITICAL MICELLE CONCENTRATION OF SODIUM DODECYL SULFATE

Ref. ADAMSON, A.W. 'Physical Chemistry of surfaces' p-374  
Interscience Publishers Ltd, London 1960

or micelles. The concentration at which the concentration of micelle suddenly becomes appreciable is referred to as the critical micellar concentration (7) or cmc as shown in Fig.1.3.

For various cationic and anionic surfactants, the cmc can be expressed by the equation,

$$\log \text{cmc} = A - BN_c$$

where  $N_c$  is the number of carbon atom in the long hydrocarbon chain. B is a constant approximately equal to 0.29. A is a constant for a particular temperature and a homologous series.

#### 1.4.3 Theory of Micellization:

As a chemical system tends towards a state of minimum free energy, the micellization process must result in a free energy decrease. The changes occurring during the process of micellization are:

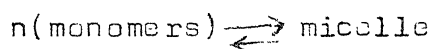
1. Decrease in hydrocarbon/water interfacial energy.
2. The micellization process with regard to monomers is a disorder to order transition, meaning that there is a negative entropy change.

However, there is loss of water structure form around the hydrocarbon chain. This loss of water structure gives a transformation from ordered state to disordered with regard to water, meaning that there is a positive entropy change during the process. There is an overall decrease in free energy and

increase in entropy of the system. The above two factors provide driving forces for the micellization process.

Furthermore, for an ionised surfactant, the bringing together of monomers into a micelle means that work has to be done against the electrostatic repulsion between similarly charged polar head groups. This restricts indefinite growth of micelles and for a particular concentration of an ionic surfactant solution, there is an optimum micellar size. Non-ionic detergents, for which no electrical force is expected to oppose micellization, form micelles at concentrations lower than those for ionic ones.

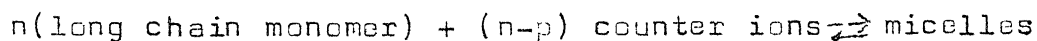
For nonionic detergents, the equilibria can be written as:



$$K = C_{\text{mic}} / C_{\text{mon}}^n$$

where K is the equilibrium constant, and activity has been replaced by concentration.

For ionised detergents:



$$K = \frac{C_{\text{mic}}}{C_{\text{mon}}^n C_{\text{ci}}^{n-p}}$$

$C_{ci}$  = concentration of counter ion,

$p$  = effective charge on micelle.

The free energy gain for  $\text{CH}_2$  group entering the micelle is found to be about  $1.25 \text{ kT}$ . The work of adsorption of a  $\text{CH}_2$  at an oil-water interface is about  $1.37 \text{ kT}$ . The relatively close agreement in energy values indicates that the interior of the micelle has a hydrocarbon liquid-like character.

The collector concentrations used in the flotation recovery are usually far below their respective critical micelle concentrations. But the concentrations of frother actually used may be high enough to produce micelles. This justifies some detailed studies on the micellar properties of frother and collector-frother systems. Such studies may furnish evidences of collector-frother interaction in the bulk phase. Conductivity studies may yield evidences of pre-micellar interaction as well.

The link between the interfacial and bulk interaction studies is provided in terms of similar nature and energetics of the collector-frother interaction in mixed micelles (bulk) and in mixed hemi-micelles (on the solid surface).



## I.5 PHILOSOPHY OF THE PROBLEM:

During the last fifteen years, considerable efforts have been put to study the anionic-nonionic interactions in solutions using various surface-active agents. But the literature on specific interaction between a collector (ionic surfactant) and a frother (non-ionic surfactant) is scanty. Some indirect evidences of collector-frother interaction at different interfaces in a flotation system have been obtained by some workers (1-5). We have not come across any literature giving evidence of interaction in the bulk liquid phase (pre-micellar and micellar interaction) between collector and frother molecules. The reason for this might be that for many years cresols and pine oils were the commonly used frothers, and these frothers have very limited solubility in water. Hence interactions study for frother solutions over a wide concentration range was out of question. But recently, alkyl ethers of poly propylene glycol have been introduced as effective frothers. These frothers are readily soluble in water and one could use several sophisticated techniques to study their interaction with collectors over a wide range of concentrations. Further introductory remarks and other details about the techniques used shall be made in the forth-coming chapters.

In our work we have used the anionic surface active agents (sodium oleate and sodium dodecyl benzene sulfonate) as collectors, and purified nonionic (Dowfroth type) surface active agents (Tripropylene glycol monomethyl ether and Tetrapropylene glycol monomethyl ether) as frothers.

#### I.6 STATEMENT OF THE PROBLEM:

Collector-frother interactions have been studied on the following points:

1. Interaction at the different interfaces in a flotation system:

Interaction at different interfaces in a flotation system has been studied by the following techniques:

(a) Surface Tension Measurements: Surface tension measurements have been used to study the interaction at liquid-gas interface and to study the effect of frother on the cmc of sodium oleate (collector) and vice versa.

(b) Adsorption and Zeta Potential Measurement: Adsorption of sodium oleate on rutile and the effect of nonionics (frothers) on the adsorption of sodium oleate have been measured (and vice versa) to study the collector-frother interaction at the solid-liquid interface. Zeta potential measurements have also been carried out to study the effect of frother on the zeta potential of rutile in sodium oleate solution and to

substantiate the conclusions derived from the adsorption data. Infra-red measurements have also been carried out to study the adsorption of sodium oleate and nonionics on rutile mineral.

(c) Flotation Recovery and Contact Angle Measurement: The effect of frothers (nonionics) on the flotation recovery of rutile and calcite, and the effect of frothers on the contact angle in rutile (single crystal) - sodium oleate solution -air system have been studied to evaluate the interaction at liquid-solid gas interface.

(2) Interaction in the Bulk Liquid Phase (Pre-micellar and Micellar Interaction):

Interaction study in the bulk liquid phase has been done by studying the micellar properties of collector (sodium oleate and sodium dodecyl benzene sulfonate) and frother (nonionic). The following techniques have been used for such a study:

(a) Conductivity Measurements: Conductivity values of sodium dodecyl benzene sulfonate solutions have been measured in the pre-micellar and post-micellar regions. The interaction between the sodium dodecyl benzene sulfonate (collector) and the frother has been studied by measuring the effect of nonionic (frother) on the conductance value of sodium dodecyl benzene sulfonate solution in pre-micellar and post-micellar regions and the equivalent conductance values were compared with the theoretical Onsager values.

(b) Light-Scattering Measurements: The interactions between the collectors Na-DBS (Sodium Dodecyl Benzene Sulfonate) and Na-OL (Sodium Oleate) and nonionics frothers have been studied by light-scattering technique through measurements of the micellar weights of nonionic (frother) and the radii of gyration of nonionic micelles, and the effect of Na-DBS and Na-OL (Sodium Oleate) on the nonionic (frother) micellar weight, shapes and sizes.

(c) Nuclear Magnetic Resonance: The technique of nuclear magnetic resonance (nmr) has been used to study the interaction between Na-DBS and nonionic in the micellar region by measuring the chemical shift and integration values of propylene oxide groups on the addition of Na-DBS.

To recapitulate, the present series of investigation has been oriented towards obtaining evidences of collector-frother interaction in typical flotation systems. These interactions were believed to happen in the various interfaces and in the bulk aqueous phase of pre- and post-micellar concentrations. Detailed studies on energetics of such interactions were not included in this series of investigations.

## REFERENCES

1. Leja, J.  
Interaction at Interfaces in Relation to Froth Flotation  
(1957), Proc. 2nd. Int. Congr. Surf. Activity, Butterworth's,  
London, 3, 273-295.
2. Fuerstenau, D.W., and Yamada, B.J.  
Neutral Molecules in Flotation Collection  
(1962), Trans. Am. Min. Engrs., 223, 50-52.
3. Schubert, H. and Schneider, W.  
Über die rolle der assoziation der unpolaren gruppen  
bei der sammleradsorption  
(1969), In. Proc. 8th. Int. Miner. Process Congr. 2,  
315-324, (Russian text): Preprint S-9.
4. Lekki, J., and Laskowski, J.  
On the Dynamic Effect of Frother-Collector Joint  
Action in Flotation  
(1971), Trans. Inst. Min. Metall. (Section C, Mineral  
Process. Extr. Metall.), 80, C 174-180.
5. Lekki, J., and Laskowski, J.  
A New Concept of Frothing in Flotation System and  
General Classification of Flotation Frother  
(1975), XI. Int. Mineral. Process. Congr., Cagliari,  
preprint 15.
6. Fuerstenau, D.W., Healy, T.W., and Somasundaram, P.  
The Role of the Hydrocarbon Chain of Alkyl Collectors  
in Flotation  
(1964), Trans. Am. Inst. Min. Engrs., 229, 321-325.
7. Adamson, A.W.  
Physical Chemistry of Surfaces  
(1960), Interscience Publishers Ltd., (London) 374-375.

## CHAPTER II

### MATERIALS

In this chapter, detailed accounts of the chemicals and materials used are given.

#### II.1 MINERALS:

Rutile and calcite were used as minerals for flotation study while only rutile was used for adsorption study. The rutile sample used in the present studies was procured from the Indian Rare Earth Ltd. It was claimed to be of 99 percent purity by the suppliers. For contact angle experiments a 1 cm dia-cylindrical rutile crystal was used. This crystal with (100) planes cut and polished was supplied by Linde Co., Chicago, USA.

##### II.1 a Sample Preparation for Flotation Experiments:

The original samples supplied as coarse grains were ground, sieved and the fraction -85 + 100 mesh size was collected. The fraction collected was thoroughly washed with water and then with dilute hydrochloric acid. This was followed by repeated washing. The sample was stored under distilled water.

## II.1b Sample Preparation for Adsorption Studies:

The original sample was washed thoroughly and further ground in an alumina pebble mill. The fraction - 300 + 325 mesh was collected. The sample was washed with water and then with dilute hydrochloric acid, and then suspended in 1.5 litres of water in a 2 litre beaker. The fraction which settled in the first 10 minutes was taken and the rest removed by decantation. This was repeated several times. The finer fraction, after decantation, was dried in an oven and was thoroughly mixed in a pebble mill. The thoroughly mixed material was again washed several times. The washed material was stored under redistilled water in a glass jar for adsorption studies.

## II.2 COLLECTOR:

Sodium oleate and sodium dodecyl benzene sulfonate were used as collectors throughout the course of these investigations.

### II.2.1 Oleic Acid:

The untagged oleic acid was obtained from the Hormel Institute's fatty acid project at University of Minnesota, U.S.A. Estimated purity was more than 99 percent as determined by gas-liquid and thin layer chromatography analysis. Iodine value was found out to be 89.9 and diene conjugation .03 percent.

### II.2.2 Preparation of Sodium Oleate:

The procedure followed for the preparation of sodium oleate from oleic acid was similar to that of Kajiji (1). Equivalent amounts of oleic acid and analytical grade sodium hydroxide were transferred to a round bottom flask and 50 ml. of dry absolute alcohol was added. The ethyl alcohol used had been distilled, kept over-night over quick lime and redistilled.

The whole mass was refluxed over a water bath for about an hour. Subsequently, excess alcohol was removed by evaporation and syrupy mass was poured hot in acetone which had been distilled after keeping over night with  $\text{CaCl}_2$ . Sodium oleate thus precipitated was filtered and washed with acetone. The dried powder was stored in a cool dry place.

### II.2.3 Labelled Oleic Acid:

The  $\text{C}^{14}$  labelled oleic acid was obtained from International Chemical and Nuclear Corporation, California, U.S.A. The specific activity of the acid was reported to be 10 mc/min. The full scale deflection of the compound was given as 100,000 cpm. The labelled oleic acid was obtained in benzene solution.

### II.2.4 Preparation of Radioactive Sodium Oleate Solution:

A suitable quantity of the tagged oleic acid was transferred from the vial to a 500 ml. volumetric flask. Excess of sodium hydroxide solution was added to make the volume around



15 ml. The mixture was kept in a thermostat maintained at 40°C for about 36 hrs. It was frequently shaken and the stopper opened to allow the benzene vapor to escape. At the end of this period, saponification was assumed to be complete. The resulting product was then added in definite proportion to a solution of ordinary (untagged) sodium oleate. The solution was stocked for further use.

#### II.2.5 Sodium Dodecyl Benzene Sulfonate:

Sodium dodecyl benzene sulfonate of A.R. quality was obtained from Peltz and Bauer Inc., N.Y.

#### II.3 FROTHER:

Tripropylene glycol monomethyl (PPG-3) ether and tetrapropylene glycol monomethyl (PPG-4) ether were used as frothers. These are nonionic in nature and are low viscosity liquids, readily soluble in water and have the general formula  $\text{CH}_3(\text{OC}_3\text{H}_6)_n\text{-OH}$ . Dow Chemical Co. research laboratory purified the commercial material usually known as Dow froth 200, 250 to obtain components in the purest state possible. Two purified materials were obtained by us through their courtesy. From the stereochemistry, it is shown that eight isomers are possible for tripropylene glycol monomethyl (PPG-3) ether and 16 isomers are possible for the tetra propylene glycol monomethyl ether (PPG-4). The analysis of the purified

products are given below:

Sample 1: Tri propylene glycol monomethyl ether (PPG-3)

99.7 percent Isomer A,

.2 percent Isomer B.

Sample 2: Tetrapropylene glycol monomethyl ether (PPG-4)

96.7 percent Isomer X,

1.9 percent Isomer Y,

1.2 percent Isomer Z.

In the thesis, the above-mentioned chemicals have been often mentioned as low mol.wt. or PPG-3 and high mol. wt. nonionic or PPG-4 respectively.

#### II.4 OTHER CHEMICALS:

Other chemicals such as 2,4 dinitrophenyl hydrazine, Rhodamine 6G and p-nitrophenol used for analytical purposes were all of analytical grade.

#### REFERENCE

1. Kajiji, S.S., and Desai, D.M.  
Properties of Sodium Oleate  
(1954), Science and Culture (India), 20, 39-43.

## CHAPTER III

### COLLECTOR - FROTHER INTERACTION AT DIFFERENT INTERFACES IN A FLOTATION SYSTEM

#### III.1 INTRODUCTION:

Froth flotation is usually induced by the addition of a collector and frother to an aqueous suspension of suitably comminuted minerals. The action of the collector is to adsorb on to the surface of the minerals to be separated, sensitizing them to bubble adherence. The action of the frother has so far been believed to involve froth formation only, brought on by a lowering of the air-water interfacial tension.

Leja and Schulman (1,2,3) showed that frother molecules become particularly effective when there is a suitable degree of molecular interaction with the collector molecules at the interfaces. Fuerstenau and Yamada demonstrated (4) the effect of a neutral molecule, (decyl alcohol) on the flotation recovery of corundum with sodium dodecyl sulphate or trimethyl dodecyl ammonium chloride as the collector. The increase in flotation recovery was explained on the basis of co-adsorption of the neutral molecules with the collector ions. It was postulated that adsorption of neutral molecules is essentially through van der Waals attractive force between the hydrocarbon chains of the adsorbed soap ions and those of the neutral

molecules. Lekki and Laskowski (5) showed the beneficial effect of  $\alpha$ -terpineol (frother) on the zeta potential, thickness of fluid film on the surface of chalcocite and adsorption of xanthate on chalcocite. The phenomenon was explained on the basis of joint action of frother and collector. Joint action of collector and frother was also confirmed by Plaksin (6), and Mukai (7).

We have not come across any literature in which the effect of collector on the behaviour of frother molecules in a flotation system has been studied. The main reason might be that quantitative estimation of the frother in the flotation system is very difficult due to the very limited solubility of the conventional frother (pine oil, cresylic acid) in water. The adsorption of some of the frothing agents ( $\alpha$ -terpineol, Diacetone) on mercury from aqueous solution was investigated by Zembala and Pomianowski (8). Plaksin (6) used  $C^{14}$  ethyl alcohol for studying the adsorption of ethyl alcohol on the mineral surface, and showed that the alcohol was found to be adsorbed on galena surfaces even without xanthate. The increase in flotation recovery of galena in presence of aliphatic alcohols was explained on the basis of adsorption of ethyl alcohol on the mineral surface.

Lekki and Laskowski (9) observed that some surface-inactive substances like diacetone alcohol and ethyl acetal are

readily soluble in water and they adsorb on solid surfaces and thus improve the flotation recovery. They contended that the 'frother' need not be surface-active to influence three-phase contact. However, this issue is not relevant in our studies, since we have specifically chosen conventional frothers (PPG-3 and PPG-4) which are surface-active. Recently Dorn (10) has determined the adsorption isotherm of Triton X-100 (nonionic surfactant) on quartz, and classified this nonionic surfactant as a collector in a study of the pH dependence on the flotation recovery of quartz. The frothing characteristic of this nonionic surfactant is however not known. Evidently, comprehensive studies in this regard are called for.

In this chapter, we describe our studies on the interaction between the collector and frother at different interfaces by the measurement of surface tension, contact angle, adsorption of frother and collector on mineral surfaces and the effect of frother on flotation recovery. Some of these results have been published (11).

### III.2 INTERACTION AT THE LIQUID - GAS - INTERFACE:

To investigate possible interaction of collector (sodium oleate) and frother (PPG-3 and PPG-4) molecules at the liquid gas interface, surface tension measurements were made by a Conco Du Nouy Tensiometer at room temperature ( $27 \pm 1^{\circ}\text{C}$ ). Usual precautions were taken during these measurements.

Sufficient time was allowed for aging (15-20 minutes) and time-independent surface tension values were obtained. Fig. 3.1 shows surface tension values of sodium oleate solutions of different concentrations containing fixed quantity of one nonionic (PPG) frother. Surface tension values of PPG solutions and the effect of small amount of sodium oleate are presented in Fig. 3.2.

Interaction between the collector and frother in the liquid-gas interface are quite evident from the data given in Figs. 3.1 and 3.2. Surface tension of sodium oleate solutions are lowered by the presence of nonionics (PPG), more so by the low molecular weight nonionic (PPG-3). This effect could not be attributed to the surface activity of the nonionic material itself since the concentration of nonionic used was low (vide Fig. 3.1). Similarly, a very small proportion of sodium oleate in water, which by itself does not correspond to much surface activity, reduces surface tension of PPG solutions substantially (Fig. 3.2). This is clearly a synergistic effect indicating co-adsorption of collector-frother molecules in the liquid-gas interface.

Figs. 3.1 and 3.2 clearly show that the low molecular weight nonionic surfactant (PPG-3) is more surface-active than the high molecular weight (PPG-4) material. This is

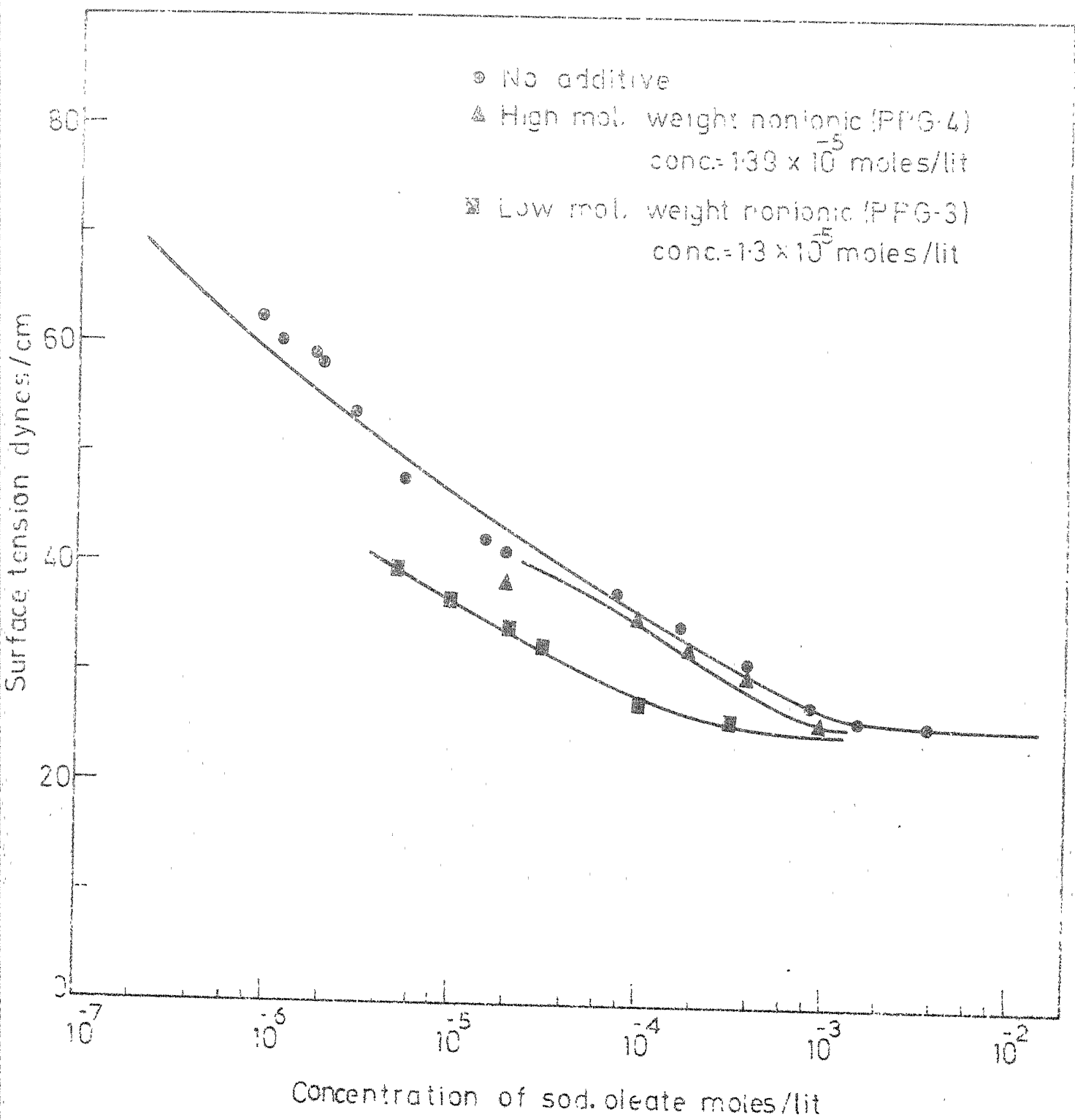


FIG. 3-1 EFFECT OF NONIONIC (PPG) ADDITIVES ON SURFACE TENSION VALUES OF SODIUM OLEATE SOLUTION

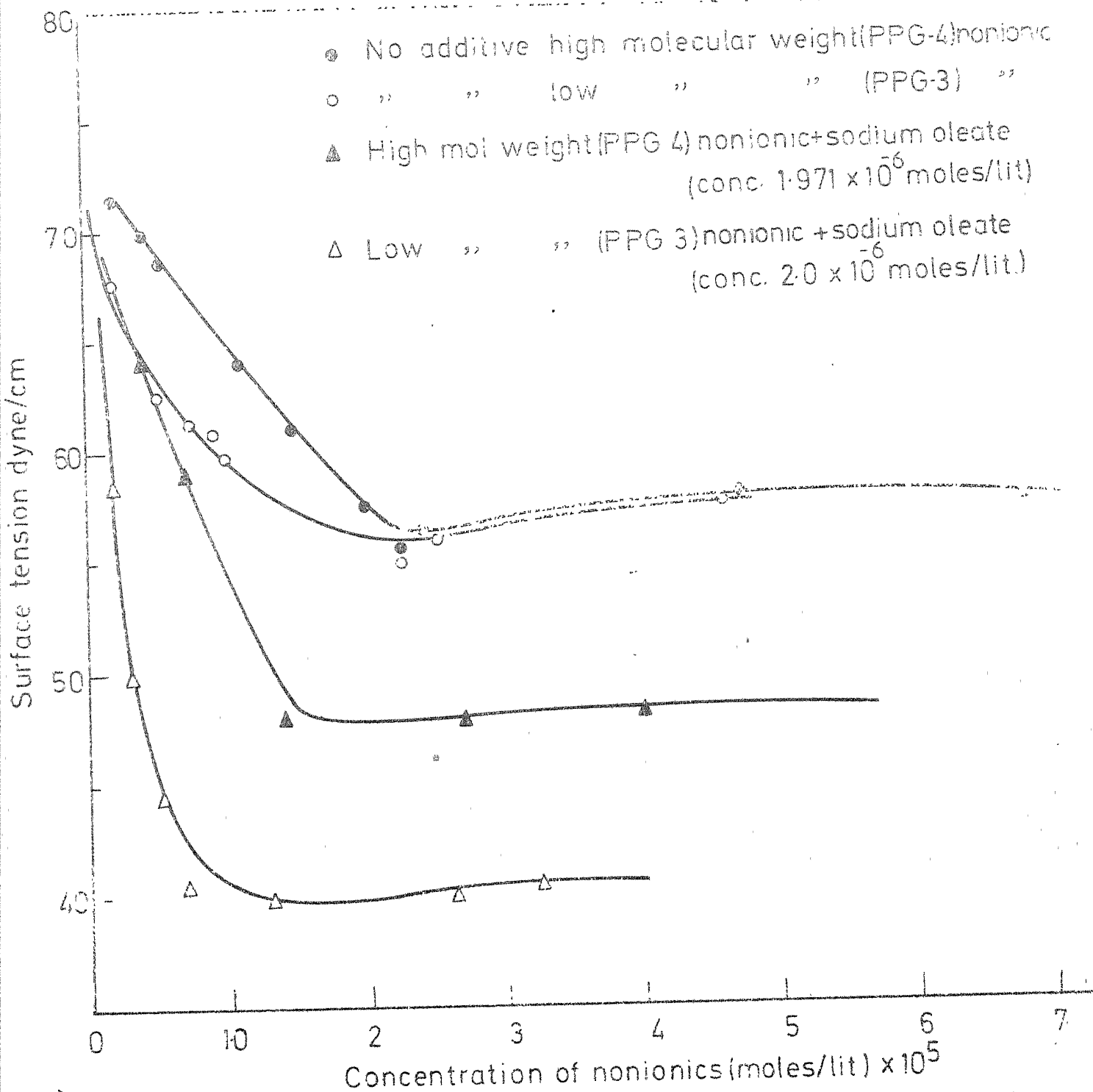


FIG.32 EFFECT OF SODIUM OLEATE ADDITIVE ON SURFACE TENSION VALUE OF NONIONIC SOLUTION



possibly due to the fact that the repetitive unit in the polyoxypropylene surfactant series is hydrophilic in nature as opposed to the conventional ionic surfactant series in which greater chain length is provided by additional hydrophobic units such as  $-\text{CH}_2$ . Quite significantly, Fig. 3.2 reveals that the cmc of PPG-3 ( $1.7 \times 10^{-5}$  m/l) is lower than the cmc of PPG-4 ( $2.2 \times 10^{-5}$  m/l).

For the micellization of nonionic molecules like PPG-3 or PPG-4 one may write the following reaction:

$[n[m] \rightarrow [M]]$  where  $[M]$  represents the molar concentration of micellar species and  $[m]$  that of monomeric species.  $K_M$  is the equilibrium constant for such a reaction. The Gibbs free energy change for micellization per monomer molecule,

$$\Delta G = - \frac{RT \ln K_M}{n}$$

$$\frac{\Delta G}{2.303 kT} = - \frac{\log K_M}{n} = - \frac{\log [M]}{n} + \log [m]$$

$\approx \log [m]$  since  $n$  is very large for PPG-3 and PPG-4, of the order of  $10^3$  (from light-scattering measurement Table 5.2). Hence  $\Delta G \approx 2.303 \log [\text{c.m.c.}] kT$  and equals  $-10.99 kT$  and  $-10.73 kT$  for PPG-3 and PPG-4 respectively. Each propylene oxide unit contributes to an increase in  $\Delta G$  to the extent of  $0.26 kT$ . Similar results were obtained by Mukherjee (12). Mukherjee used various data including those for octyl

polyoxyethylene glycole monoethers (13) and computed the head group self-interaction contribution to  $\Delta G$  for hexaoxyethylene glycol-mono ether to be  $\sim 1.2$  kT per molecule which works out to be about 0.2 kT per single oxyethylene group. Leja and Nixon (14) have suggested that polyoxyethylene ether frothers also show a definite critical micelle concentration and their surface tension values increase with increase in the molecular weight of frother.

It is also significant that the cmc values of PPG-3 and PPG-4 are lowered by small additions of sodium oleate. This constitutes a proof of mixed micellization and interaction of collector and frother in the bulk phase. This aspect will be discussed in some detail later in this thesis.

### III.3 INTERACTION AT LIQUID-SOLID-AIR INTERFACES:

The interaction in the solid-liquid-air system was studied by flotation and contact angle experiments.

The flotation experiments were carried out in an all glass laboratory flotation cell. About 30 g. of calcite prepared for an experiment were transferred to a 600 ml glass beaker and to it was added sodium dodecylbenzene sulfonate and frother (PPG). The volume was made upto 375 cc, and the pH was adjusted to  $7 \pm .05$  after 4-5 minutes. The pulp was then conditioned for 5 min. and the conditioned pulp was transferred to the flotation cell and the flotation experiment

was conducted by passing air from a compressor through a gas regulator for about two minutes. The concentrate and tailings were collected in trays, dried and weighed.

Experimental results on flotation recovery of calcite are shown in Figs. 3.3 and 3.4. Fig. 3.3 shows the effect of Na-DBS concentration on the flotation recovery of calcite at different concentrations of the nonionic frother (PPG-3). The flotation recovery results of calcite with different concentrations of purified nonionics (PPG) at constant concentrations of Na-DBS are shown in Fig. 3.4. It is seen from Fig. 3.3 that the flotation recovery increases as concentration of Na-DBS increases for a constant concentration of PPG-3. It is also seen from Fig. 3.3 and 3.4 that the recovery of calcite increases with an increase in PPG-3 concentration. This increase in flotation recovery is much greater at the lower concentration range of Na-DBS, and the hemi-micelle concentration (concentration at which a sharp increase in flotation recovery occurs), decreases as the concentration of PPG increases (Fig. 3.3).

Similar experimental results were obtained by us earlier for the system rutile-sodium oleate and nonionics frother (PPG-3 and PPG-4) (11,15). The effect of nonionic (PPG) on the flotation recovery of rutile at constant concentration of sodium oleate is shown in Fig. 3.5.

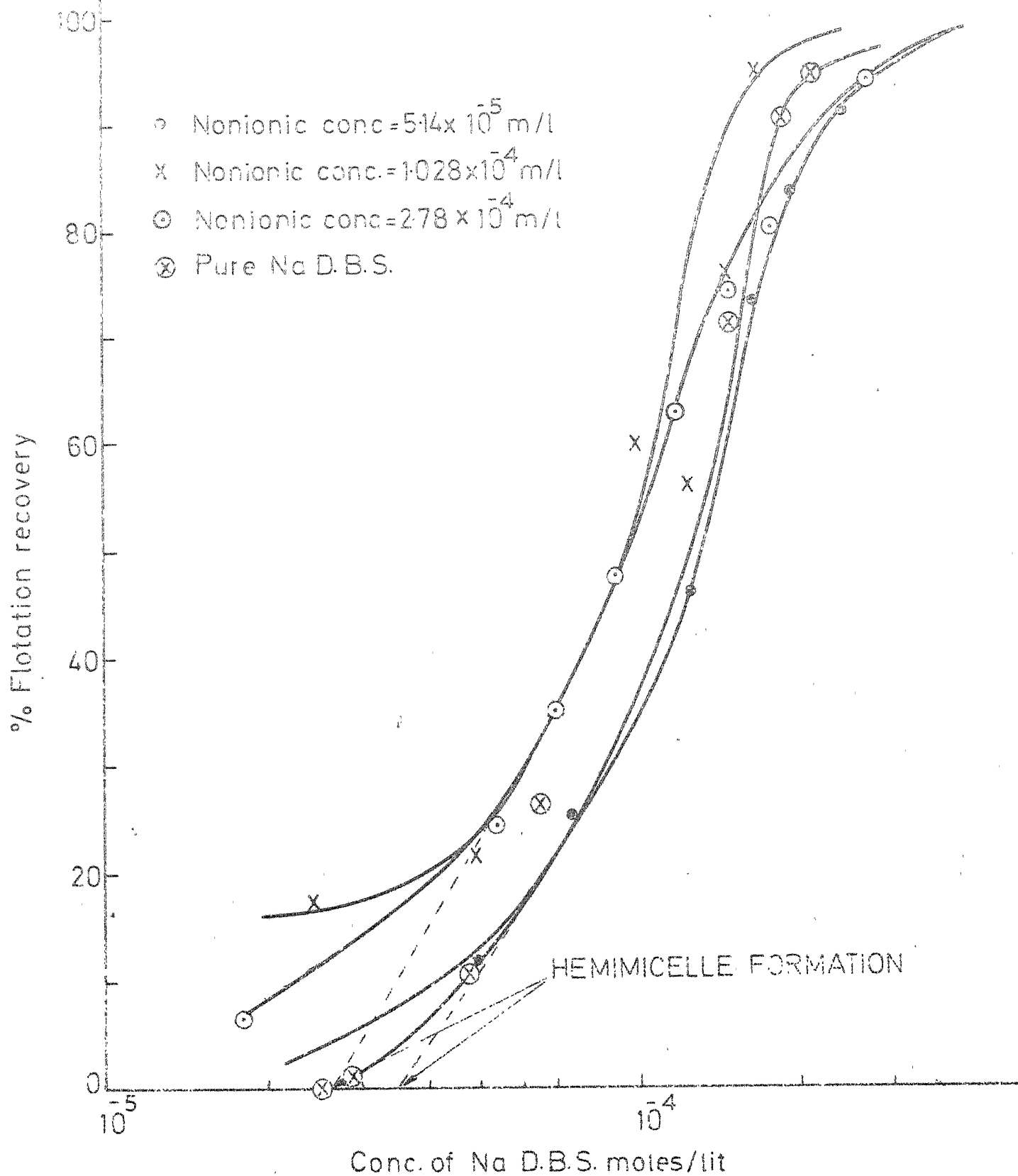


FIG.33 EFFECT OF NONIONIC (LOW MOL WEIGHT) ON FLOTATION RECOVERY - CALCITE FLOTATION BY Na-D.B.S.

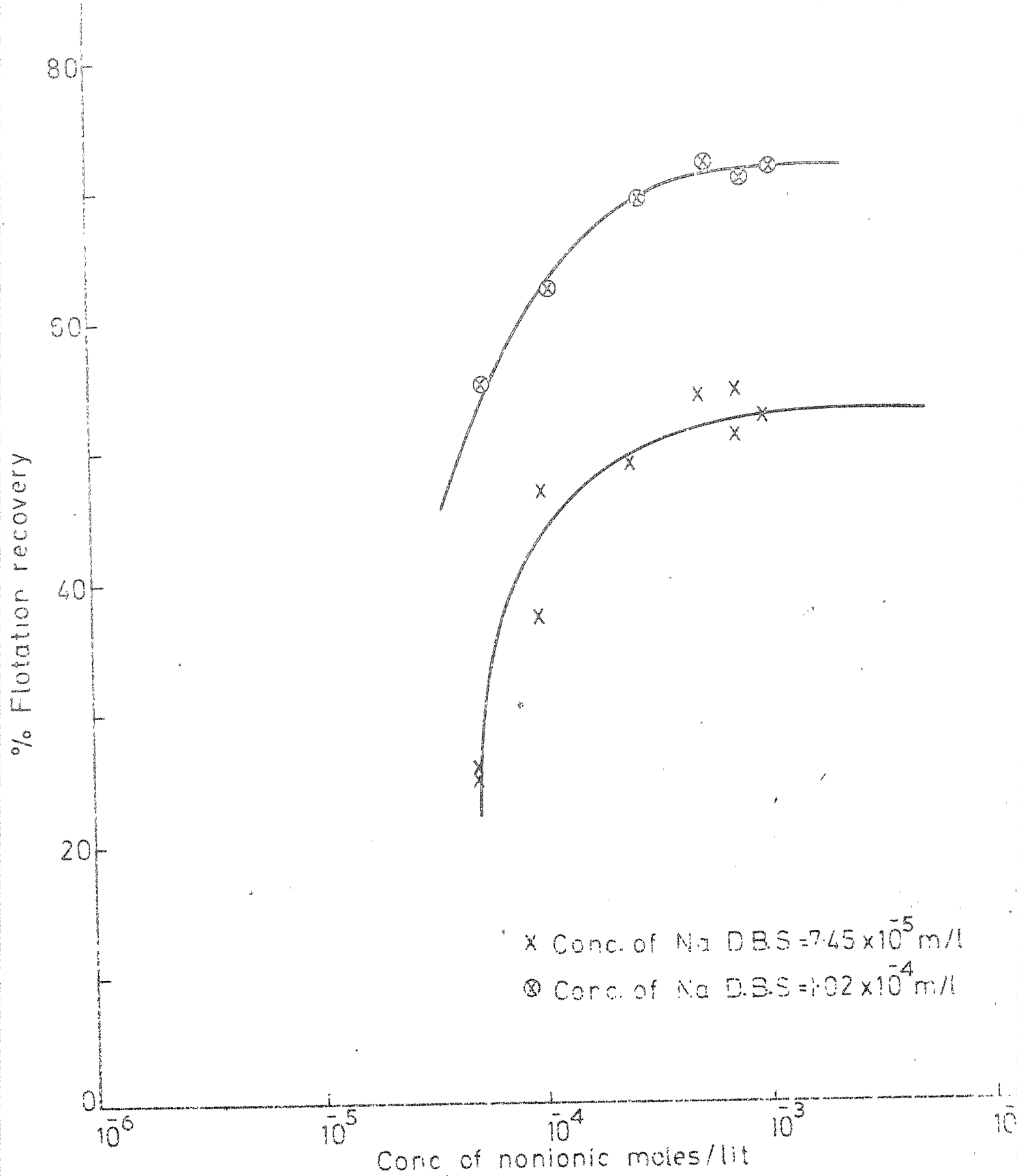


FIG 3.4 EFFECT OF LOW MOL. WEIGHT NONIONIC ON FLOTATION RECOVERY OF CALCITE

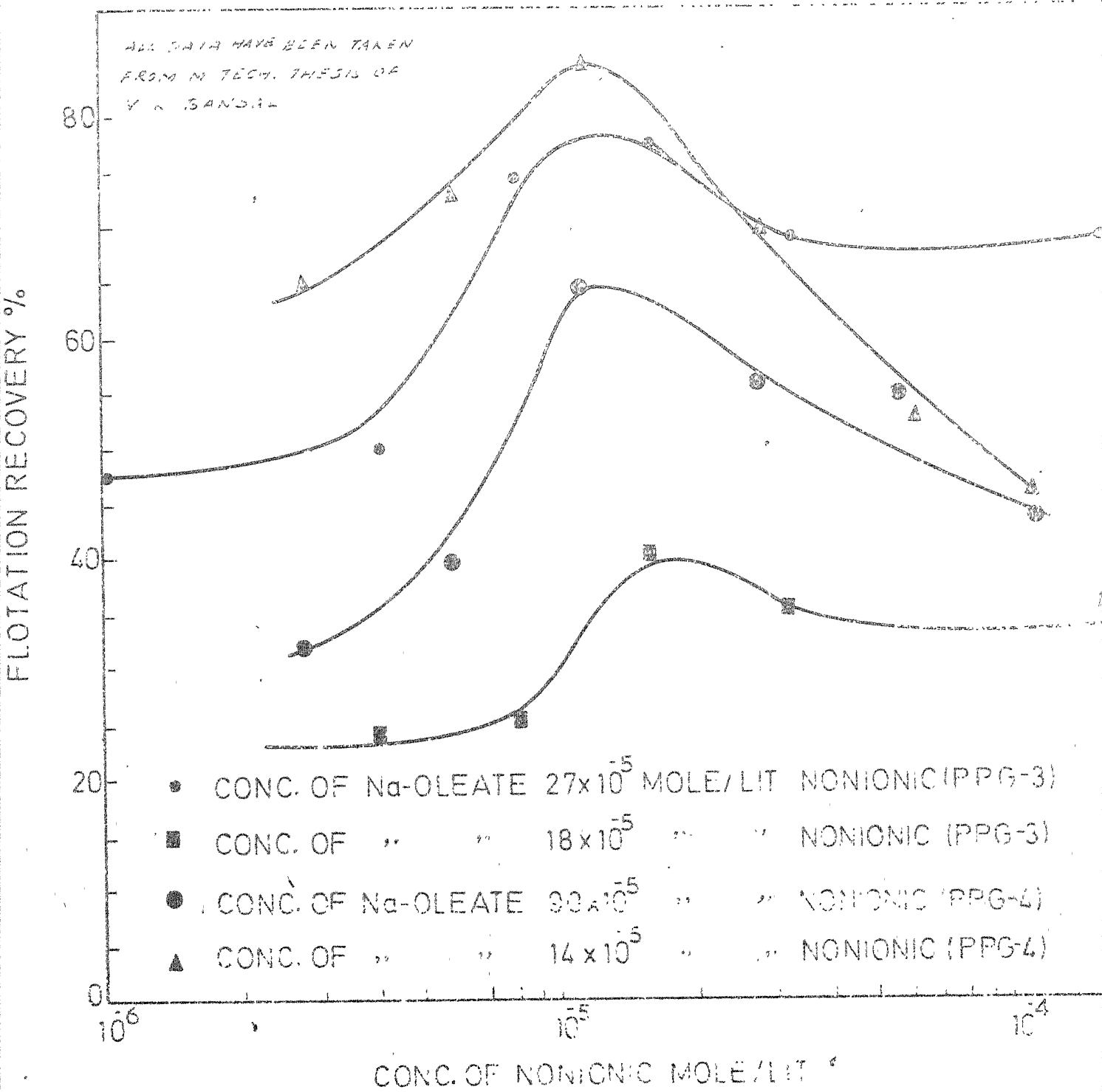


FIG. 3.5 EFFECT OF NONIONIC ON THE FLOTATION RECOVERY OF RUTILE

The effect of the frother (PPG) may be two-fold:

(1) it may increase frothing action, or (2) it may enhance the collection action. The enhancement of collection may be due to (1) increase in adsorption of Na-DBS and sodium oleate (collector) on the solid surface, or (2) concurrent adsorption of frother molecule on mineral surface. From Fig. 3.5, it is clear that the recovery of rutile decreases when the concentration of PPG (nonionic frother) increase above its cmc ( $2.0 \times 10^{-5}$  m/l). The decrease in flotation recovery of rutile at higher concentration of nonionics can be attributed to the mixed micellization of nonionics and sodium oleate. The mixed micelle thus formed would be a type of nonionic micelle with the oleate ions incorporated into nonionic micelle and causing a depletion of collector molecules from the bulk phase.

This type of observation is not observed in the case of calcite flotation. This might be due to a weaker interaction between Na-DBS (collector) and nonionic frothers, as compared to that between sodium oleate and nonionics. This point would be again discussed in the context of micellar studies. Thus the decrease in the concentration of collector molecule (Na-DBS) might be less as compared to sodium oleate during the formation of mixed micelle of collector and frother.

The interaction between collector and frother at liquid-solid-gas interface has also been studied by monitoring the

effect of frother on the contact angle established between rutile, sodium oleate solution, and air. For the measurement of contact angles, the captive bubble technique was used. The sodium oleate solution with different concentration of non-ionic frother was taken in a cuvette and a single crystal of rutile was submerged in it. Air bubbles were attached on the single crystal with the help of a bubble holder. The image of the bubble was projected on a flat paper surface, and the contact angles were measured by drawing tangents at the interface and measuring the angle in the aqueous phase between the tangent and the projected interline.

The results so obtained are shown in Fig. 3.6, which shows that the contact angle increases as the concentration of sodium oleate increases, and when the concentration of sodium oleate reaches  $10^{-4}$  m/l, the values of contact angle start falling. This decrease in contact angle beyond this concentration of sodium oleate can be attributed to the formation of a double layer after the monolayer coverage has been completed on the single crystal surface. The double layer formation will decrease the hydrophobicity of the single crystal which was obtained upto the monolayer coverage and thus will decrease the contact angle.

From Fig. 3.6 it is also clear that the effect of the frother (nonionic PPG-4) on the contact angle, if any, is not measurable (reading error is about  $2^\circ$  and reproducibility is



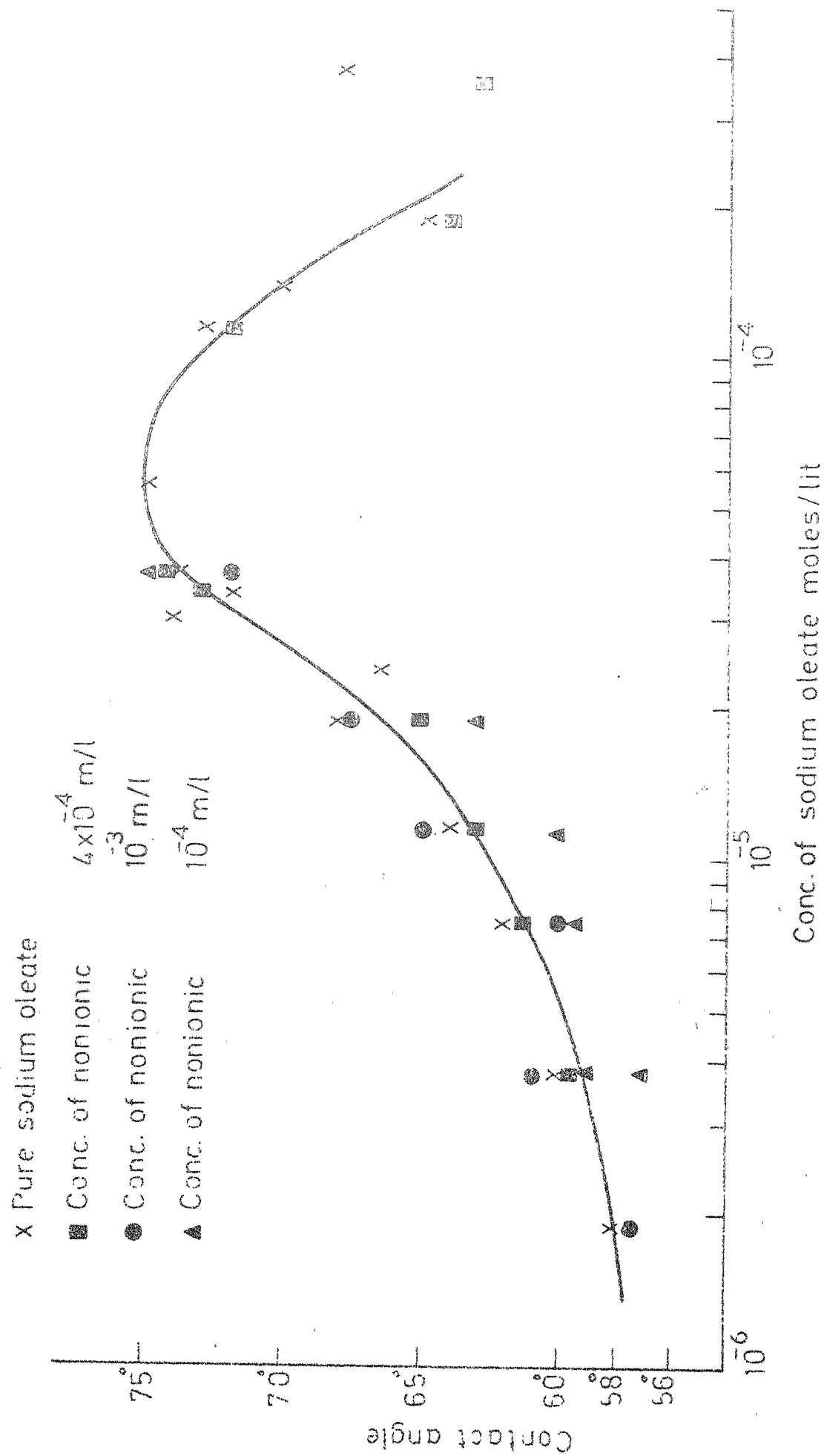


FIG.3.6 EFFECT OF HIGH MOLECULAR WEIGHT NONIONIC (PPG-4) ON CONTACT ANGLE SYSTEM Na-oleate - RUTILE-AIR

5 to 10 percent). The absence of any appreciable change in the contact angle on the addition of frother and the establishment of contact angle in sodium oleate solution alone can be used as an argument against the collector - frother interaction.

However, if the expression,

$$\cos \theta = \frac{\gamma_{a/s} - \gamma_{s/l}}{\gamma_{a/l}} \quad \text{is considered,}$$

where,

$\theta$  = contact angle,

$\gamma_{a/s}$  = interfacial energy between air-solid interface,

$\gamma_{s/l}$  = interfacial energy between solid-liquid interface,

$\gamma_{a/l}$  = interfacial energy between air-liquid interface,

then an addition to a collector solution of a frother which changes  $\gamma_{a/l}$  by a few dynes/cm should also cause a change in  $(\gamma_{a/s} - \gamma_{s/l})$  in order to keep  $\cos \theta$  constant. Therefore, the fact that frother does not affect the contact angles developed in collector solutions, is really an argument for the existence of collector - frother interaction, since a change in  $(\gamma_{a/s} - \gamma_{s/l})$  could be brought about only by the adsorption of frother or by augmenting collector adsorption on the solid surface. Such an argument was presented earlier by Leja (2).

### III.4 INTERACTION AT THE LIQUID-SOLID INTERFACE:

Interaction at liquid-solid interface has been studied by the effect of nonionics (frother) on the amount adsorbed of collector (sodium oleate) on rutile powder and vice versa. The effect of nonionics (frother) on the zeta-potential of rutile in the system rutile-sodium oleate has also been studied to establish the interaction between them.

#### III.4.1 Estimation of Adsorption of Sodium Oleate:

##### (a) Solution Method:

Finely divided rutile powder had to be used so that the difference in concentration of sodium oleate in aqueous solution before and after equilibration could be appreciable. The surface area of the rutile sample was determined by the p-nitrophenol method as suggested by Gilos (16). The surface area of the sample was found to be  $2.108 \times 10^4 \text{ cm}^2/\text{g}$ .

Solutions of sodium oleate were tagged with C-14  $\beta$ -active tracer. A constant ratio between the concentration of labelled and unlabelled oleic acid was maintained. For adsorption experiments, the solid sample (about 3 g) was equilibrated with sodium oleate solution at  $30 \pm 1^\circ\text{C}$  for 5 hrs. Supernatant solution was centrifuged to remove any suspended solid, and 2.0 ml of the clear solution was transferred to a specially prepared planchet having a cavity of the same volume and evaporated at  $40^\circ\text{C}$  for 10 hrs. in an oven. The radio-activity counting was done in a  $\beta$ -ray Geiger counter. The

adsorption magnitude was obtained from initial and equilibrium solute concentrations utilising a standard calibration curve. The adsorption data are shown in Fig. 3.7.

(b) Direct Estimation on Solid Method:

Although the previous method was superior to the conventional colorimetric method in estimating very low concentrations of sodium oleate, some reservation remained regarding the usefulness of adsorption data on finely divided particles in view of the coarseness of the particles used in flotation experiments. Active site surface concentration and hence collector adsorption density may not be identical in the latter sample.

Therefore, direct adsorption estimations on solid of coarser size were also made. Size distribution of -65 + 100 mesh rutile samples (as used for flotation) was obtained by microscopic observations and with this data, and assuming non-porosity of particles, the surface area of the sample was computed to be  $4.4 \times 10^2 \text{ cm}^2/\text{g}$ .

For calibration, 10 g of solid samples were mixed with known and variable quantities of sodium oleate in solution containing a fixed proportion of labelled chemical. Water was evaporated and 4.5 g of dried rutile containing proportionate and known amounts of sodium oleate on the surface were taken in the planchet for radio-activity counting. The count rate was related to the known adsorption density.

All data taken from Figure 3.7 in Tech. Thesis of W. K. Bumsol

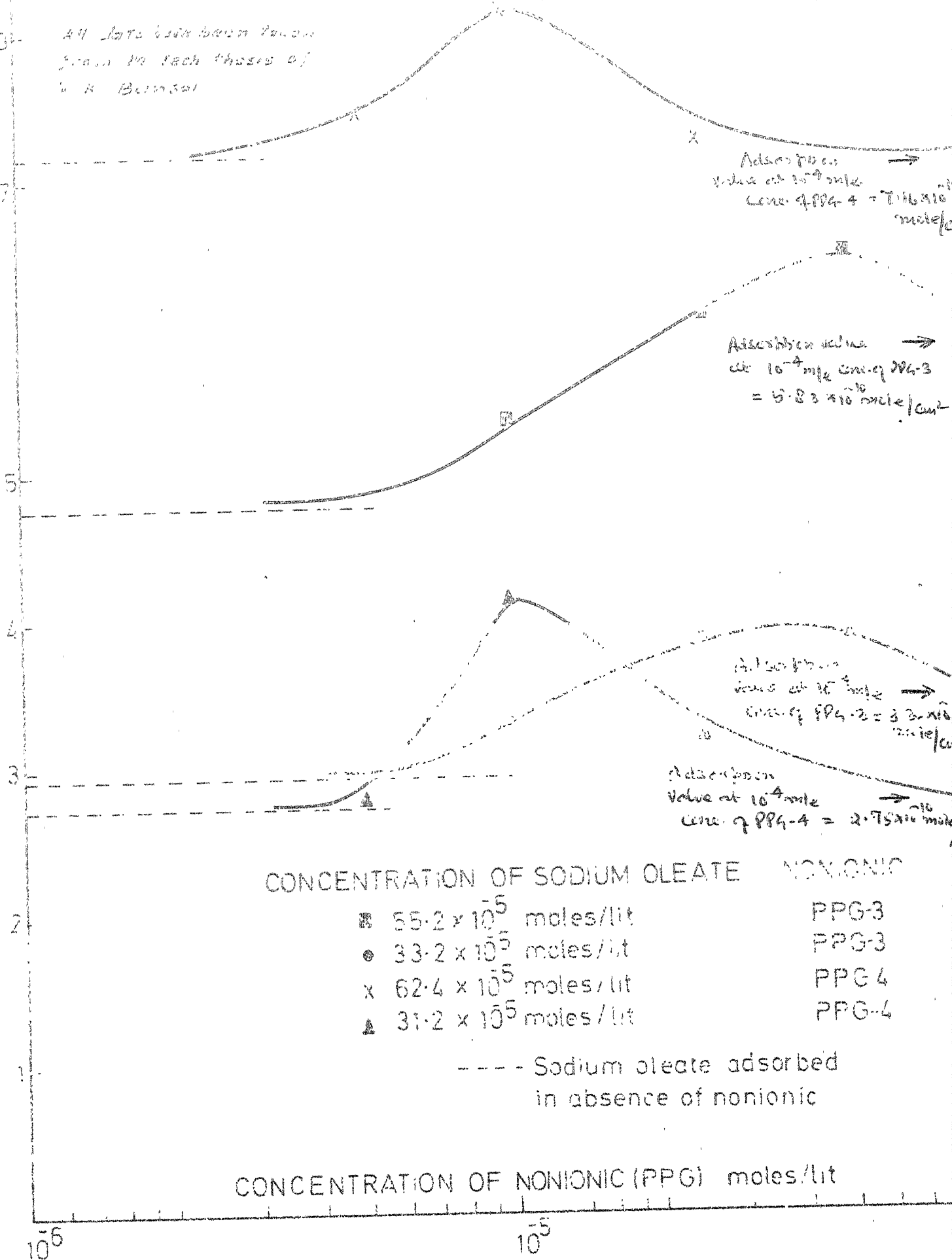


FIG. 3-7 EFFECT OF NONIONIC (PPG) ON ADSORPTION OF SODIUM OLEATE

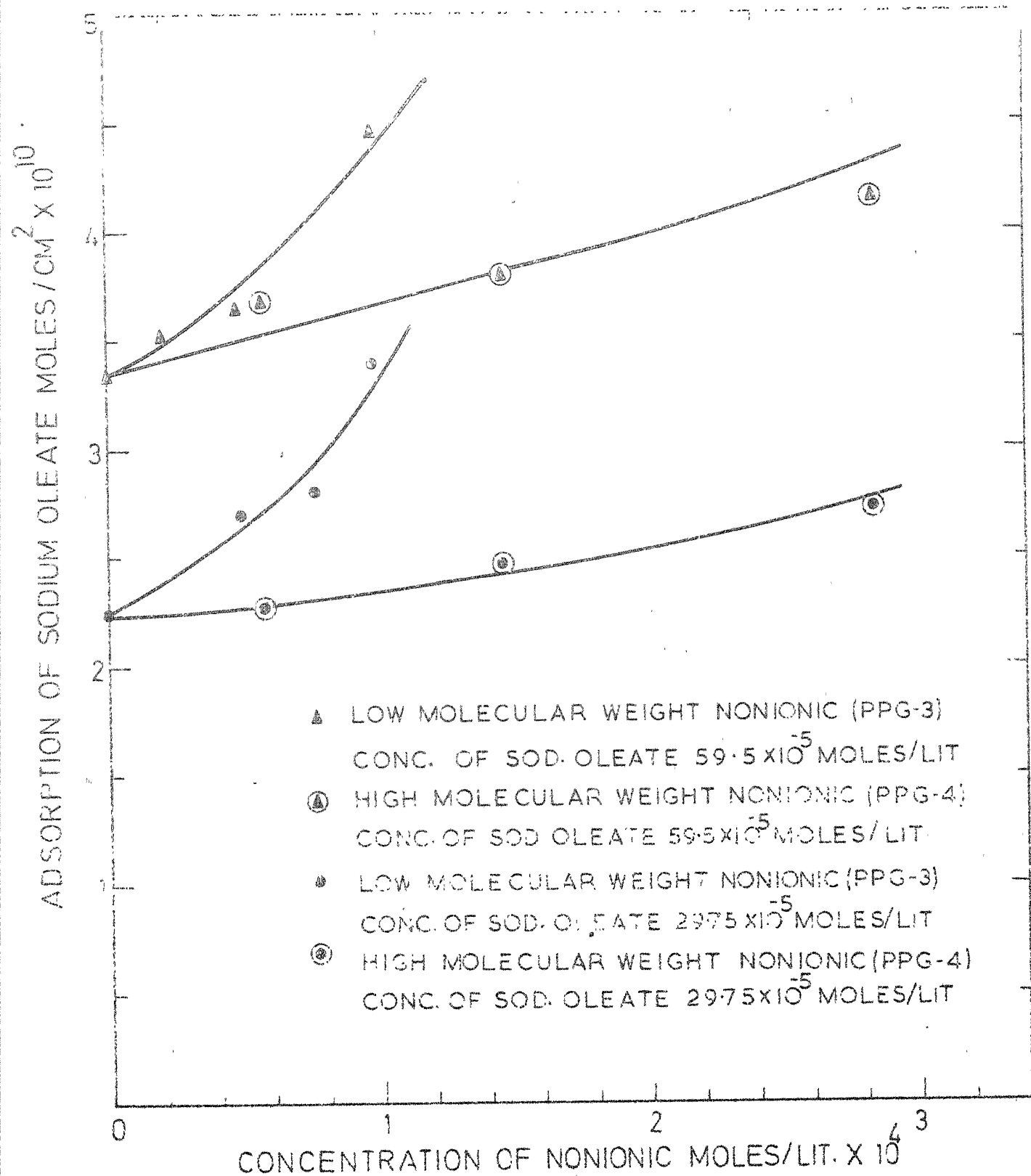


FIG. 3.8 EFFECT OF NONIONICS (PPG) ON ADSORPTION OF SODIUM OLEATE (DIRECT ESTIMATION ON SOLID METHOD)

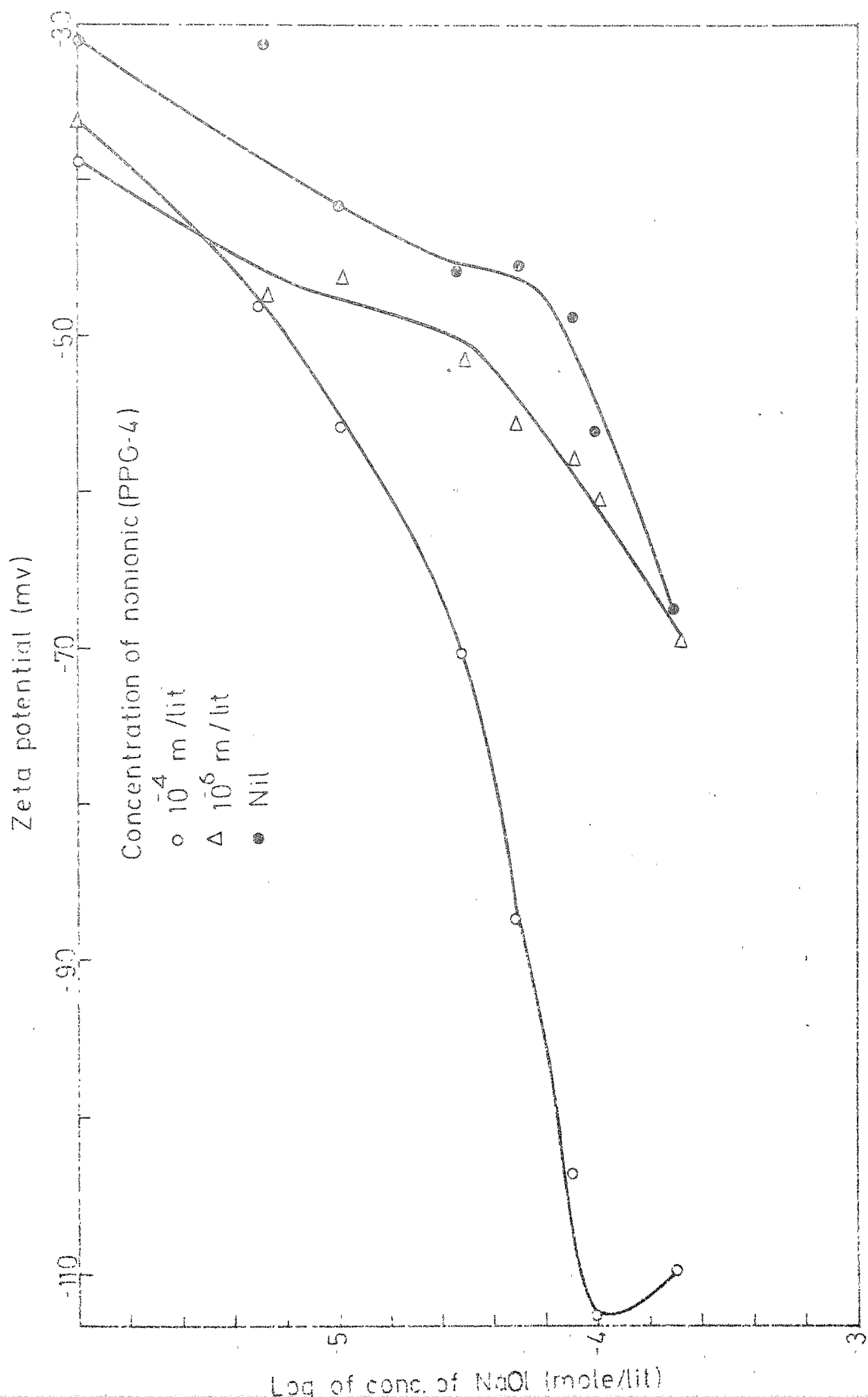


FIG 3-9 EFFECT OF CONCENTRATION OF SODIUM OLEATE & NONIONIC(PPG-4) ON ZETA POTENTIAL OF RUTILE

For adsorption determination, 10 g of sample was equilibrated with 10 ml of sodium oleate solution of known concentration, decanted and the rutile samples were washed with 10 ml. of double distilled water once. The samples were dried. After drying 4.5 g of sample was transferred to the planchet for counting. The adsorption of sodium oleate was calculated from the standard curve. The reproducibility of the experiments was about  $\pm 5$  percent.

The effects of variable concentrations of purified nonionics on the adsorption of sodium oleate were studied at different constant sodium oleate concentration and the data so obtained are shown in Fig. 3.8.

#### III.4.2 ZETA POTENTIAL DETERMINATION:

Zeta potential values of rutile mineral surface in presence of various concentrations of sodium oleate and purified nonionic (PPG-4) were computed from the electrophoretic mobility of solid particles. Electrophoretic mobility measurements were carried out in a Numinco Model MLC-1201 Mass Transport Analyser. The data are plotted in Fig. 3.9.

#### III.4.3: Adsorption of Non-ionic Frothers on Solid Surface:

Gatewood and Graham (17) have provided a colorimetric method for estimation of polypropylene oxide type of nonionics. The method consists in interaction of the above kind of



nonionic with 2,4 dinitrophenyl hydrazine in acetone-free alcoholic solution (water bath refluxing for 15 min.) and development of colour with 10% alcoholic KOH in ice-bath temperature. The peak of colour intensity was found to be at 535  $\mu$ . The calibration curve for both the nonionics (on molar basis) was found to be identical. Colour intensity was found to be significant and measurable only when the nonionic concentration exceeded  $10^{-3}$  m/l.

Weighed and dry solid samples (about 5 g) were equilibrated with nonionic solution with or without sodium oleate. After equilibration, the supernatant solution was removed. From this, sodium oleate was abstracted by more than equivalent quantity of Dowex 1-X8 anion exchange resin of 2.1 meq/g. ion exchange capacity. After removal of sodium oleate, the non-ionic solution was evaporated to a suitable higher concentration so that the colorimetric technique could be employed.

In flotation experiments, nonionic concentration has been around (usually less than)  $10^{-5}$  m/l. Colorimetric technique as described above is not feasible for such a dilute solution unless this is subjected to evaporation to obtain more than 100 fold increase in concentration which is tedious. Therefore, the original nonionic concentration had to be kept at higher values. There was no adsorption of nonionic frother on rutile in absence of sodium oleate.

nonionic with 2,4 dinitrophenyl hydrazine in acetone-free alcoholic solution (water bath refluxing for 15 min.) and development of colour with 10% alcoholic KOH in ice-bath temperature. The peak of colour intensity was found to be at 535 m $\mu$ . The calibration curve for both the nonionics (on molar basis) was found to be identical. Colour intensity was found to be significant and measurable only when the nonionic concentration exceeded  $10^{-3}$  m/l.

Weighed and dry solid samples (about 5 g) were equilibrated with nonionic solution with or without sodium oleate. After equilibration, the supernatant solution was removed. From this, sodium oleate was abstracted by more than equivalent quantity of Dowex 1-X8 anion exchange resin of 2.1 meq/g. ion exchange capacity. After removal of sodium oleate, the non-ionic solution was evaporated to a suitable higher concentration so that the colorimetric technique could be employed.

In flotation experiments, nonionic concentration has been around (usually less than)  $10^{-5}$  m/l. Colorimetric technique as described above is not feasible for such a dilute solution unless this is subjected to evaporation to obtain more than 100 fold increase in concentration which is tedious. Therefore, the original nonionic concentration had to be kept at higher values. There was no adsorption of nonionic frother on rutile in absence of sodium oleate.

Nonionic adsorption was noticed in certain concentration ranges of sodium oleate as reported in Table 3.1.

Table 3.1

Adsorption of Nonionic Frother on Rutile Surface

Concentration of sodium oleate m/l	Concentration of nonionic m/l	Adsorption of nonionic moles/cm <sup>2</sup>
PPG-4 sample		
Nil	$5.4 \times 10^{-3}$	Nil
$3.626 \times 10^{-4}$	$5.4 \times 10^{-3}$	$8.0 \times 10^{-10}$
PPG-3 sample		
Nil	$4.51 \times 10^{-3}$	Nil
$3.58 \times 10^{-4}$	$4.51 \times 10^{-3}$	$1.1 \times 10^{-10}$
$7.16 \times 10^{-4}$	$4.51 \times 10^{-3}$	$2.45 \times 10^{-9}$

#### III.4.4 Infra-red Analysis:

We next attempted to obtain evidence of adsorption of sodium oleate and nonionics on rutile surface by infra-red spectral studies using a Perkin-Elmer model 137 I.R. spectrophotometer. The infra-red absorption spectral charts for sodium oleate, nonionics and rutile were obtained separately. The peak at  $1545 \text{ cm}^{-1}$  in case of sodium oleate is the characteristic peak for the anti-symmetrical vibration of the  $\text{C} = \text{O}$  group. The ether  $\text{C}-\text{O}-\text{C}$  group in the case of nonionics is represented by the peak at  $1123-1100 \text{ cm}^{-1}$ . None of these

peaks were observed on the rutile surface after equilibration of -300 mesh rutile powder with sodium oleate-nonionic solutions. The peaks were not revealed probably due to low magnitude of adsorption and removal of weakly adhering molecules during washing.

Viswanathan and Mazumdar showed (18) that rutile treated with sodium oleate solution gave I.R. adsorption peak at  $1510-1530\text{ cm}^{-1}$ , characterising oleate anion-metal cation surface product. This could not be confirmed in the present series of experiments.

### III.5 DISCUSSION:

The adsorption data obtained by the solution method (Fig. 3.7) clearly reveal augmentation of collector adsorption on the rutile surface with increase in nonionic frother concentration. Since very finely divided rutile powder was used for the solution method adsorption experiments, some doubt remained as to whether these data are relevant in explaining flotation behavior of coarse particles. Adsorption experiments with coarse particles by 'direct estimation on solid method' revealed similar trends regarding the effect of nonionic frothers in augmenting collector adsorption on rutile (Fig. 3.8). The data given in Fig. 3.8 are not strictly comparable with Fig. 3.7, since the coordinates represent initial concentration, and equilibrium concentration values could differ between 'solution method'.

peaks were observed on the rutile surface after equilibration of -300 mesh rutile powder with sodium oleate-nonionic solutions. The peaks were not revealed probably due to low magnitude of adsorption and removal of weakly adhering molecules during washing.

Viswanathan and Mazumdar showed (18) that rutile treated with sodium oleate solution gave I.R. adsorption peak at  $1510-1530\text{ cm}^{-1}$ , characterising oleate anion-metal cation surface product. This could not be confirmed in the present series of experiments.

### III.5 DISCUSSION:

The adsorption data obtained by the solution method (Fig. 3.7) clearly reveal augmentation of collector adsorption on the rutile surface with increase in nonionic frother concentration. Since very finely divided rutile powder was used for the solution method adsorption experiments, some doubt remained as to whether these data are relevant in explaining flotation behavior of coarse particles. Adsorption experiments with coarse particles by 'direct estimation on solid method' revealed similar trends regarding the effect of nonionic frothers in augmenting collector adsorption on rutile (Fig. 3.8). The data given in Fig. 3.8 are not strictly comparable with Fig. 3.7, since the coordinates represent initial concentration, and equilibrium concentration values could differ between 'solution method'.

involving fine particles and 'direct method' involving coarse particles. The discrepancy could also be due to (a) errors in measurement of surface area of the samples and (b) possible higher surface density of adsorption sites in the case of finer samples as used in the solution method.

Adsorption values as obtained by different methods and using samples of different specific surface area are of the same order of magnitude. In both cases, the beneficial effects of nonionic frothers in improving collector adsorption on rutile are clearly manifest. This is also confirmed by the zeta-potential data presented in Fig. 3.9. Increasing nonionic concentration makes negatively charged rutile particles even more negatively charged. This process is augmented by the presence of nonionic frother indicating heightened adsorption of collector anion.

The beneficial effect as described above is possibly due to co-adsorption of collector and frother (nonionic) molecules on the solid surface. Estimation of nonionic frother in dilute solution by the known colorimetric method is difficult and tedious. Thus, adsorption of nonionic frothers on rutile from dilute solutions could not be confirmed. At a concentration slightly above  $10^{-3}$  m/l, nonionic frothers are found to be adsorbed in presence of collector, (Table 3.1). There is no adsorption in absence of collector,

or if the collector concentration is too low. This seems to be a typical case of synergism between collector and frother molecules - each inducing adsorption of the other on the solid surface. Nonionic molecules are possibly adsorbed in between collector hydrocarbon chains anchored to the solid surface. The presence of adsorbed nonionic molecules in its turn induces further adsorption of collector.

Experimental data(11, Fig.3.7) at higher concentrations of nonionics (concentration above their cmc) also shows that the adsorption of sodium oleate on rutile decreased. The technological implication of this result is that a high concentration of frother is to be avoided just as high collector dosage is known to be harmful.

Leja and Nixon (14) observed the deleterious effect of excessive addition of poly-oxy ethylene type of frother. They postulated that excessive addition of nonionic increases collector adsorption to the extent of double layer formation at the mineral surface rendering it less hydrophobic. The adsorption data obtained in the present system (Fig. 3.7) are however not in agreement with Leja and Nixon's postulate. At high sodium oleate concentration, adsorption of this collector (Na-Ol) on rutile is decreased if nonionic concentration approaches or exceeds its cmc. Thus the flotation and adsorption data for higher nonionic concentration are

better explained by the postulate of mixed micellization and depletion of collector molecules from the bulk phase.

The binding force between the adsorbed collector and frother molecules is possibly of the van der Waal type between the hydrophobic chain of collector and nonionic molecules. Cohesion strength of the collector film on the mineral surface is enhanced due to rise in association energy and improves the adsorption condition as demonstrated in the case of n-alkane addition to the quartz n-alkyl ammonium salt system (19). There may be additional hydrogen bond linkages between the electronegative atoms in the polar parts of the collector and frother molecules. Sandwiched nonionic molecules decreases the force of repulsion between adsorbed collector anions.

The adsorption density of the ions in the Stern layer is given by

$$\Gamma_i = 2rC \exp \left( - W_i/kT \right)$$

where  $\Gamma_i$  is the adsorption density in mole/cm<sup>2</sup>, r the radius of adsorbing ion, C the bulk concentration of the collector in mole/ml, k the Boltzmann constant, T the temperature in degrees Kelvin and  $W_i$  is the work required to bring an ion from the bulk of the solution to the double layer. Using the adsorption data obtained through the 'solution method',



the value of  $W_i$  for oleate ion to be adsorbed on rutile has been computed. This is of the order of  $-10$  kT in absence of nonionic, and there is an increase of about  $.2$  kT in the absolute magnitude of  $W_i$  in presence of optimum proportions of nonionic frothers.

To summarise, clear evidence has been obtained regarding the interaction of collector and frother molecules in a rutile flotation system -both in the solid-liquid as well as the liquid-gas interface. Increasing nonionic frother concentration increases flotation recovery as well as collector adsorption density on the rutile surface. As the nonionic concentration approaches or exceeds its cmc, the above two parameters decrease, probably due to abstraction of collector ions from the bulk to the mixed micelle phase.

Below the cmc of nonionic frother, there is augmentation of collector adsorption with concurrent adsorption of non-ionic frother molecules on the solid surface. Similar synergistic effect is noticed in the liquid-gas interface in which not only frother molecules but also the collector molecules get adsorbed through mutual interaction. Somasunderan and Fuerstenau (20) had postulated earlier that collector species are adsorbed both at the solid-liquid and liquid-gas interface. The collector adsorbed at the liquid-gas interface, that is, at the interface of the gas bubble, facilitates,

**CENTRAL INDEX**

Acc. No. **A 45527**

reduction of the time necessary for the formation of the solid-gas interface, since the collector ions are now carried to the solid surface by the bubble. The amount of collector that could be transferred to the solid-gas interface from the bubble surface upon contact is significantly higher than that which could be transferred from the solid-liquid interface.

Marcus and Sandvik (21) also proposed that under normal flotation conditions the adsorption of surface-active collector on solid surfaces is governed, to a large extent, by a transfer of collector from the gas-liquid interfaces to the solid surfaces. Thus the adsorption densities found in solid-liquid system are often not representative for solid-liquid-gas system. Transfer of collector as well as frother molecules from the liquid-gas interface to the solid surface during the establishment of the three phase contact can be justifiably proposed. This constitutes an additional step of collector-frother interaction.

Thus the conventional notion that collector is active at the solid-liquid interface and frother at the liquid-gas interface only, is over-simplistic. Much of the phenomenon of mineral particle-air bubble contact in a flotation system is due to mutual interaction and co-adsorption of collector and frother molecule at the different interfaces.

## REFERENCES

1. Leja, J., and Schulman, J.H.  
Flotation Theory: Molecular Interaction Between Frothers and Collectors at Solid-Liquid-Air Interfaces (1954), Trans. AIME, Mining Engineering, 6, 221-228.
2. Leja, J.  
Interaction at Interfaces in Relation to Froth Flotation (1957), Proc. 2nd. Int. Congr. Surf. Activity, Butterworth, London, 3, 273-295.
3. Leja, J., and Schulman, J.H.  
Flotation Theory: Molecular Interactions Between Frothers and Collectors at Solid-Liquid-Air Interfaces (1954), Trans. Am. Inst. Min. Engrs., 199, 221-228.
4. Fuerstenau, D.W., and Yamada, B.J.  
Neutral Molecular Association in Flotation (1962), Trans. Am. Inst. Min. Engrs., 223, 50-52.
5. Lukki, J., and Laskowski, J.  
On the Dynamic Effect of Frother-Collector Joint Action in Flotation (1971), Trans. Inst. Min. Met., (Section C), 80, C174-180.
6. Plaksin, I.N., Khazinskaya, G.N., and Maksimore, D.V.  
On Joint Action of Collectors and Frothers (1960), Obogaschenic poleznykti iskopaemykh, Izd. Akad. Nauk. URSS, Moscow, (Russian Text), 60.
7. Mukai, S., Wakamatsu, T., and Takahashi, K.  
Mutual Interaction Between Collector and Frothers in Flotation (1972), Memoirs of the Faculty of Engineering, Kyoto University, 34, 279-288.
8. Zembala, M., and Pomianowski, A.  
Adsorption of Flotation Frothers on a Surface of Mercury (1970), Paper Presented at the 9th Symposium on Physicochemical Problems of Mineral Processing, Gliwice (Gliwice: Silesian University of Technology) (Polish Text).

9. Lekki, J., and Laskowski, J.  
A New Concept of Frothing in Flotation System and  
General Classification of Flotation Frothers  
(1975), Eleventh Inter. Miner. Process. Congr., Cagliari,  
Preprint 15.
10. Doron, A., Vargas, D., and Goddard, J.  
Nonionic Surfactants as Flotation Collectors.  
(1975), Trans. Inst. Min. Metall., (Section C), 84, C 34-37.
11. Bansal, V.K., and Biswas, A.K.  
Collector-Frother Interaction at Different Interfaces  
in a Flotation System  
(1975), Trans. Inst. Min. Metall., (Section C), 86,  
C 131-135.
12. Mukherjee, P.  
The Nature of the Association Equilibria and Hydrophobic  
Bonding in Aqueous System of Association Colloids  
(1967), Adv. Colloid. Interf. Sci., 1, 241-245.
13. Corkill, J.M., Goodman, J.F., and Harrold, S.P.  
Thermodynamics of Micellization of Nonionic Detergents  
(1964), Trans. Farad. Soc., 60, 202-207.
14. Leja, J., and Nixon, J.C.  
Ethylene Oxide and Propylene Oxide Compounds as  
Flotation Reagents  
(1957), 2nd. Inter. Congr. Surf. Activity, Butterworth  
Scientific Publication, 297-307.
15. Bansal, V.K.  
Collector-Frother Interaction  
(1971), M.Tech. Thesis, Indian Institute of Technology,  
Kanpur, India, Figs. 11, 12 and 13.
16. Giles, C.H., and Nakhwa, S.N.  
The Measurement of Specific Surface Areas of Finely  
Divided Solids by Solution Adsorption  
(1962), J. Appl. Chem., 12, 266-273.
17. Gatewood, L. Jr., and Graham, H.D.  
A Spectrophotometric Method for the Detection and  
Quantitative Determination of Polyoxyethylene Surface  
Active Agents  
(1961), Anal. Chem., 33, 1393-1396.

18. Viswanath, K.V., and Majumdar, K.K.  
Collector-Regulator Interactions in the Flotation of  
Beach Minerals Under Conditions of Soap Flotation  
(1973), Trans. Indian Inst. Met., 26(1), 55-60.
19. Schubert, H. and Schneider, W.  
Role of Non-Polar Groups Association in Collector  
Adsorption  
(1963), 8th Int. Min. Process. Congr. Proceedings  
(Leningrad), 315-324, Preprint 5-9.
20. Somasundaran, P., and Fuerstenau, D.W.  
On Incipient Flotation Conditions  
(1968), Trans. Am. Min. Engrs., 241, 102-104.
21. Marcus, D., and Sandvik, K.L.  
Adsorption of Anion on Quartz Through Bubble Interaction  
(1968), Trans. Inst. Min. Metall., (Section C), 77  
C 61-64.

## CHAPTER IV

### CONDUCTIVITY MEASUREMENT OF COLLECTOR-FROTHER INTERACTION

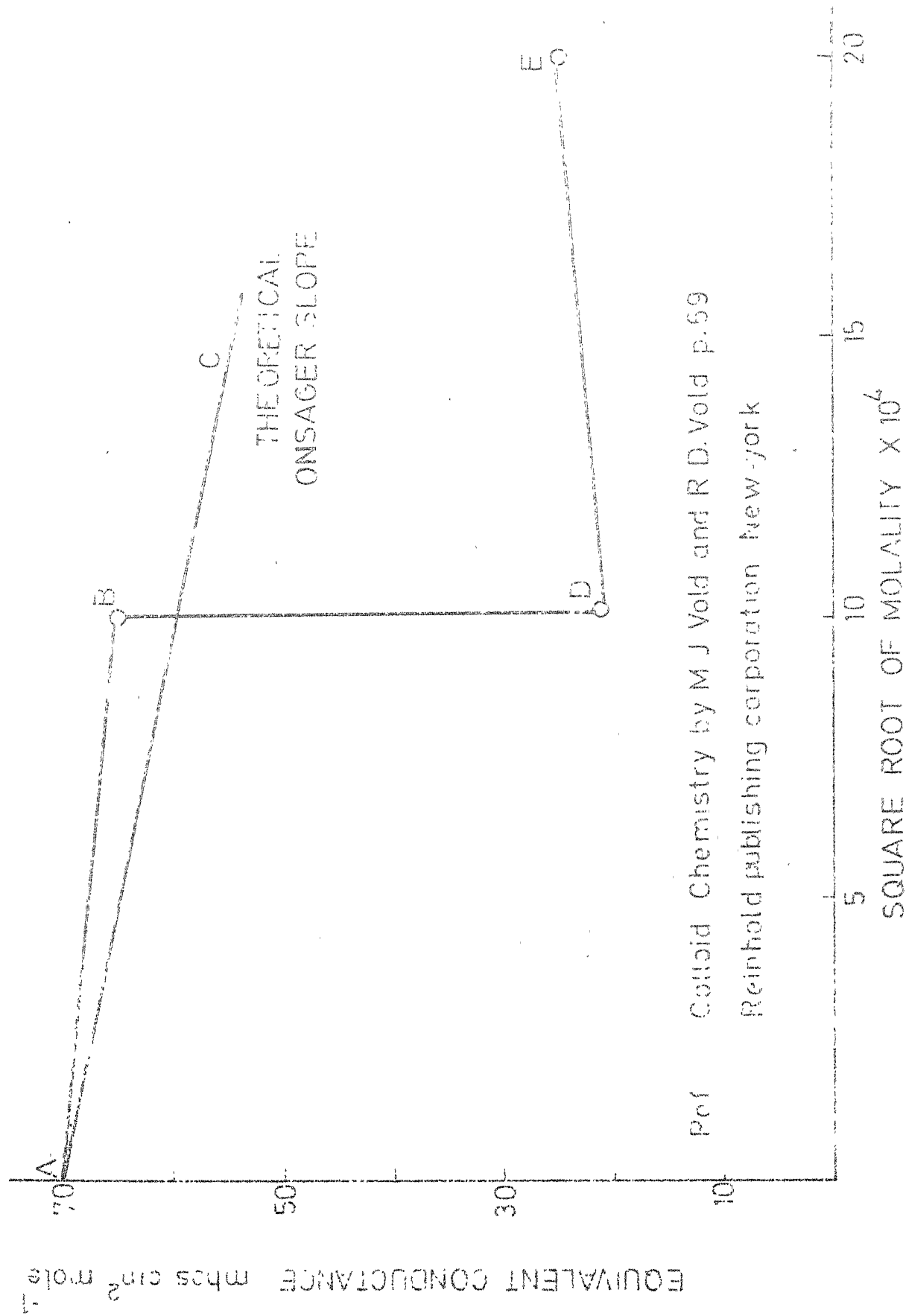
#### IV.1 INTRODUCTION:

The electrical conductivity of a solution is due to the movement of the charged species of different kinds present in the solution. It is measured in a conductivity cell with electrodes of suitable area a suitable distance apart, and the values so obtained may be used to calculate equivalent conductance ( $\Lambda$ ) by the formula  $\Lambda = 1000 k/c$  where  $k$  is specific conductance,  $c$  is concentration in moles/lit.  $\Lambda$  is the conductivity that would have been observed if the electrodes had been one cm apart, and large enough area to have between them a volume of solution sufficient to contain one equivalent of solute.

The variation of equivalent conductance of strong uni-univalent electrolytes is given by the Onsager relation;

$$\Lambda = \Lambda_0 - (\Lambda_0 A + B) \sqrt{c}$$

where  $\Lambda_0$  is the equivalent conductance of the solution at infinite dilution, and  $\Lambda$  the conductance at the concentration of  $c$  moles/lit. and  $A$  and  $B$  are constants for the system. The Onsager plot involves plotting  $\Lambda$  against  $\sqrt{c}$ , from where constants  $A$  and  $B$  can be evaluated. Useful information about



Ref Colloid Chemistry by M J Vold and R D. Vold p.69  
Reinhold publishing corporation New York

FIG.4.1 EQUIVALENT CONDUCTIVITY OF SODIUM DODECYL SULFATE IN WATER AS A  
FUNCTION OF THE SQUARE ROOT OF THE MOLALITY

the solution behaviour of surfactants in water has been obtained by such plots. As an example, we show the Onsager plot for the anionic detergent sodium dodecyl sulfate (SDS) in Fig. 4.1, taken from Vold and Vold (1). At very low concentrations, the conductance behavior of SDS follows the Onsager relation. At the critical concentration region BC, the equivalent conductance drops sharply, but finally, in fairly concentrated solutions, it again rises slowly. Such a behaviour is typical of systems that aggregate to form micelles and the critical micelle concentration (cmc) is deduced to be in the region BC. The cmc value for SDS is seen from Fig. 4.1 to be  $10^{-2}$  m/l.

Conductivity measurements were used by Biswas and Mukherjee (2) and also by Tokiwa and Moriyama (3) to study the effect of nonionic surfactants on the cmc values and conductance values of some anionic surfactants. Biswas and Mukherjee (2) used Lubrol W as the nonionic and Lissapol C as the anionic surfactant. From the conductance vs. concentration curves for the (Lissapol C:SDS) system they concluded that conductance increases with the addition of nonionics and the inflection point gradually tends to disappear. They explain that the role of the nonionic is not only to replace the  $\text{Na}^+$  ions in the micelle, thereby increasing the conductance in the micellar zone, but also to form mixed micelles even at lower concentrations. The effect of dodecyl polyoxyethylene



ethers ( $C_{12}$ POE) on the micellization of SDS has been studied by Tokiwa and Moriyama (3). They studied the effect by changing the mole ratio of SDS/ $C_{12}$ POE, and the chain length of POE, in order to study the mixed micelles formed by the ionic and nonionic components. It was found that at low concentrations of SDS, the specific conductance ( $k$ ) of the mixed solutions of SDS and  $C_{12}$ POE are smaller than those of the solutions of pure SDS alone. This was explained as due to the incorporation of the ionic components ( $DS^-$  ions) into the nonionic micelles. In the region of high concentrations of SDS, on the other hand, the values of  $k$  for the mixed solutions were found to be greater than those for the pure anionic solutions. It thus appears that equivalent conductance measurements would be of value in monitoring the interactions between nonionic (frother) and anionic (collector) surfactants, and in identifying the mixed micelles that may form in these binary aqueous solutions.

We have studied the effect of nonionics (PPG-3 and PPG-4) on the specific conductance value of sodium dodecylbenzene sulfonate (Na-DBS) solutions, both at pre- and post-micellar concentrations. The results are reported in this chapter. The value of  $\Lambda_0$  of Na-DBS in water alone, and in presence of nonionics at different concentrations, are also calculated by extrapolation to zero concentration. The effect of nonionics on the conductance of Na-oleate solution

was studied earlier by the author of this thesis and the gist of the results is mentioned in brief.

#### IV.2 EXPERIMENTAL:

The conductivity of aqueous solution of sodium dodecyl benzene sulfonate alone, and mixed with tetrapropylene and tripropylene glycol monomethyl ether (PPG-4 and PPG-3) was determined by using a conductivity cell of known cell constant and a conductance bridge, Metrohm AG konduktometer E 382, at  $35.0 \pm .1^\circ\text{C}$ . The water used in preparing the solutions had a specific conductance approximately of  $1.0 \times 10^{-6} \text{ ohm}^{-1} \text{ cm}^{-1}$ . Dye titration experiments to detect the micelle formation was used as per Corrin and Harkins (4).

#### IV.3 RESULTS AND DISCUSSION:

The specific conductance values of Na-DBS in aqueous solution in the absence, and in the presence of PPG-3 are shown in Figs. 4.2, and 4.3. The values were plotted as specific conductance vs. concentration of Na-DBS. The inflexion point so obtained is the cmc of Na-DBS and its value is about  $2 \times 10^{-3} \text{ m/l}$ . This value of cmc was also confirmed by the dye-titration method using Rhodamine 6G as a dye (4). Fig.4.2 shows that the specific conductance increases upon the addition of PPG-3, at concentrations of PPG-3  $10^{-5} \text{ m/l}$  and  $10^{-4} \text{ m/l}$ . The intrinsic contribution of PPG-3 to the conductivity is negligible since the specific conductance of nonionic solutions in the absence of Na-DBS is about  $2\text{-}3 \times 10^{-6} \text{ mhos}$ .

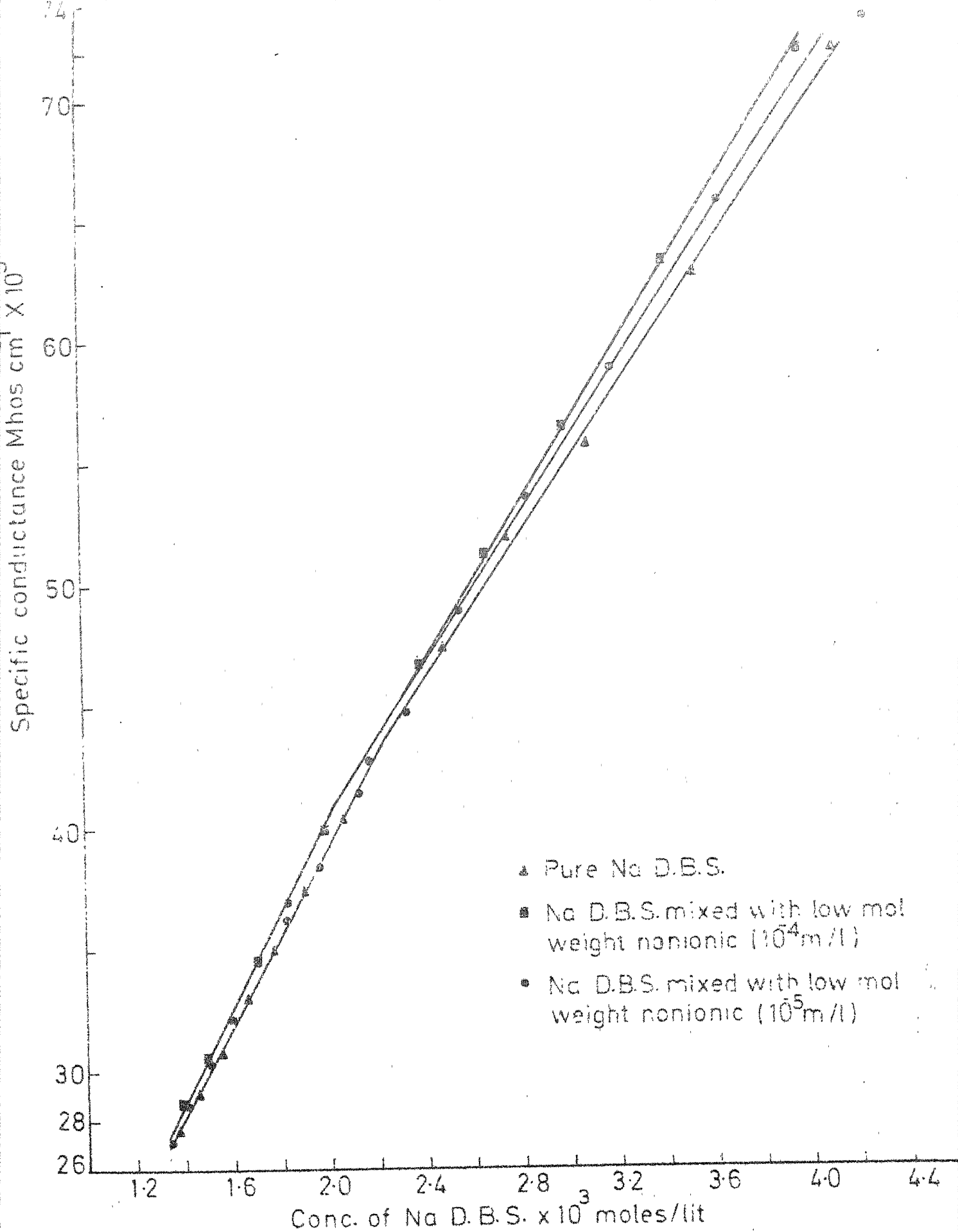


FIG.4.2 EFFECT OF LOW MOL.WEIGHT NONIONIC ON SPECIFIC

Specific conductance  $\text{Mhos cm}^{-1} \times 10^5$

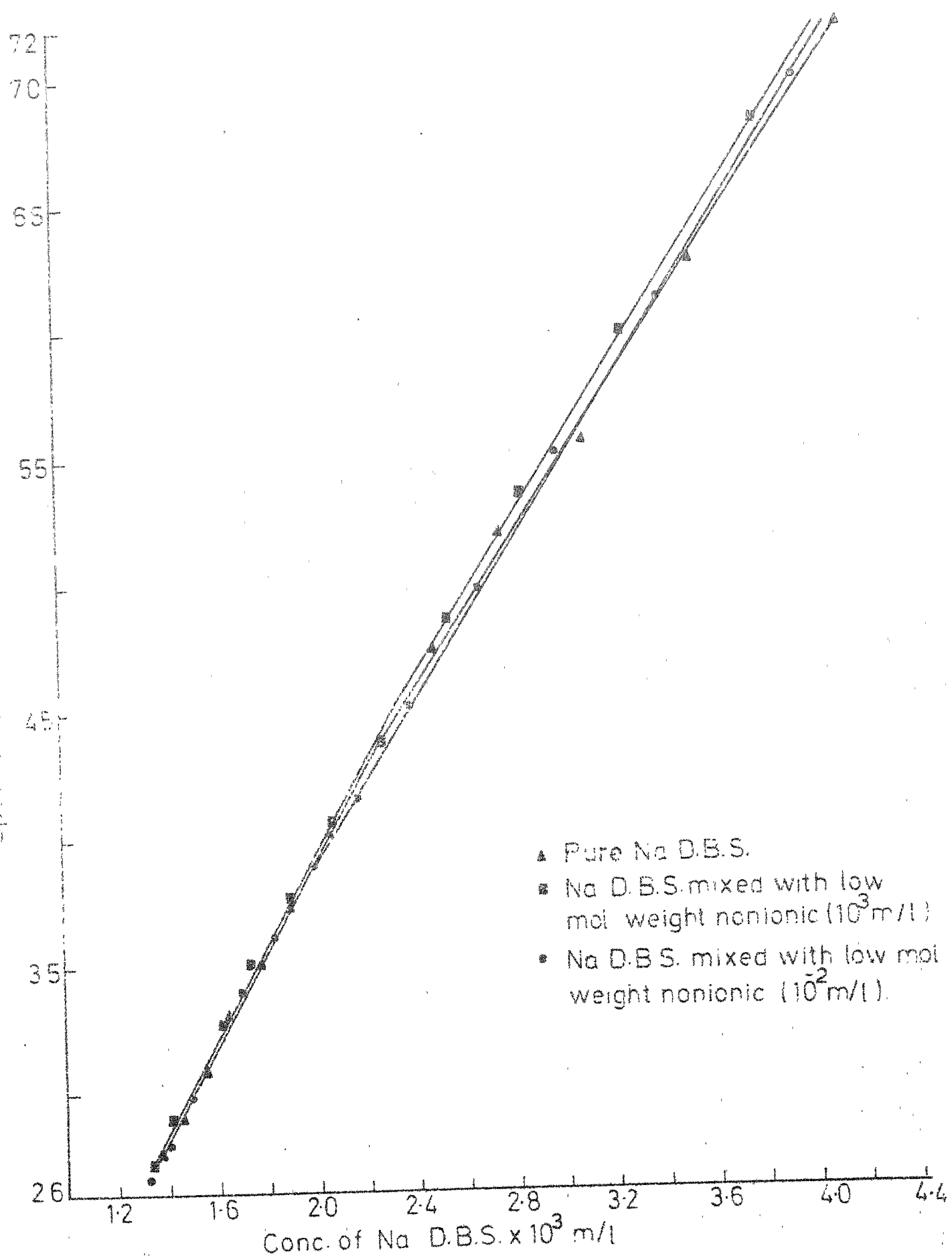


FIG. 4.3. EFFECT OF LOW MOL. WEIGHT NONIONIC ON SPECIFIC

- NaDBS Alone
- CONC. OF PPG-3  $10^{-5}$  m/l
- ▲ CONC. OF PPG-3  $10^{-4}$  m/l
- CONC. OF PPG-3  $10^{-3}$  m/l
- ⊙ CONC. OF PPG-3  $10^{-2}$  m/l

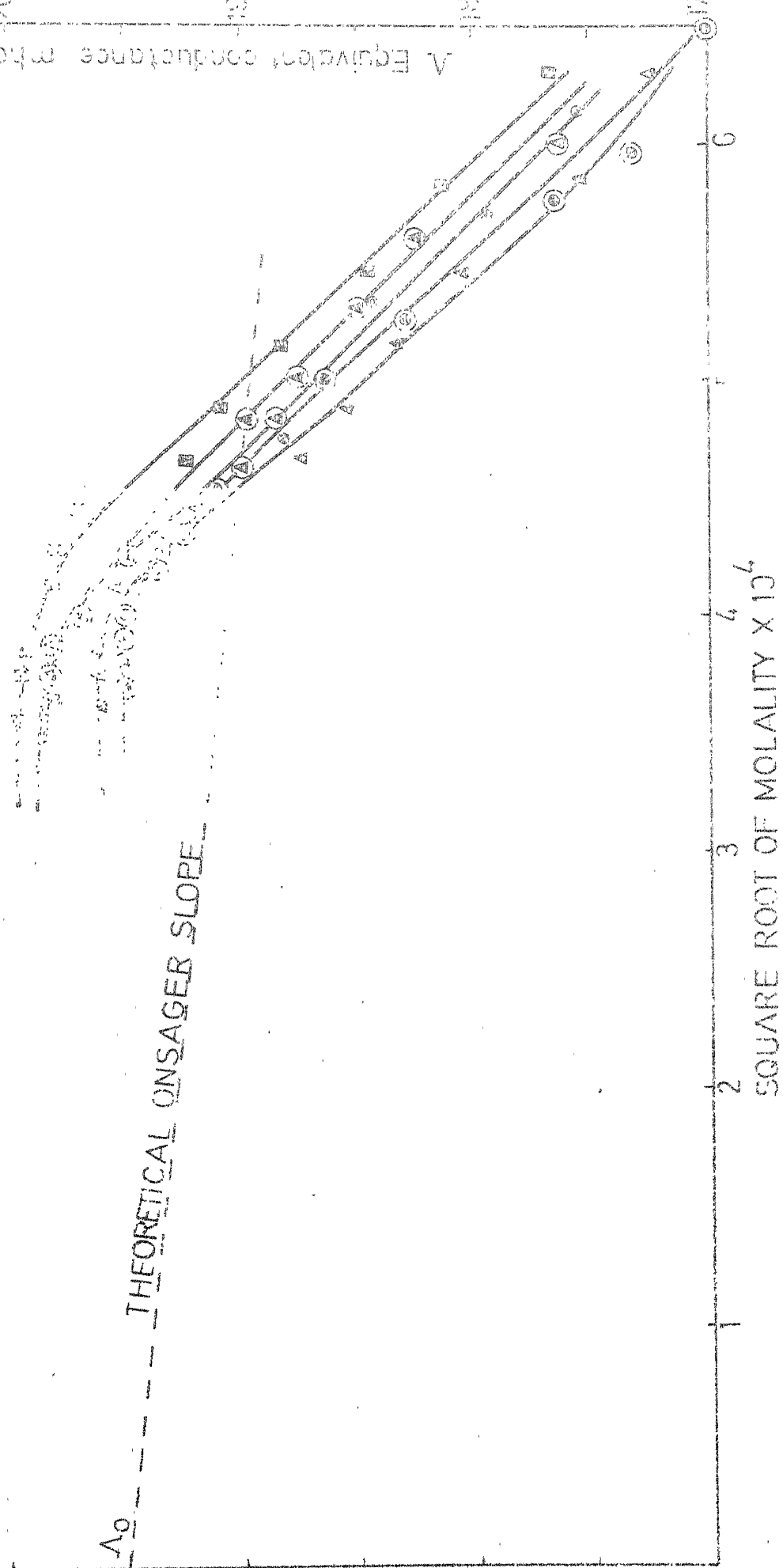


FIG 44. EFFECT OF LOW MOLECULAR WEIGHT NONIONIC (PPG-3) ON EQUIVALENT CONDUCTANCE OF NaDBS

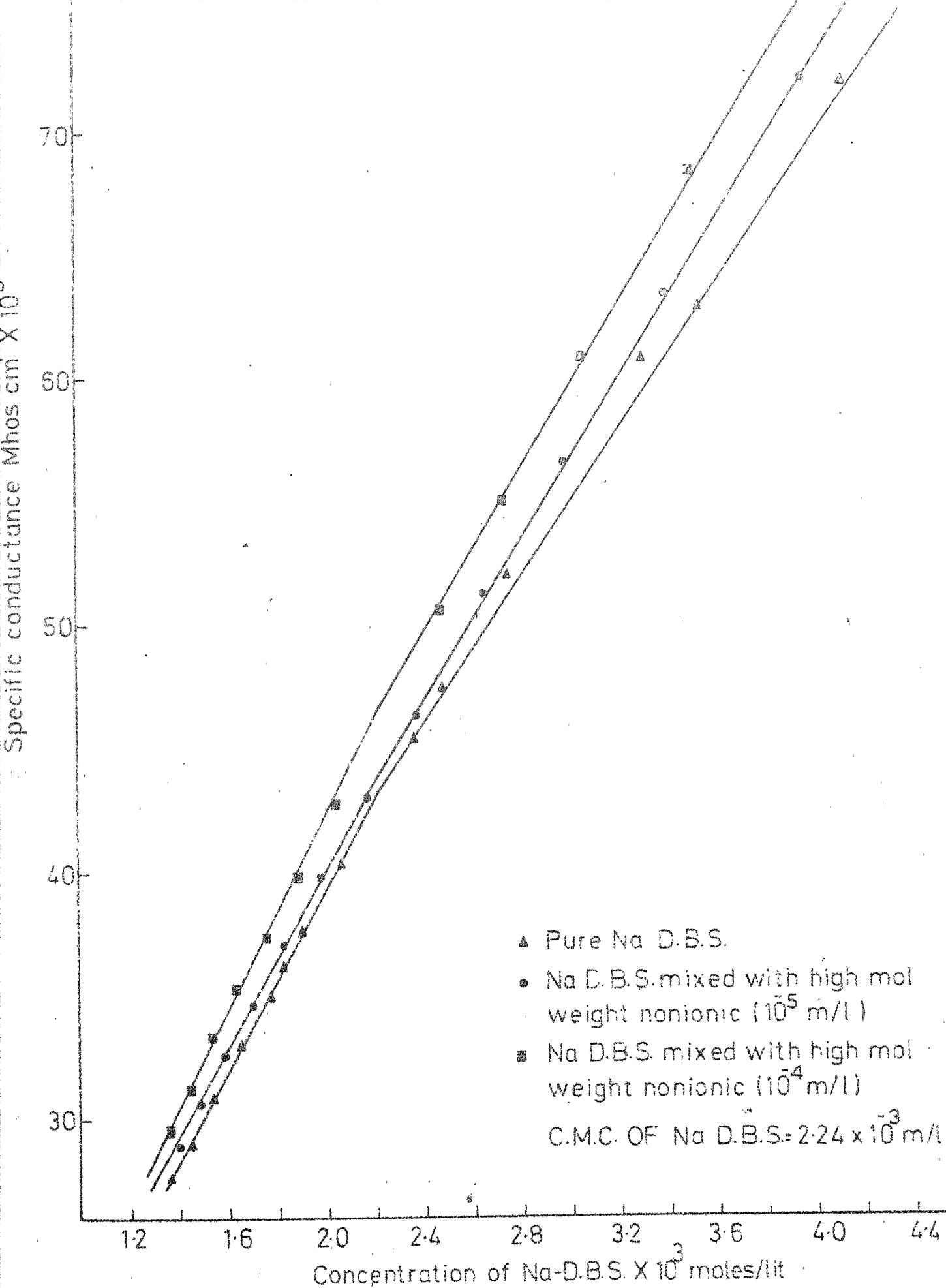
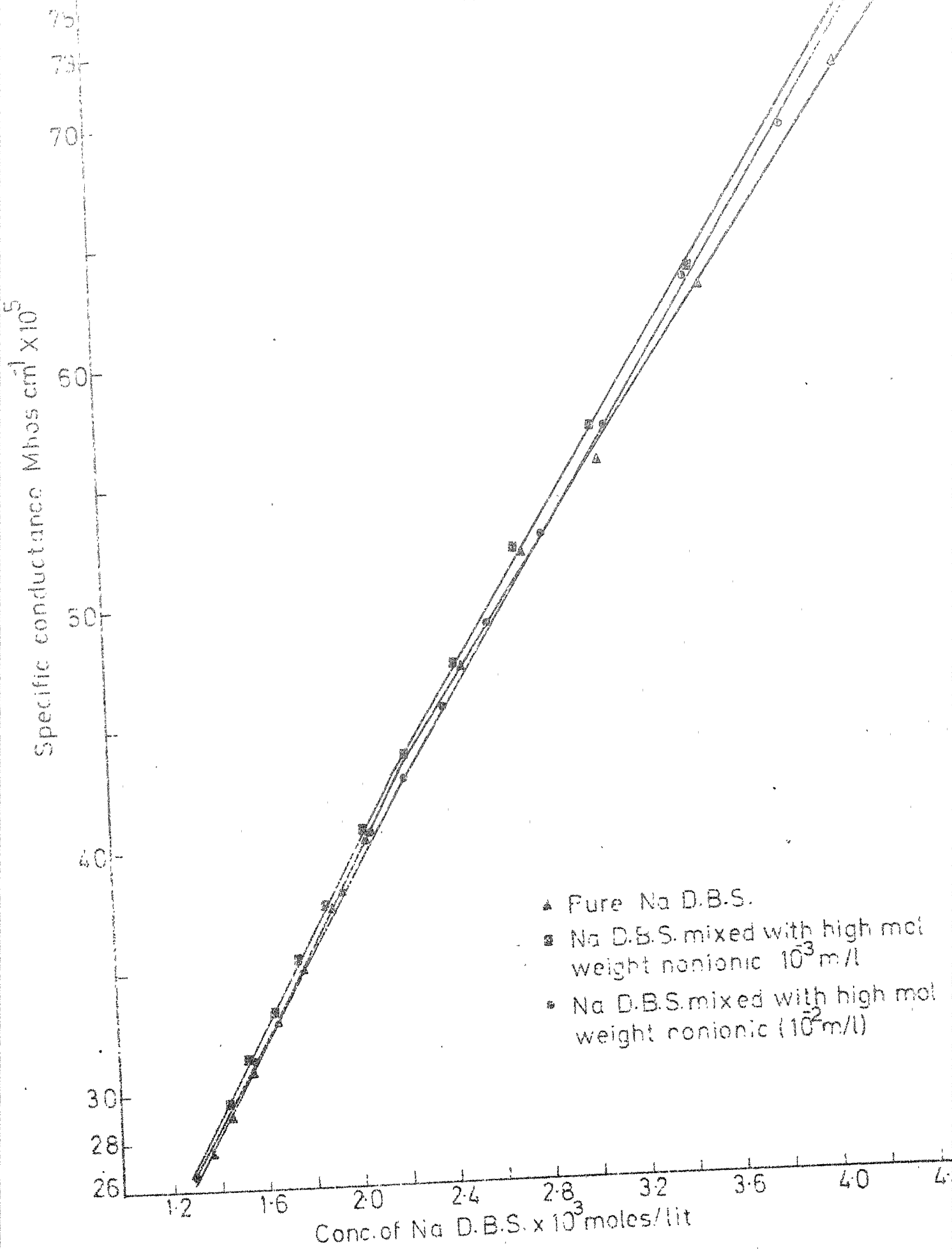


FIG. 18. EFFECT OF HIGH MOL. WEIGHT NONIONIC ON SPECIFIC

Identical results were obtained for the system Na-DBS: PPG-4, again when the concentration of (PPG-4) was  $10^{-4}$  m/l and  $10^{-5}$  m/l as shown in Fig. 4.5. This increase in conductance of Na-DBS solution at concentrations above its cmc accompanying the addition of nonionics such as PPG-3 and PPG-4 might be due to two factors, as considered by Biswas and Mukherjee. (1) The abundance and mobility of free ions ( $\text{Na}^+$  ions) obtained as dissociation products, (2) The mobility of the mixed micelles.

In a typical sodium dodecyl benzene sulfonate micelle, the electrostatic repulsion of like-charged DBS-ions is counter balanced by the gegenions viz.  $\text{Na}^+$ , which are sandwiched in between. The nonionic (PPG-3 and PPG-4) molecules may substitute  $\text{Na}^+$  while at the same time reducing electrostatic repulsion as referred to above. Added to this, there may be additional low energy bonding between the nonionic molecule and the anionic chain such as hydrophobic association. The  $\text{Na}^+$  ions released through the above process would obviously increase the conductivity of the Na-DBS, solution. Somewhat similar observations were made and interpreted by Tokiwa and Moriyama (3) as well.

It is also found from Figs. 4.3 and 4.6 that at a given concentration of Na-DBS (above its cmc) the conductance value starts decreasing when the concentration of nonionics (PPG-3

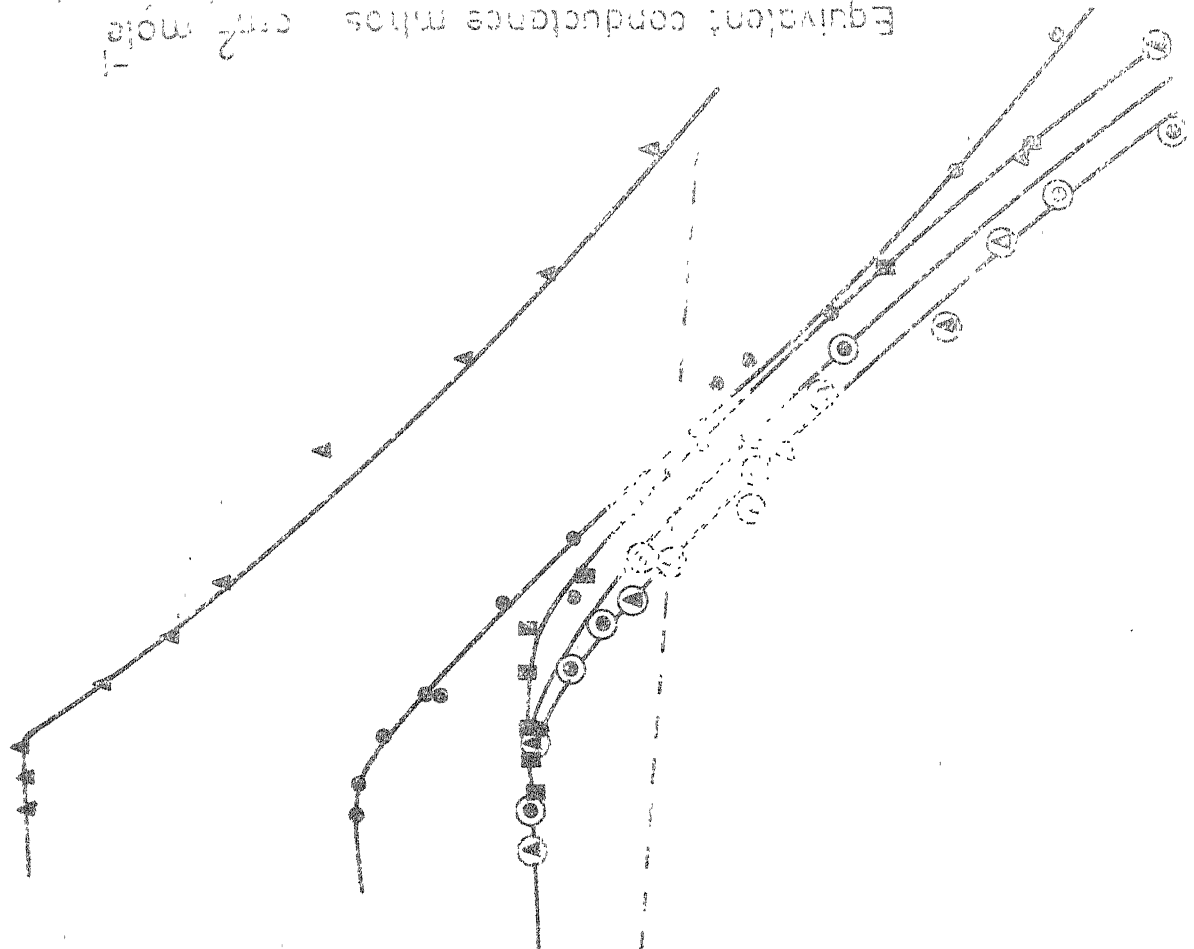


EFFECT OF HIGH MOL. WEIGHT NONIONIC ON SPECIFIC



- NaDES Alone
- CONC. OF PPG-4  $10^5$  m/l
- ▲ CONC. OF PPG-4  $10^4$  m/l
- CONC. OF PPG-4  $10^3$  m/l
- ⊙ CONC. OF PPG-4  $10^2$  m/l

$\Lambda_0$  ----- THEORETICAL ONSAGER SLOPE



SQUARE ROOT OF MOLALITY X  $10^3$

FIG. 4.7 EFFECT OF HIGH MOLECULAR WEIGHT NONIONIC (PPG-4) ON EQUIVALENT CONDUCTANCE OF NaDES

and PPG-4) are raised upto  $10^{-3}$  m/l or beyond. This decrease in specific conductance of Na-DBS at these concentration of PPG-3 and PPG-4 (well above their own cmc) is probably due to the incorporation of the anionic collector (Na-DBS) within the nonionic (PPG-3 and PPG-4) micelles, which decreases the apparent concentration of Na-DBS molecules upon the formation of mixed micelles.

The effect of PPG-3 and PPG-4 on the equivalent conductance of Na-DBS is shown in Figs. 4.4 and 4.7 respectively. There is an increase in the equivalent conductance upon the addition of  $10^{-5}$  to  $10^{-4}$  m/l of PPG. The addition of larger amounts of PPG ( $10^{-3}$  m/l) decreases the equivalent conductance of Na-DBS, indicating the formation of mixed micelles of PPG where Na-DBS is incorporated in PPG-micelles. The value of  $\Lambda_0$  have been calculated to infinite dilution. The theoretical Onsager slopes are also shown as dotted line in Figs. 4.4 and 4.7. The effect of PPG on the  $\Lambda_0$  value of Na-DBS is tabulated in Table 4.1.

Inspection of Table 4.1 reveals that  $\Lambda_0$  values of Na-DBS undergoes small, but significant changes in the presence of the nonionic PPG molecules. In some cases the change in  $\Lambda_0$  value is only marginally above experimental error while in others it is significant. This is contrary to the anticipated invariance in the  $\Lambda_0$  values. Indeed, Scott and Tartar (5)

Table 4.1

Effect of Nonionic (PPG) on  $\Lambda_0$  Value of Na-DBS at 35°C.

Sl. No.	Concentration of tripropylene Glycol monomethyl Ether (PPG-3), in m/l.	$\Lambda_0$ Value mho cm <sup>2</sup> /m	Concentration of tetrapropylene Glycol monomethyl Ether (PPG-4) in m/l.	$\Lambda_0$ Value mho cm <sup>2</sup> /m
1.	0	200*	0	200*
2.	10 <sup>-5</sup>	204	10 <sup>-5</sup>	206
3.	10 <sup>-4</sup>	205	10 <sup>-4</sup>	217
4.	10 <sup>-3</sup>	204	10 <sup>-3</sup>	200
5.	10 <sup>-2</sup>	201	10 <sup>-2</sup>	200

\* This is equivalent to  $\lambda_{DBS^-} = 140$  since  $\lambda_{Na^+}$  is 60 at 35°C.

noticed no changes in  $\Lambda_0$  value in the aqueous solutions of sodium ethyl benzene sulfonate. However, our results for Na-DBS show slight positive deviation in  $\Lambda_0$ . Mukherjee and Mysels (6), and Mukherjee (7) have suggested that there may be dimeric association of ionic surfactants even at pre-micellar concentrations. Conductivity data on dilute aqueous solutions of ionic surfactants show (6,8) deviation from the Debye Huckel Onsager expression. The higher conductance values, experimentally obtained in these cases have been stated to be due to the dimerization of the surfactant ions in which the ions heads are held far apart and the flexible hydrocarbon

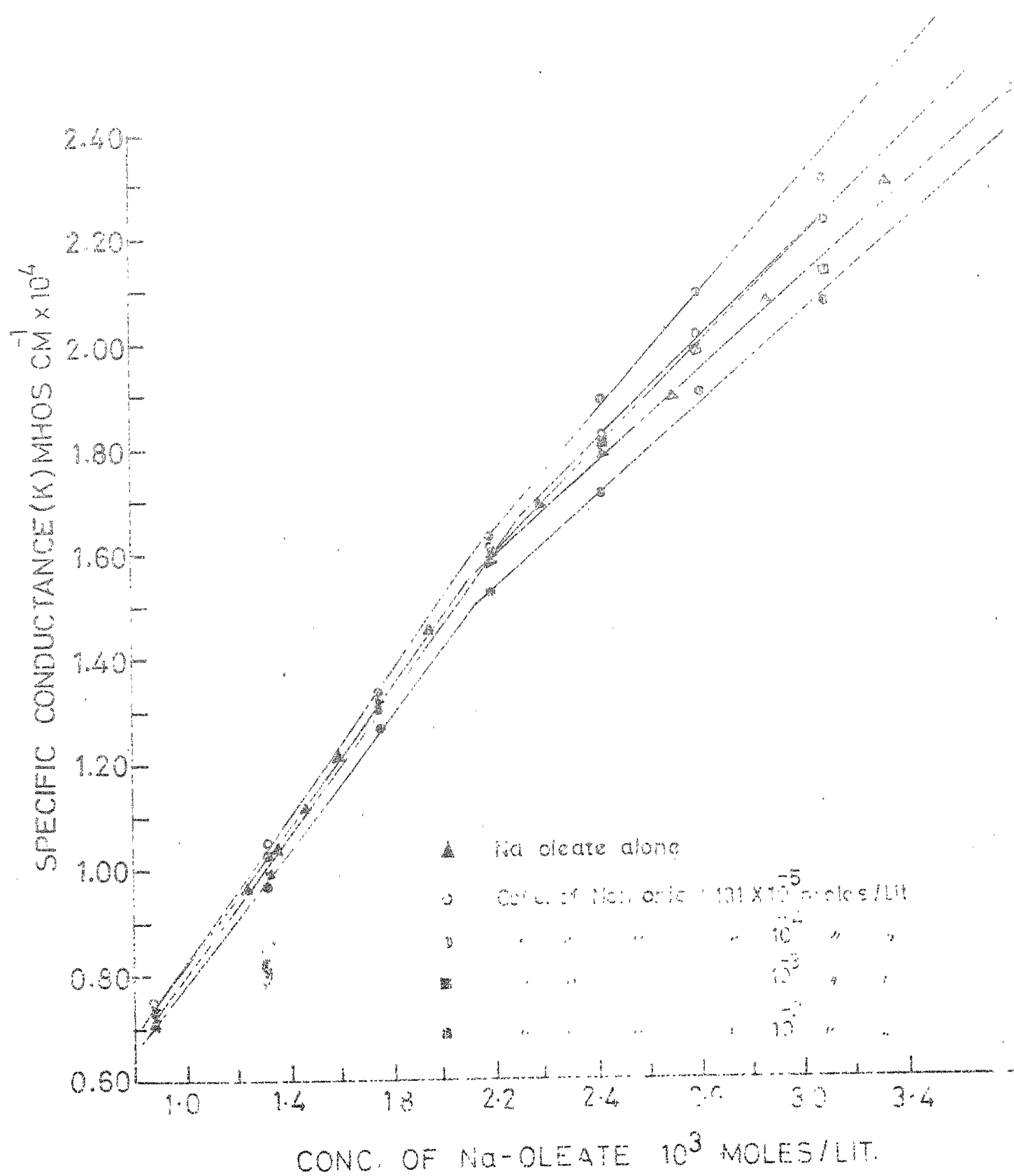


FIG.4-8 SPECIFIC CONDUCTANCE AGAINST CONCENTRATION FOR Na-OLEATE ALONE AND MIXED WITH NONIONIC ( LOW MOLECULAR WEIGHT) AT 25°C

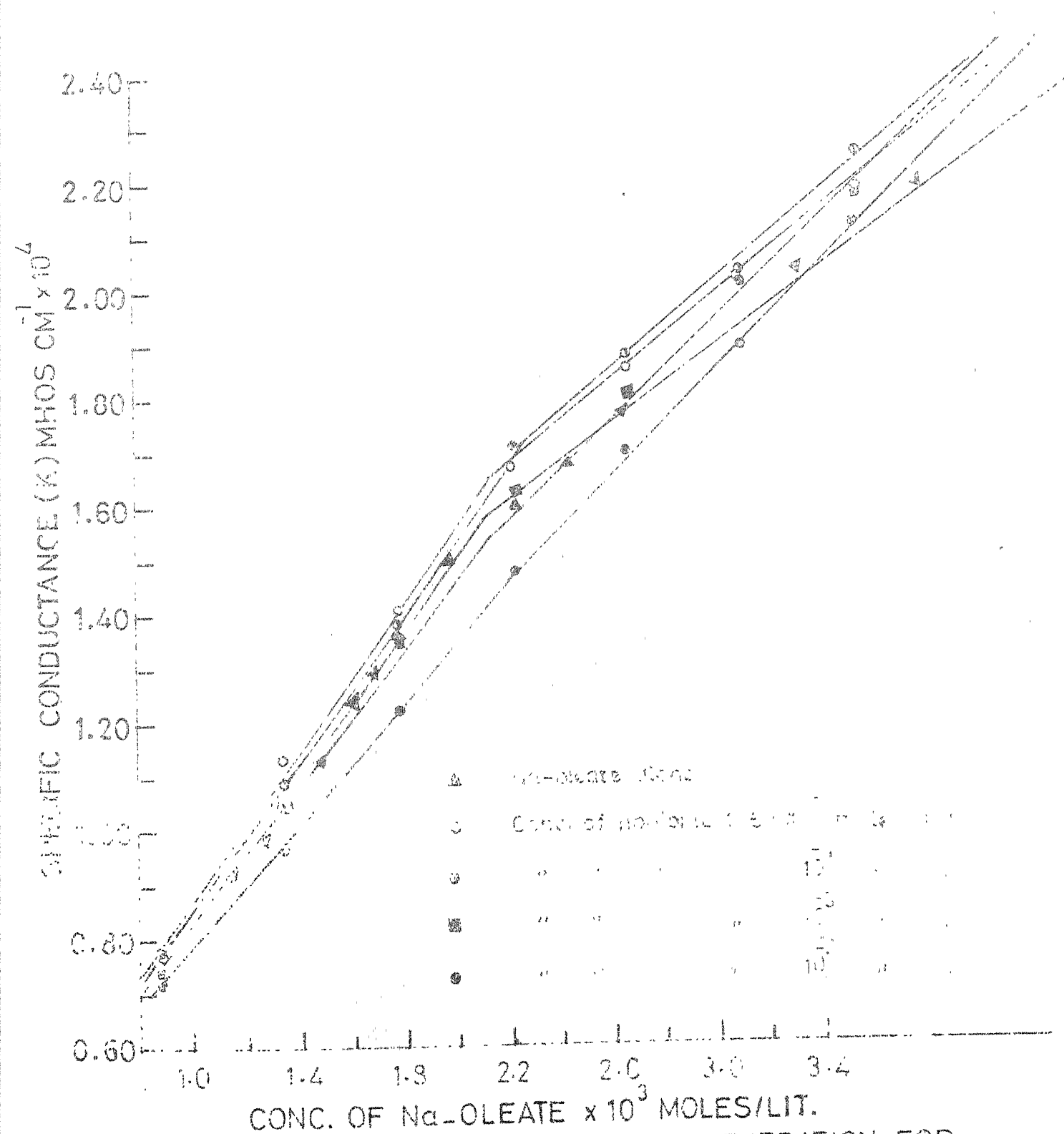


FIG.4.9 SPECIFIC CONDUCTANCE AGAINST CONCENTRATION FOR Na OLEATE ALONE AND MIXED WITH NONIONIC (HIGH MOLECULAR WEIGHT.) AT 25°C

chains are inter coiled. This would result in a reduction in the hydrodynamic resistance for the dimeric ions during their movement. This postulate has been supported from experiments on the transference no. of SDS, which is found to be higher than the theoretical value (7). It is likely that we are encountering a similar possibility of dimerization of Na-DBS, since in this case: (a)  $\Lambda_p$  shows slight positive deviation, and (b) the equivalent conductance of the anionic surfactant increases in the presence of low concentrations of PPG. Further experiments on such pre-micellar aggregation would be of use in validating this possibility.

We have studied earlier (9) the effect of PPG on the conductance of the second anionic surfactant Na-Oleate. The results of these study are presented in Figs. 4.8 and 4.9. The behavior in this system parallels to a large extent what is being seen in the case of Na-DBS. For sodium oleate,  $\Lambda_p$  works out to be 83.5, and  $\Lambda_{ol-}$  to be 23.5 mho cm<sup>2</sup>/mol. at 25°C. This value is much lower than the corresponding value for Na-DBS. In presence of nonionic, the conductance of sodium oleate solution increases slightly both in the micellar as well as post-micellar zone, provided the nonionic concentration is not much above its cmc. However, if the nonionic concentration is maintained at a relatively high value (above its cmc), such as 10<sup>-3</sup> or 10<sup>-2</sup> m/l, there is appreciable decrease in conductance

particularly at higher concentrations of sodium oleate. This decrease is much more prominent for sodium oleate than for Na-DBS, indicating stronger interaction of the former within the PPG-micelle.

In studies involving sodium oleate, a special problem need to be considered. It has been suspected that sodium salts of fatty acids, such as Na-Oleate may undergo hydrolysis. If this were to happen, a straight forward interpretation of conductance data here will be difficult. It has been suggested (10) that in soap solutions of pre-micellar concentrations, there are not only soap anions ( $X^-$ ), but also acids (HX), and complexes such as  $(HX_2^-)$ ,  $(X_2^-)$ , and  $(HXX)_2$ . The change in free energy for the dimerization of the oleate anions has been estimated (11) to be -7 cal/mol., suggesting that in the carboxylic acid solutions of soaps, aggregation at the pre-micellar stage occurs as prelude to conventional micellization.

To summarize, conductivity measurement of Na-DBS alone and in presence of PPG-3 and PPG-4 at different concentrations shows that when concentration of PPG is low there is mixed micelle formations by incorporating PPG molecules in Na-DBS micelle but if the concentrations of PPG is well above its cmc value the decrease in conductance value of Na-DBS can be explained only in terms of the proposed formation of mixed micelle of type nonionic micelle and Na-DBS molecules incorporated in nonionics micelle.

## REFERENCES

1. Vold, M.J., and Vold, R.D.  
Colloid Chemistry  
(1964), Reinhold Publishing Corporation, New York, p.61.
2. Biswas, A.K., and Mukherjee, B.K.  
Studies on Micellar Growth in Surfactant Solutions  
(1960), J. Phys. Chem., 64, 1-4.
3. Tokiwa, F., and Moriyama, N.  
Mixed Micelle Formation of Anionic and Nonionic  
Surfactants  
(1969), J. Coll. Interf. Sci., 30, 338-344.
4. Corrin, M.L., and Harkins, W.D.  
Determinations of the Critical Concentration for  
Micelle Formation of Colloidal Electrolyte by the  
Spectral Change of Dye  
(1947), J. Am. Chem. Soc., 69, 679-683.
5. Scott, A.B., and Tartar, H.V.  
Electrolytic Properties of Solutions of Paraffin-Chain  
Quarternary Ammonium Salts  
(1943), J. Am. Chem. Soc., 65, 692-698.
6. Mukherjee, P., Mysels, K.J., and Dulin, C.I.  
Dilute Solutions of Amphipathic Ions I. Conductivity  
of Strong Salts and Dimerization  
(1958), J. Phys. Chem., 62, 1390-1396.
7. Mukherjee, P.  
Dilute Solutions of Amphipathic Ions, II, Transference  
Number  
(1958), J. Phys. Chem., 62, 1397-1400.
8. Mukherjee, P.  
The Nature of the Association Equilibria and Hydro-  
phobic Bonding in Aqueous Solutions of Association  
Colloids  
(1967), Adv. Coll. Interf. Sci., 1, 241-245.



9. Bansal, V.K.  
Collector-Frother Interaction  
(1971), M.Tech. Thesis, Indian Institute of Technology  
Kanpur, p. 30.
10. Eagland, D., and Franks, F.  
Association Equilibria in Dilute Solutions of  
Carboxylic Acid Soaps.  
(1965), Trans. Farad. Soc., 51, 2468-2477.
11. Mukherjee, P.  
Dimerization of Anions of Long-Chain Fatty Acids in  
Aqueous Solutions and the Hydrophobic Properties of  
the Acids  
(1965), J. Phys. Chem. 69, 2821-2827.

## CHAPTER V

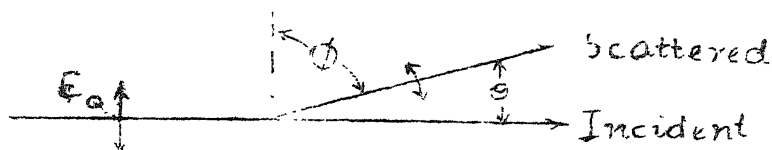
### LIGHT - SCATTERING STUDIES ON THE SIZES AND SHAPES OF THE MICELLES OF PPG, AND ON THE INTERACTION BETWEEN PPG AND IONIC SURFACTANTS

#### V.1 INTRODUCTION.

During the elastic scattering process involving radiation of frequency  $\nu$  (or wavelength  $\lambda = c/\nu$ ) and incident electric field  $E_o$ , the field strength of the scattered photons  $E_s$  is given by

$$E_s = \frac{4\pi^2\nu^2}{c^2 r} \alpha E_o \sin \theta \quad (5.1)$$

where  $\alpha$  is the polarizability of the scatterer,  $c$  is the velocity of light,  $r$  is the distance between the scattering element and the observer, and angle  $\theta$  is the angle formed between the dipole axis and the line of observation as shown below:



The intensity ratio is given by:

$$\frac{I_s(\theta)}{I_o} = \frac{16\pi^4\alpha^2}{\lambda^4 r^2} \left( \frac{1 + \cos^2 \theta}{2} \right) \quad (5.2)$$

where  $I_o$  and  $I_s$  are the intensities of the incident and out-coming beams and  $\theta$  is the angle found between the incident and scattered beams. This is the basic-Rayleigh equation of light-scattering for a single scattering element.

The quantities actually measured experimentally are the Rayleigh ratio  $R_\theta$  which is given as,

$$R_\theta = r^2 \left[ \frac{I_s(\theta)}{I_o} \right] (1 + \cos^2 \theta) \quad (5.3)$$

$$\text{or the turbidity } \frac{I_o - I_s}{I_o} = e^{-\tau} \quad (5.4)$$

These are related as,

$$\tau = \frac{16 \pi R_\theta}{3} \quad (5.5)$$

$I_s$  being the total scattered intensity, we have then,

$$R_\theta = \frac{8 \pi^2 \alpha^2}{\lambda^4} \quad (5.6)$$

The above relation is valid under the following conditions:

- (a) The incident beam is monochromatic and parallel;
- (b) The particles scatter independently of each other (infinite dilute solution);
- (c) Each particle is randomly oriented in space;
- (d) There is no absorption of the radiation;

(c) The particles are isotropic; and the interaction between the scattered and incident radiations inside the particles may be neglected, as for example, secondary scattering.

The solution, we deal no longer with single non-interacting particles immersed in vacuum. Keeping temporarily the assumption of independent particles, we immerse them now in a medium, which itself has a polarizability  $\alpha_0$ ; the observed increase in scattering when the solute is introduced into the pure solvent represents now the excess polarizability of the solute - over that of solvent molecules. The particles in solution are in constant thermal motion. Consequently, the real factor to consider is not the polarizability  $\alpha$  itself, but the fluctuation  $\Delta\alpha$  in various volume elements in the medium. Since polarizability itself is related to the refractive index  $n$ , the term  $\Delta\alpha$  can be written in terms of the refractive index increment  $(\partial n/\partial c)$ , following Debye. The Debye expression for light scattering is then written, including the virial terms, as below:

$$\frac{Hc_2}{\Delta\tau_\theta} = \frac{Kc_2}{R_\theta} = \frac{1}{M_2} [1 + 2Bc_2 + 3C c_2^2 + \dots] \quad (5.7)$$

where  $K = 2\pi^2 n^2 (\partial n/\partial c_2)^2 / N_A \lambda^4$ , and  $H = 16\pi K/3$ .

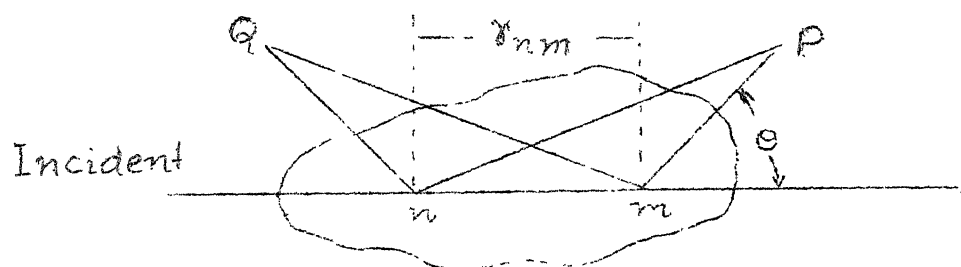
The subscript 2 refers to the solute whose concentration is expressed in g/ml. and molecular weight  $M_2$ .  $N_A$  is the Avagadro number,  $n$  the refractive index of the solvent (for

dilute solutions) and  $\lambda$  the wavelength of photons used for scattering.  $R_\theta$  and  $\Delta\tau$  are the excess Rayleigh ratio and excess turbidity respectively of the solutions over pure solvent, and  $(\partial n/\partial c_2)$  is the refractive increment which has to be determined, using a refractometer (usually a differential refractometer).

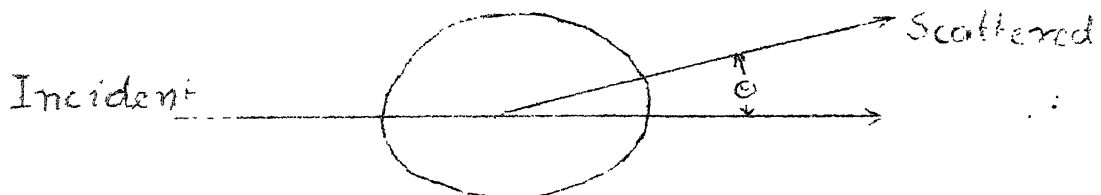
Thus, in a two component system when there is no interference effect, a plot of the scattering function  $\frac{Kc_2}{R_\theta}$  or  $\frac{Kc_2}{\Delta\tau_\theta}$  as a function of the concentration gives a curve, the intercept of which is the reciprocal of the molecular weight, and whose limiting slope is the second virial coefficient.

#### Large Particles and Particle Geometry:

When the dimensions of the particle are of a magnitude comparable to the wavelength of the radiation, interference occurs between the radiation scattered from individual elements within a particle. As a result, the scattering envelope is assymmetric. The reason for this is shown below:



The particle is large with respect to the wavelength of the radiation. Let us consider scattering from elements  $n$  and  $m$  observed at points  $P$  and  $Q$ . We find that when radiation scattered from elements  $n$  and  $m$  reaches point  $P$  (in the forward direction), there is no great difference between the path lengths of two rays, so that they are not much out of phase with each other and interference is small. However, when the radiation scattered from  $n$  and  $m$  reaches point  $Q$  (in the backward direction) the total distance travelled by the ray  $m$  is much greater than that from  $n$  (greater by  $nm + mQ - nQ$ ). As a result, the two rays can become completely out of phase, leading to serious interference. In the forward direction, i.e. along the incident beam, scattered radiation from  $n$  and  $m$  is fully in phase, there is no interference, and the observed scattering is the sum of the scattering from all elements within the particle. The scattering envelope then has a shape similar to that shown below:



In order to obtain the correct unattenuated scattering intensity, it becomes necessary to extrapolate the data to zero angle.

Quite generally the effect of large size of the particle is described by a function  $P(\theta)$  known as the 'scattering function' defined as

$$P(\theta) = \frac{\text{Scattering intensity for a large particle}}{\text{Scattering intensity without interference}}$$

$P(\theta)$  usually has a value less than unity when  $\theta$  is large, but increases steadily to a limiting value of unity as  $\theta$  reduces to zero degree. Thus for large particles, eq.(5.7) will apply when  $\theta = 0$ , i.e. if the data are obtained at several angles  $\theta$  and extrapolated to  $\theta = 0^\circ$ . This limit is usually expressed as

$$\frac{Hc_2}{4\pi_0} = \frac{Kc_2}{R_{00}} \quad .$$

The general equation for the particle scattering factor  $P(\theta)$  has been given by Debye as

$$P(\theta) = \frac{1}{\sigma^2} \sum_{i=1}^{\sigma} \sum_{j=1}^{\sigma} \frac{\sin \mu r_{ij}}{\mu r_{ij}} \quad (5.8)$$

where  $\mu = \frac{4\pi}{\lambda} \sin(\theta/2)$ ;  $r_{ij}$  is the vector distance between two scattering points  $i$  and  $j$  of a total set of  $\sigma$  scattering points within the large particles.  $P(\theta)$  has also been related to the radius of gyration (root mean square average) of the scattering particle as;

$$\lim_{\theta \rightarrow 0} \frac{1}{P(\theta)} = 1 + \frac{16\pi^2}{3\lambda^2} R_G^2 \sin^2(\theta/2) \quad (5.9)$$

This equation is valid only at very low concentration and therefore it is necessary to extrapolate the data at each angle to zero concentration. Again for a large particle eq. (5.7) is valid only at the limit  $\theta = 0^\circ$ . Zimm has formulated a method for plotting  $\frac{Kc_2}{R_\theta}$  (or  $\frac{Hc_2}{\Delta\tau_\theta}$ ) vs.  $\sin^2\theta/2 + kc$  where  $k$  is an arbitrary constant chosen to accommodate all the data in a graph sheet. The  $c = 0$  line and  $\theta = 0^\circ$  line both should meet at  $y$ -axis giving an intercept of  $1/M_2$ . The slope of  $c = 0$  line gives  $R_G$  and the slope of  $\theta = 0^\circ$  line gives the value of second virial coefficient.

#### $P(\theta)$ , $R_G$ , and Their Relation to the Particle Shape:

The angular dependence of  $P(\theta)$  for a flexible coil, for a sphere, for a rod and for ellipsoids of revolution with various axial ratios  $p$  has been given in the literature and a representative report of this is due to Koch (1). In general  $P^{-1}(\theta)$  is plotted against the product  $[\frac{4\pi}{\lambda} \sin(\theta/2) a]$ , where  $a$  is the relevant dimension of the scattering particle. Alternatively it can also be plotted vs.  $[\frac{4\pi}{\lambda} \sin(\theta/2) R_G]$ . Such a plot is shown in Fig. 5.11. The relation between  $P(\theta)$  and  $R_G$  has already been given in eq. (5.9).

It is possible to calculate  $R_G$  for various shapes of scattering particles. For a solid sphere of radius  $R$ ,  $R_G^2 = 3/5R^2$ ; for a long straight rod of length  $L$ ,  $R_G^2 = L^2/12$ ; for a flexible coil of end to end distance  $(h^2)^{1/2}$ ,  $6R_G^2$  equal to  $h^2$ ; and



for a prolate ellipsoid of revolution of semi axes  $a$ ,  $a$ ,  $b$  and axial ratio  $p = b/a$ ;  $R_G = a \left( \frac{p^2 + 2}{5} \right)^{1/2}$ . Thus a study of light-scattering is of great use in the determination of molecular weights and shapes of large scattering particles such as polymers and micelles.

Table 5.1 lists the scattering function and radii of gyration for various particle shapes.

Light-scattering studies on surfactant micelles have been reported predominantly for ionic surfactants (2-13). It has been possible to derive the molecular weights and shapes of micelle from such studies. On nonionic surfactants there have been increasing reports in literature of the use of light-scattering technique (14-30). However, while people have derived the size of the micelles, there has been very little information available on the shape, radii of gyration and scattering functions. Becher (30), Tokiwa (31) and Schick (32,37) have done useful work in this area. Becher and Arai have suggested (30) possible models for the shapes of nonionic lauryl surfactants. Light-scattering studies on mixed micellar systems (31-36) have been few and even in these cases information on  $R_G$  has been sparse. However, other techniques such as viscosity and NMR have been used to study the molecular organization in mixed micelles.

Table 5.1

Scattering Function and Radii of Gyration for Various Structures

Structure	$P(\theta)$	Radius of Gyration
Sphere	$\left[ \frac{3}{x} (\sin x - x \cos x) \right]^2$ $x = \frac{hD}{2}$ $D = \text{diameter of sphere}$ $h = \frac{4\pi}{\lambda} \sin \theta / 2$	$\left( \frac{3}{5} \right)^{1/2} \frac{D^2}{2}$
Thin Rod	$\frac{1}{x} \int_0^{2x} \frac{\sin w}{w} dw - \left( \frac{\sin x}{x} \right)^2$ $x = \frac{hL}{2}$ $L = \text{length of rod}$	$\left( \frac{L^2}{12} \right)^{1/2}$
Ellipsoid	$\sum_{n=0}^{\infty} \frac{(-1)^n}{3 \times 4!} \frac{(2n+2)(2n+5)}{(2n+6)!} 2^{2n}$ $* x^{2n} \sum_{r=0}^n \frac{n!}{r!(n-r)!} \frac{p^r}{2r+1}$ $p = \frac{b^2 - a^2}{a^2}$ $x = \frac{4\pi a \sin \theta / 2}{\lambda}$ $b = \text{semi-major axis}$ $a = \text{semi-minor axis}$	$\left[ \frac{(2 + (b/a)^2)}{5} \right]^{1/2}$

Contd...

Table 5.1 contd...

<u>Structure</u>	<u>P(<math>\theta</math>)</u>	<u>Radius of gyration</u>
Thin Disc:	$\frac{2}{x^2} [1 - \frac{1}{x} J_1(2x)]$	$R/\sqrt{2}$
	$x = hR$	
	$R = \text{radius of disc}$	
	$J_1 = \text{Bessel function of order 1.}$	
Random Coil	$\frac{2}{x^2} (e^{-x} + x - 1)$	
	$x = \frac{h^2 \langle r^2 \rangle_{av}}{6}$	$(\frac{\langle r^2 \rangle_{av}}{6})^{1/2}$
	$\langle r^2 \rangle_{av} = \text{root mean square}$	
	$\text{end to end distance}$	

In this chapter we have used the technique of light-scattering to study the micellar aggregation of two frothers belonging to the polypropylene glycol monomethyl ether family i.e. the trimer and tetramer denoted respectively as PPG-3 and PPG-4. We show that these indeed form micelles in aqueous solutions but the exact shape of micelles cannot be unequivocally stated. We have also been able to monitor the formation of mixed micelles between the frothers and collectors such as sodium dodecyl benzene sulfonate (Na-DBS), and Na-Oleate (Na-OL). Some information about the molecular organization within the mixed micelles is reported in Chapter VI by the use of NMR spectroscopy.

## V.2 EXPERIMENTAL:

### V.2.1 Preparation of Dust Free Solutions:

The main problem in light scattering measurements is the preparation of solutions completely free of particulate matter such as air-borne dust, solid particles which may be abraded from the apparatus etc. This requirement of ultra-clean solutions is unique and does not occur to a similar extent in any other physical measurement. Not only must the solutions directly examined be completely free of extraneous particles, but there must be an auxiliary source of relatively large quantities of dust free-solvent for use in washing pipettes, cell covers and for dilutions.

Organic solvents, and solutions in them, are probably easy to clean because of their generally low viscosity and their low polarity, and for the same reasons, particulate contaminants which may accidentally enter the solution after clarification tend to settle out in the cell and not to contribute to the scattering. With aqueous solution, it seems that the higher polarity of water has an effect probably electrical, on dust particles, which inhibit their removal from the bulk of the solvent and rapidly cause their suspension once they are separated.

The normal mode of downward filtration under vacuum cannot be used with detergent solutions, since splashing and foaming result in the formation of stable foams which may cause the solution to be dirtier than before filtration. With aqueous solutions, the higher viscosity and polarity of water render centrifugation much more time-consuming, and subsequent contamination is likely to cause more trouble. The method we have adopted is the cleaning of solvents and stock solution of additives by pressure filtration through a 100 $\mu$  pore size Millipore filter in an assembly made of stainless steel. The filter assembly with its attachments is shown in Fig. 5.1. The whole assembly was thoroughly cleaned with triple glass distilled water. The ion exchange water was always avoided due to the possible presence of some ion-exchange

resin particles which reduces the efficiency of the filter. The millipore filter was placed in the middle flange with supporting stainless steel mesh as shown in Fig. (5.1). The filter and stainless steel mesh were tightly positioned by screwing nuts. The upper portion of assembly, filter flange and bottom portion of assembly was placed as shown in Fig. 5.1. The O" rings were placed between the two flanges in grooves made in the flanges. The flanges were tightened with the help of 6 screws to avoid any leakage. The solvent was filled through the cap in the upper portion of the assembly. Approximately 250 ml of solvent can be filtered in one filtration. The pressure in the upper part of the assembly was maintained by an inert gas so that filtration rate is 10-15 drops per minute. If the filtration rate was higher, the pressure was released through a needle valve. The first few filtrate fractions were thrown out, then the solvent was collected in a glass bottle cleaned by dust free solvent. The funnel, the pipette and all glass-ware were thoroughly cleaned by dust free solvent. After 3 or 4 filtrate fractions had been collected, the filter was replaced. The filtrate after each filtration was checked in the photometer for dust particles. Any dust particle in the solvent shines like a star in the dark chamber when seen perpendicularly. The best way to check the solvent as to whether it is free from any dust and foreign particle is to measure the dissymmetry ratio

Valve to release pressure  
 Cap for filling solution  
 Needle valve  
 To N<sub>2</sub> gas cylinder

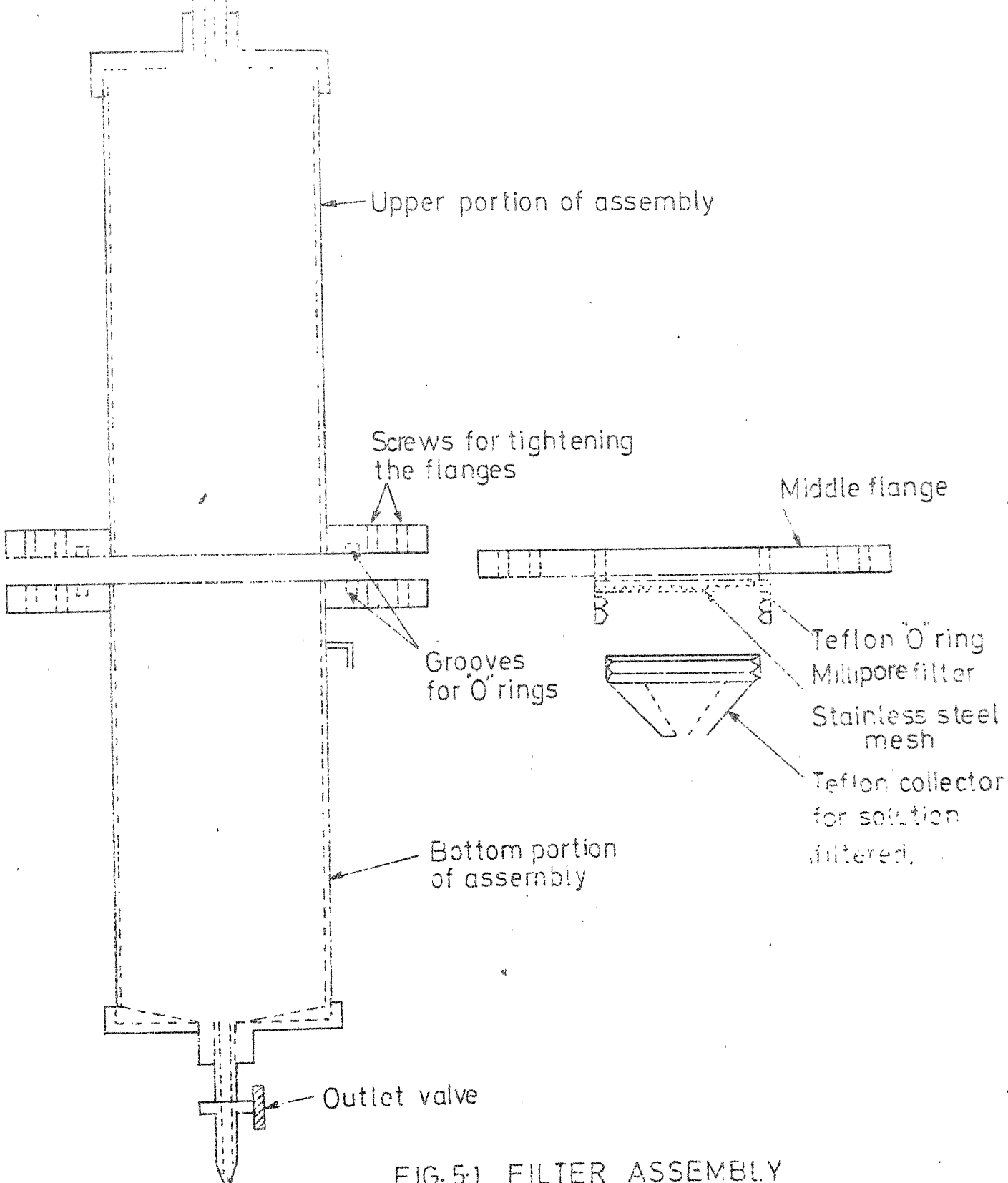


FIG. 5-1 FILTER ASSEMBLY

( $I_{45^\circ}/I_{135^\circ}$ ). When the solvent gives the dissymmetry ratio around 1, it is in the best condition for starting measurement. The solvent for each set of readings was prepared fresh and was stored in a tightly closed glass bottle. The light-scattering cell was thoroughly cleaned with the dust free solvent and dried with lid covering the cell before starting the measurement.

#### V.2.2 Refractive Index Measurements:

Any macromolecule in a solution, when affected by thermal motions of the solvent molecules, gives rise to small density fluctuations throughout the solution. These ultimately lead to the scattering of light due to the resultant micro-inhomogeneities, and some change in the refractive index. This property of the molecule can be quantitatively represented by a measurable parameter called the refractive index increment  $dn/dc$ . This term occurs in the practical light-scattering equation to the second power. This means that an error of, say, 2 percent, in its determination leads to an error of 4 percent in the derived molecular weight. Hence it becomes necessary to measure this parameter with great accuracy. The  $dn/dc$  measurements were done on Brice-Phoenix diffractometer (2000 series). The instrument consists of a mercury arc light source, with color filter to isolate either the 436 m $\mu$  blue or 546 m $\mu$  mercury green lines, a vertical illuminated slit and a thermostated square glass cell with a 25 $^\circ$  diagonal glass



partition dividing it into solution and solvent compartments. The slit image is focussed by a double convex lens and its position measured in a microscope fitted with a micrometer eyepiece. The divided cell is mounted on a turntable whose axis of rotation passes through the glass of the partitions (rotating the cell  $180^\circ$  serve to double any deviation). These optical components are mounted solidly on any optical bench. The  $dn/dc$  value was calculated from the straight line ( $n$  vs  $c$  graph).

#### V.2.3 Angular Measurements:

Angular measurements were made on the Brice-Phonex Universal Light-scattering photometer (2000 series) using the cylindrical cell C-101. Initially 30 ml of the solution was taken in the cell and the temperature was maintained at  $35^\circ \pm .1^\circ\text{C}$  by circulating water from a constant temperature bath through the water jacket which encloses the cell assembly. The deflection ( $G_\theta$ ) at various angles were read from an attached galvanometer. The procedure adopted for operating the instrument was followed as described in the operation manual. The deflection reading was always kept above 50 divisions on the scale by adjusting the combination of filters. Angular measurements at different concentrations were made by dilution. The angular measurements values were found to be  $\pm 10\%$  reproducible in the dilute concentration range.

- $n$  - Refractive index of solution;
- $R_w/R_c$  Residual refractive index correction. This factor arises because the foreshortening of the field of view of the detector is not completely corrected by the working - standard diffusor comparison. This correction decreases with decreasing cell size and for the cell used was found to be 1.1.
- $r/r'$  Calibration factor for use with the narrow diaphragms. Since the calibration factor  $r/r'$  is dependent on the refractive index of the solution, it must be determined for each solute-solvent system to be studied. Lamp replacement or small changes in alignment may effect  $r/r'$ . Consequently, its value should be checked occasionally. In our system it was found to be 0.551.
- $h$  Height of beam in cell;
- $\theta$  Angle of measurement
- $R$  is the fraction of the primary beam reflected at the exit window and is defined by

$$R = \left( \frac{n-1}{n+1} \right)^2$$

where  $n$  is the refractive index of the glass for light  $\lambda = 436 \text{ m}\mu$ . The value of  $R$  is 0.39 for cell C-101,

- $G$  Deflection at  $\theta$  angle;
- $G_w$  Deflection at  $0^\circ$  angle;

The value of H (optical constant) is calculated from the equation

$$H = \frac{32\pi^3 n^2 (dn/dc)^2}{3\lambda^4 N}$$

where,

n = refractive index of solution;

c = solution concentration in g/ml;

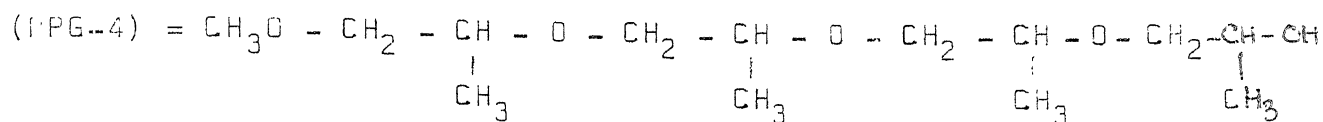
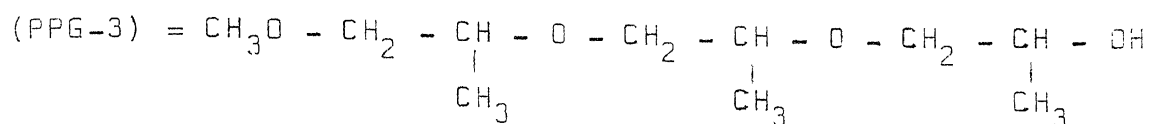
dn/dc = refractive index increment;

$\lambda$  = wavelength in vacuum;

N = Avogadro's number.

### V.3 RESULTS AND DISCUSSION:

There is indication from studies in the previous chapters that pure nonionic surfactants propylene glycol mono-methyl ethers of degree of polymerization 3 and 4 (referred to as PPG-3 and PPG-4 respectively) associate in aqueous solution to form micelles. Other authors have studied the aggregation of Lauryl derivatives ( $C_{12}$  hydrocarbon tail bearing) of polyoxymethylene in water by both hydrodynamic and spectroscopic methods and established the presence of micelles in these derivatives. Our compounds lack such a hydrocarbon tail; therefore it is of interest to study whether PPG-3 and PPG-4 also form micelles in water. The structure, of these two surfactants are given below:



In spite of the absence of any long hydrophobic groups in these, the presence of the  $\text{CH}_3$  and  $\text{OCH}_3$  groups and the absence of ionic heads which would repel each other, seem sufficient to cause micellar aggregation. In order to confirm such micelle aggregation in PPG-3 and PPG-4, we undertook careful light-scattering studies on these systems.

The results of light scattering investigation on pure fractionated PPG-3 in aqueous solution are presented in Fig. 5.2. The turbidity values  $\text{HC}/\Delta\tau_\theta$  are plotted simultaneously as a function of increasing concentration, and scattering angle  $\theta$ . Such a plot, termed the 'ZIMM PLOT', yields a parallelogram with one corner meeting the ordinate. The concentration range of PPG-3 chosen was well above the critical micelle concentration ( $\text{cmc} \sim 10^{-5} \text{ m/l}$ ) as determined by the surface tension method and was in the range  $5.8 \times 10^{-3} \text{ gm/ml}$  ( $2.8 \times 10^{-2} \text{ m/l}$ ) to  $1.59 \times 10^{-2} \text{ gm/ml}$  ( $7.7 \times 10^{-3} \text{ m/l}$ ). The angles chosen were  $0^\circ$ , and between  $45^\circ$  and  $90^\circ$ , at  $5^\circ$  interval. The constant  $k$  was chosen to be 100 in order to fit the graph in the paper. The  $0^\circ$  angle line has a slope which is nearly zero, indicating a negligible value for the second virial coefficient  $A_2$ , i.e.

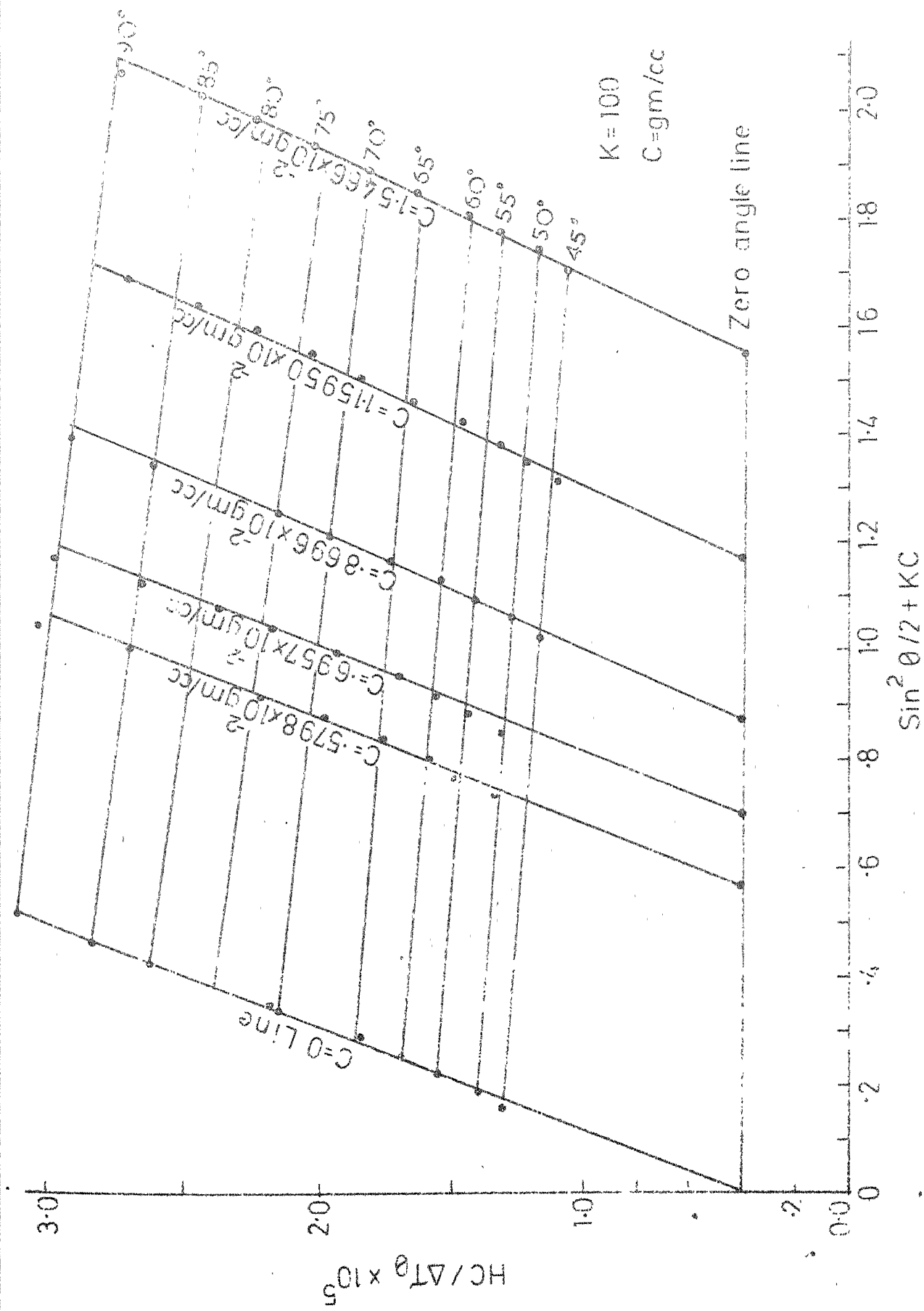


FIG.52 ZIMM PLOT FOR PURE NONIONIC MICELLE (LOW MOL WEIGHT(PPG-3)

no significant intermolecular interaction. However, the lines for all other angles do show a small negative slope. It is difficult to attach any physical significance to these small negative slopes at  $\theta \neq 0^\circ$ , since extrapolation to zero angle is necessary for large particles. The molecular mass calculated from the 'Zimm plot' for PPG-3 from Fig. 5.2 comes out to be a value of about  $2.5 \times 10^5$ . This is a clear indication that micellar aggregation of PPG-3 happens in water. Since the monomer mass of PPG-3 is 206, the number of molecules associated in a micelle is on an average about 1000, a very large number indeed. In the case of polyoxymethylated lauryl alcohol ( $C_{12}$ POE) such a large aggregation is known (37). In  $C_{12}$ POE, aggregation numbers of the order of 700 to 4000 have been reported, with practically no hydration at such degrees of association. However, with  $C_8$ POE the maximum value for the aggregation number reported by Becher (37) are about 200, while for  $C_{16}$ POE values as high as 1600 have been reported. In this light the value of  $10^3$  for PPG-3 is striking especially since PPG is devoid of any hydrophobic core. It is noteworthy that Becher has shown that the aggregation number for homogeneous surfactants are considerably larger than for polydisperse samples, the samples of PPG-3 and PPG-4 used in this thesis are fractionated and homogeneous fractions, a factor that may increase the aggregation number for PPG-3 and PPG-4.

It is also known that as temperature increases, the micellar size also increases. All our measurements were at a temperature of  $35 \pm .1^\circ\text{C}$ . The difference in chemical structure between POE and PPG-3, and a higher temperature of measurements may both contribute to the large value of  $n$  observed in our system (It is noteworthy that for hexaoxymethylated lauryl alcohol, the micellar aggregation number increases from 400 to 1400 between  $25^\circ\text{C}$  and  $35^\circ\text{C}$ . At  $45^\circ\text{C}$  the value is 4000). Presumably the  $\text{CH}_3$  groups in the repetitive side chain offer sufficient hydrophobic character resulting in micelle formation.

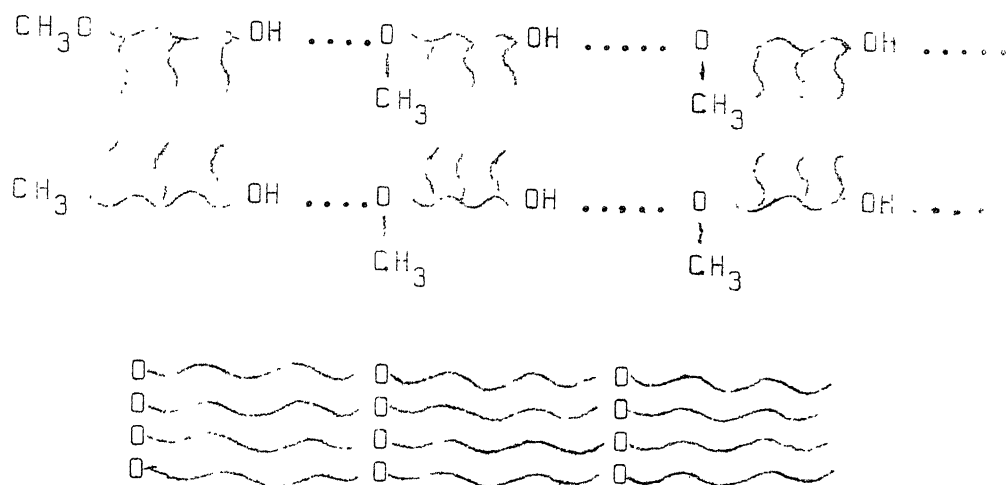
The indication that micelle aggregation occurs in PPG-3 in water, and that the average molecular weight of the micelles is of the order of  $10^5$  suggests the size of the scattering particle to be large. Hence we take recourse to use of particle scattering function  $P(\theta)$  which is defined as the ratio of scattering intensity of large particle to that occurring without interference. When  $\theta$  is relatively large,  $P(\theta)$  would be much less than one and at the limiting condition of  $\theta = 0^\circ$   $P(\theta)$  should be equal to one. Therefore one ought to use values of  $\text{HC}/\Delta\tau_\theta$  at the limiting value of  $P(\theta) = 1$  in order to obtain molecular parameters. The relation between  $P(\theta)$  and radius of gyration ( $R_G$ ) of the scattering particle is given by eq. (5.9) and the relation between  $\text{HC}/\Delta\tau_\theta$  and  $R_G^2$  is given by eq. (5.7). Calculation of such a slope from the Zimm plot

(Fig. 5.2), and from  $P^{-1}(\theta)$  vs.  $\sin^2 \theta/2$  curve given in Fig. 5.9 yield a value  $\langle R_G \rangle_{av}$  of  $1627 \text{ \AA}^0$  for PPG-3 micelles in water.

Further interpretation as to the shape of PPG-3 micelle comes by an examination of the form of  $P(\theta)$  for various particle shapes, as given in Table 5.1. One could try and calculate the geometric parameter of a sphere of radius  $R$ , and a rod of length  $L$ , or a flexible coil of end to end length  $\langle h \rangle$ . The relation between  $R_G^2$  and  $R^2$  for a sphere is  $R_G^2 = 3/5 R^2$ . Correspondingly the radius of PPG-3 micelles turns out to be  $2100 \text{ \AA}^0$ , whereas the value calculated from the molecular weight of the micelles (assuming sphericity and a density of 0.8 for the micelle) turns out to be  $50 \text{ \AA}^0$ . Thus a spherical model for the micelle is not likely. The relation between  $R_G^2$  and the length  $L$  of a long thin rod is:  $R_G^2 = \frac{L^2}{12}$ , and based on this, a value of  $L = 5640 \text{ \AA}^0$  is arrived at. If we calculate the rod length of micelle of PPG-3, using the molecular weight of  $2.5 \times 10^5$  obtained from the experiment, the calculated values do not agree with the value derived from the experimental  $R_G$ . For example a rod with a diameter of  $15 \text{ \AA}^0$  yields  $L = 2800 \text{ \AA}^0$ ; a diameter of  $30 \text{ \AA}^0$  yields  $L = 700 \text{ \AA}^0$ , with higher diameters reducing the value of  $L$  considerably. It is possible to consider 'end on' association of PPG-3 in a 'log boom' type of micelle (Fig. 5.18) but this would mean placing several PPG molecules laterally, along the major axis of the 'log boom'. Such an association does not appear likely from the



chemical structure point of view, unless one considers the association to be stabilised by regular intermolecular hydrogen bonding between terminal groups of PPG-3 monomers placed laterally. Contributions from the intermolecular hydrophobic association of the methyl groups along the backbones will add to the stability of the 'log-boom' arrangement. Such a scheme is illustrated below:



Further comment on the feasibility of such a 'log boom' type rod is unwarranted at this stage, since there is no compelling spectroscopic evidence for the presence of such hydrogen bonds in PPG-3. Hence we turn our attention to the micelle shape of an ellipsoid of revolution. Becher and Arai (30) have suggested that  $C_{12}$ PDE associates to form micelles with the hydrodynamic shape of ellipsoid. The scattering function  $P(\theta)$  has been calculated for ellipsoids with axial ratios of 2,3,4 and plotted against the product  $kS a$  (where  $k = \frac{2\pi}{\lambda}$ ,  $S = 2 \sin \theta/2$  and  $a$  = semi minor axis of the

ellipsoid) by Koch (1); the relation between radius of gyration and the parameters such as axial ratios and semi-minor axis  $a$  of an ellipsoid with axes  $2a$ ,  $2a$ ,  $2b$  is given by,

$$R_G = a \left( \frac{p^2 + 2}{5} \right)^{1/2}$$

The experimental value of  $P^{-1}\theta$  for PPG-3, when plotted against  $kSa$  do not match with either spherical or ellipsoidal shape of  $p = 1, 2, 3, 4$ . Recently the Koch plot has been modified to involve the product  $kSR_G$  rather than  $kSa$  (38). Fig. 5.11 presents such a plot of  $P^{-1}(\theta)$  against  $kSR_G$  for PPG-3. It is clear from the nature of the  $P^{-1}(\theta)$  vs.  $kSR_G$  plot, that the shape of the micelle is intermediate between an ellipsoid of small  $p$ , and a rod. We have tried calculating  $R_G$  values for ellipsoidal shapes with a variety of  $a$  values and axial ratios but in each case the agreement between the calculated  $R_G$  and the experimental value is poor. Hence it appears that if we have to consider an ellipsoidal shape it may have to be a totally asymmetric ellipsoid with each axis different from each other ( $a, b, c$ ). Favro (39), has treated the problem of rotational brownian motion of such an asymmetric shape, but to the best of our knowledge, neither the scattering function nor radius of gyration for such shapes has been reported. Hence, treatment of our data assuming an asymmetric ellipsoid has been not possible.

~~ellipsoid) by Koch (18) & the relation~~

We next turn our attention to the possibility of 'box shape' micelles, i.e. the McBain bilayer leaflets in three dimensions. A cubical box does not appear likely since it would be hydrodynamically equivalent to a sphere. We then consider a rectangular box in three dimensions of lengths  $a$ ,  $b$  and  $c$ . In the McBain (40) model,  $c = 30 \text{ \AA}$  for a bilayer of PPG-3. The volume  $V$  of such a micelle will be  $30 ab \text{ \AA}^3$ , and hence  $ab = 2 \times 10^4 \text{ \AA}^2$  which gives us several possible sets of  $n_a$  and  $n_b$  values where  $n_i$  is the number of PPG-3 molecules per axis, under the constraint  $n_a + n_b + n_c = 1200$ . A rectangular box with three non-equal axes may be considered hydrodynamically equivalent to an asymmetric ellipsoid of revolution. Becher and Arai (30) have extended the McBain model in three dimensions to yield the 'sausage' type micelles (Fig. 5.18). The present idea of a rectangular box micelle differs from the 'sausage' model in the invocation of three different axes. Unfortunately, direct experimental proof for the presence of rectangular micelles in PPG-3 are not available and thus our proposal is speculative in nature. Shah and Hamlin (41) have suggested such a model in the ternary system, Hexadecane K-oleate and water.

Light-scattering studies on PPG-4 show that this molecule also associates in water similar to PPG-3. The 'Zimm plot' for PPG-4 in water is shown in Fig. 5.3. Here again, there is virtually no intermolecular interaction as evidenced

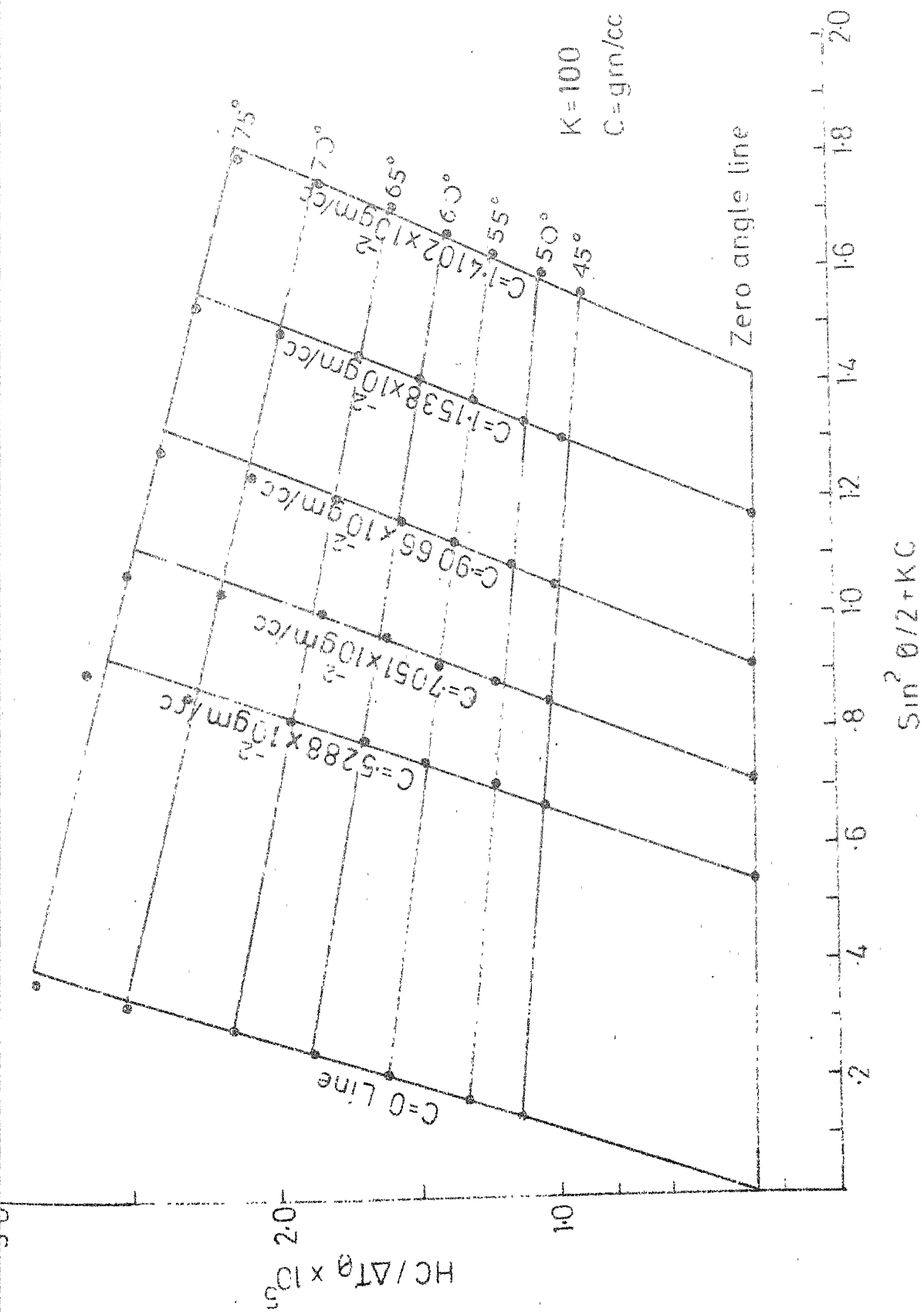


FIG. 53 ZIMM PLOT FOR HIGH MOL. WEIGHT NONIONIC MICELLE (PPG-4)

in slope of the zero angle line. The average molecular weight for PPG-4 micelle is calculated to be  $3.3 \times 10^5$ , indicating an aggregation number of about 1200 molecules, remarkably similar to the trimer nonionic. The radius of gyration of PPG-4 micelles calculated from the slope at zero concentration line of Fig. 5.3 comes out to be 2115 Å. The  $P^{-1}\theta$  dependence of  $\sin^2\theta/2$  for PPG-4 is illustrated in Fig. 5.10 and the dependence of  $P^{-1}\theta$  on the product  $ksR_g$  is illustrated in Fig. 5.11. The plot is identical with that of PPG-3, indicative of the identity of the shapes of the micelles in both cases. Once again we reiterate that this curve is incompatible with the spherical, rod like, ellipsoid of low axial ratio, or statistical coil shape for the micelle. In analogy to the argument presented for PPG-3 above, we tentatively retain the possibility of an asymmetric ellipsoid or a rectangular 'McBain box' as the shape of PPG-4 micelles.

We have also studied the interaction between the collector Na-DBS; and the frothers PPG-3 and PPG-4 by light-scattering. In particular, it is of interest to know whether mixed micelles are formed in these binary mixtures, particularly when the concentration of NaDBS is below its cmc. First, it is necessary to study the size, shape and cmc of Na-DBS micelles themselves. Fig. 5.4 gives the light scattering plot for pure NaDBS in aqueous solution in the concentration range,  $9 \times 10^{-3}$  g/ml to  $2.3 \times 10^{-2}$  g/ml ( $25-60 \frac{m}{l}$  mole/lit) and at various angles.



It is striking that the zero angle line shows a negative slope indicative of intermolecular repulsion arising due to anionic heads. The molecular weight calculated from the zero angle line of the 'Zimm plot' (Fig. 5.4) comes out to be ~~4x8~~  $4.5 \times 10^4$  and the radius of gyration calculated from the slope of  $c = 0$  line comes out to be  $400 \text{ \AA}$ . The shape of the micelle of NaDBS fits with the rod shape of L calculated from the  $R_G$  value equal to  $1400 \text{ \AA}$ ; or a prolate ellipsoid with a reasonably large  $p$ . These observations agree well with reported values in literature for anionic surfactants (9,11). The cmc of Na-DBS is higher than those of PPG-3 and PPG-4 and is approximately  $2 \times 10^{-3} \text{ m/l}$  (Fig. 4.2).

The interaction of PPG-3 with NaDBS has been studied by light-scattering and the results are shown in Figs. (5.5), (5.6), (5.9), and (5.11). The concentration of PPG-3 was always above cmc while that of Na-DBS never exceeded  $8 \times 10^{-4} \text{ m/l}$ . The results of the molecular weight, slope, and the radii of gyration for all these systems are listed in Table 5.2. Here again the 'Zimm plots' are very satisfactory and the zero angle line has essentially zero slope indicative of little net intermolecular interaction. It is interesting that radii of gyration of PPG-3 micelles increase by a factor of 2 to 2.5 upon the addition of Na-DBS and the molecular weight increases almost 20 fold. There is little doubt that we are encountering a 'mixed micelle' system here, with Na-DBS molecules solubilized

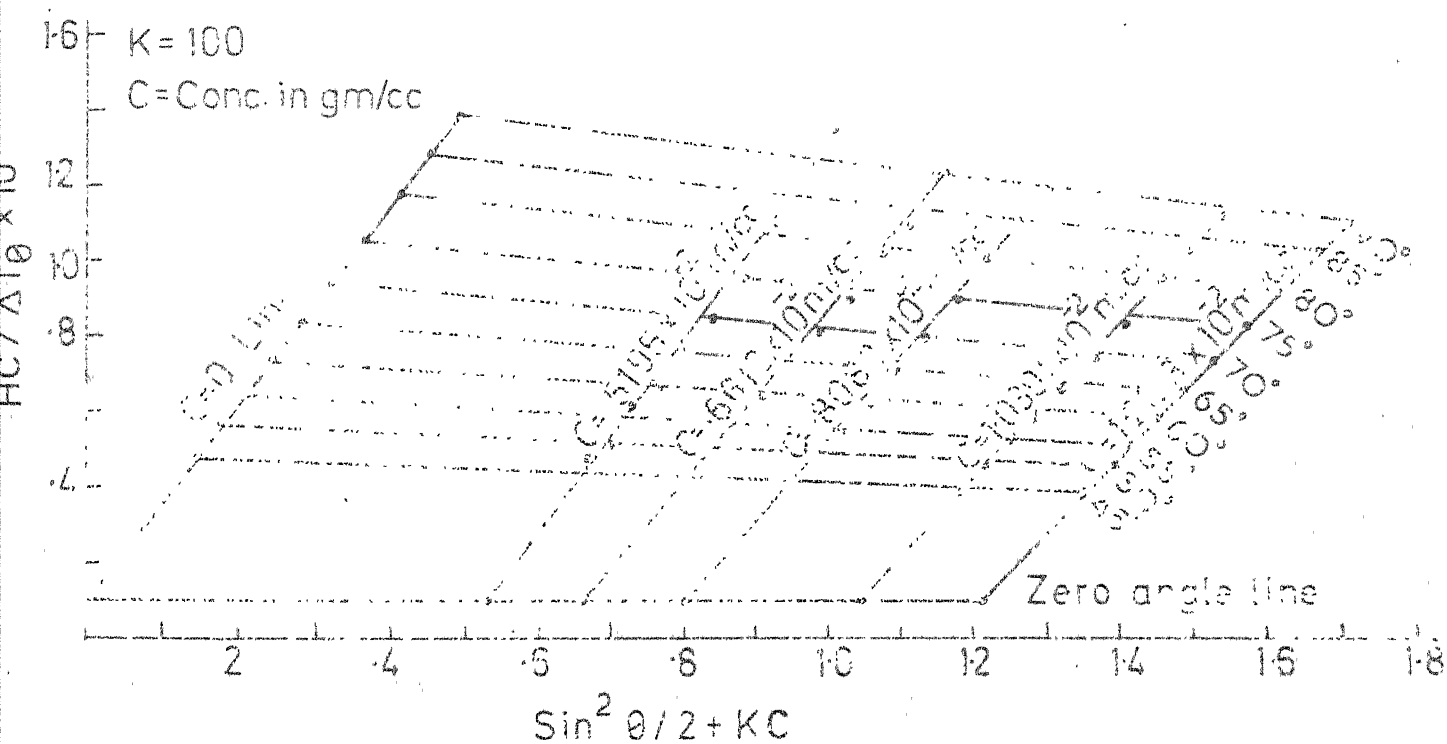


FIG.55 ZIMM PLOT FOR LOW MOL.WEIGHT NONIONIC MICELLE  
 IN PRESENCE OF Na D.B.S. CONC.  $5 \times 10^{-5}$  m/l



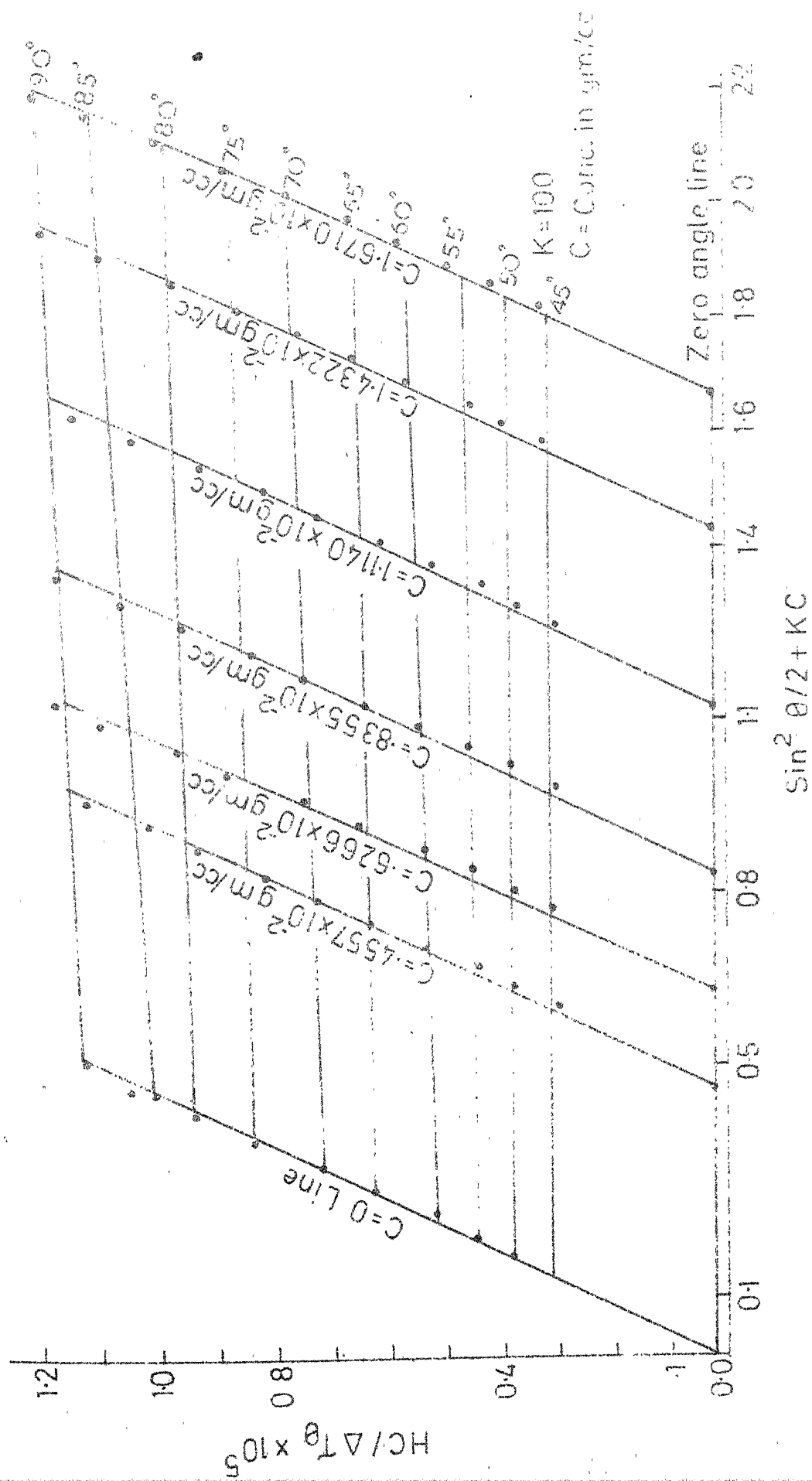


FIG.5.6 ZIMM PLOT FOR LOW MOL.WEIGHT NONIONIC MICELLE IN PRESENCE  
OF Na D.B.S. (CONC.  $8.5 \times 10^{-4}$  m/l)

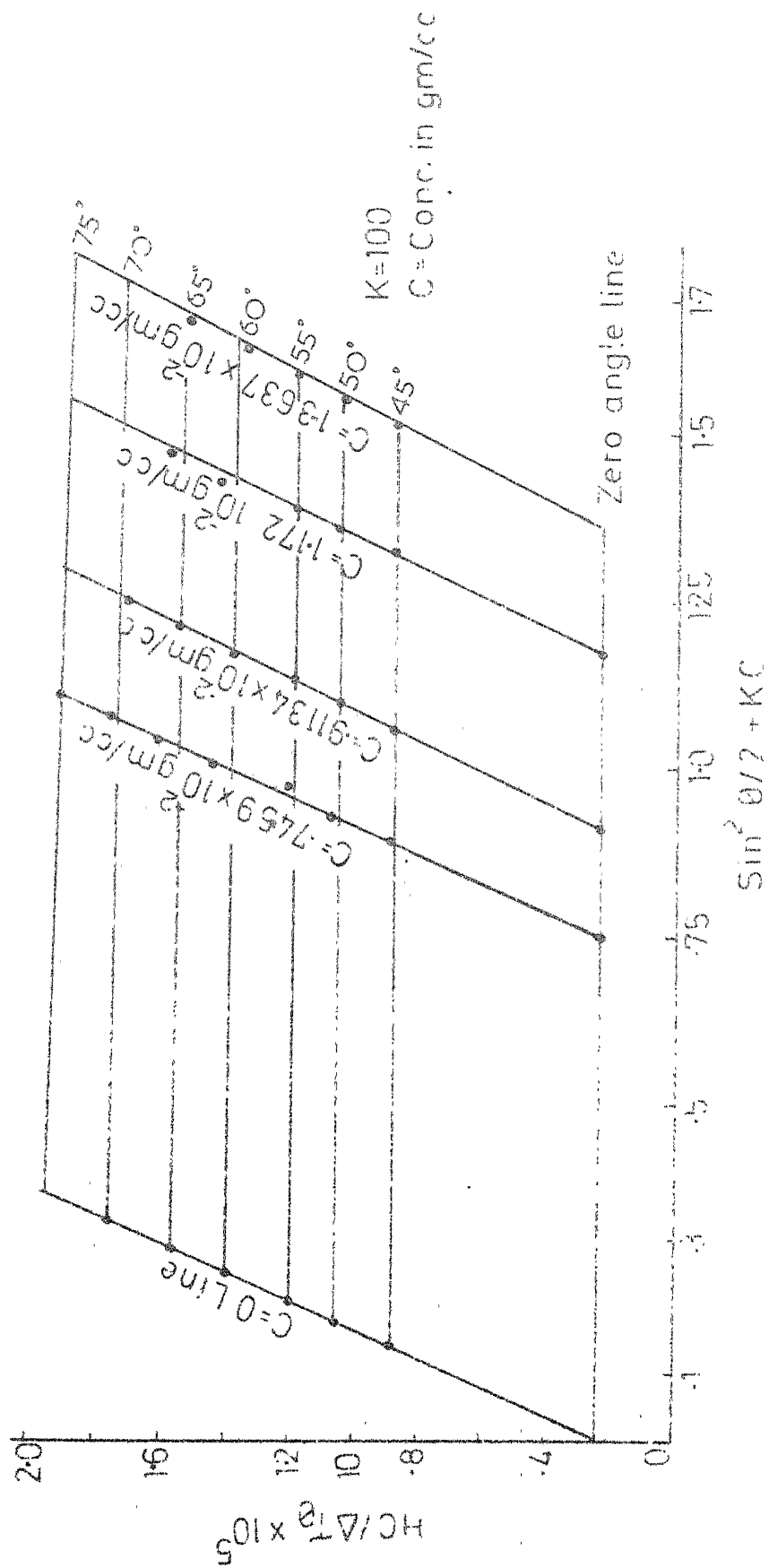


FIG. 57 ZIMM PLOT FOR HIGH MOL. WEIGHT NONIONIC (PPG-4) MICELLE IN PRESENCE OF NaDMS. CONC. =  $2.55 \times 10^{-5}$  M/L

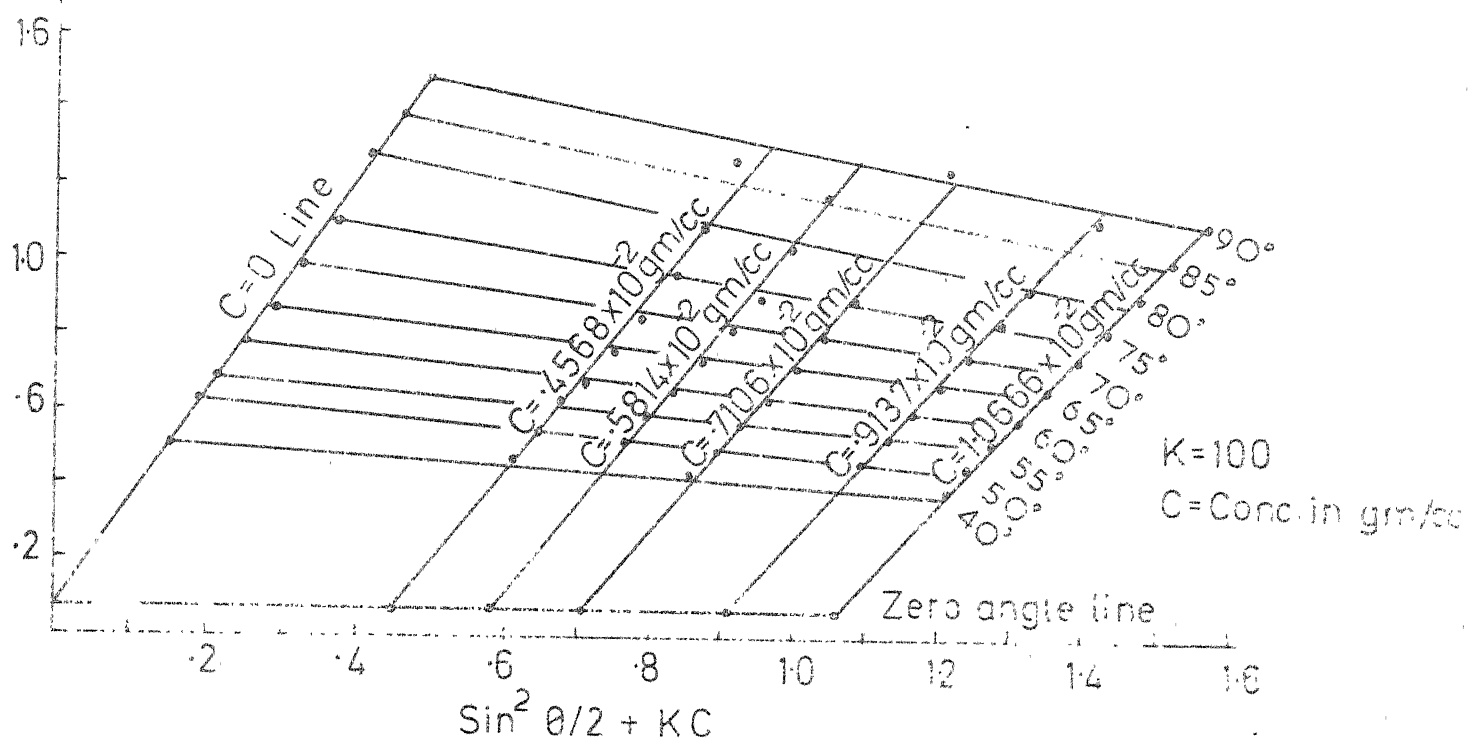


FIG. 58 ZIMM PLOT FOR HIGH MOL. WEIGHT NONIONIC MICELLE  
IN PRESENCE OF Na D.B.S. (CONC- $5 \times 10^{-5}$  m/l)

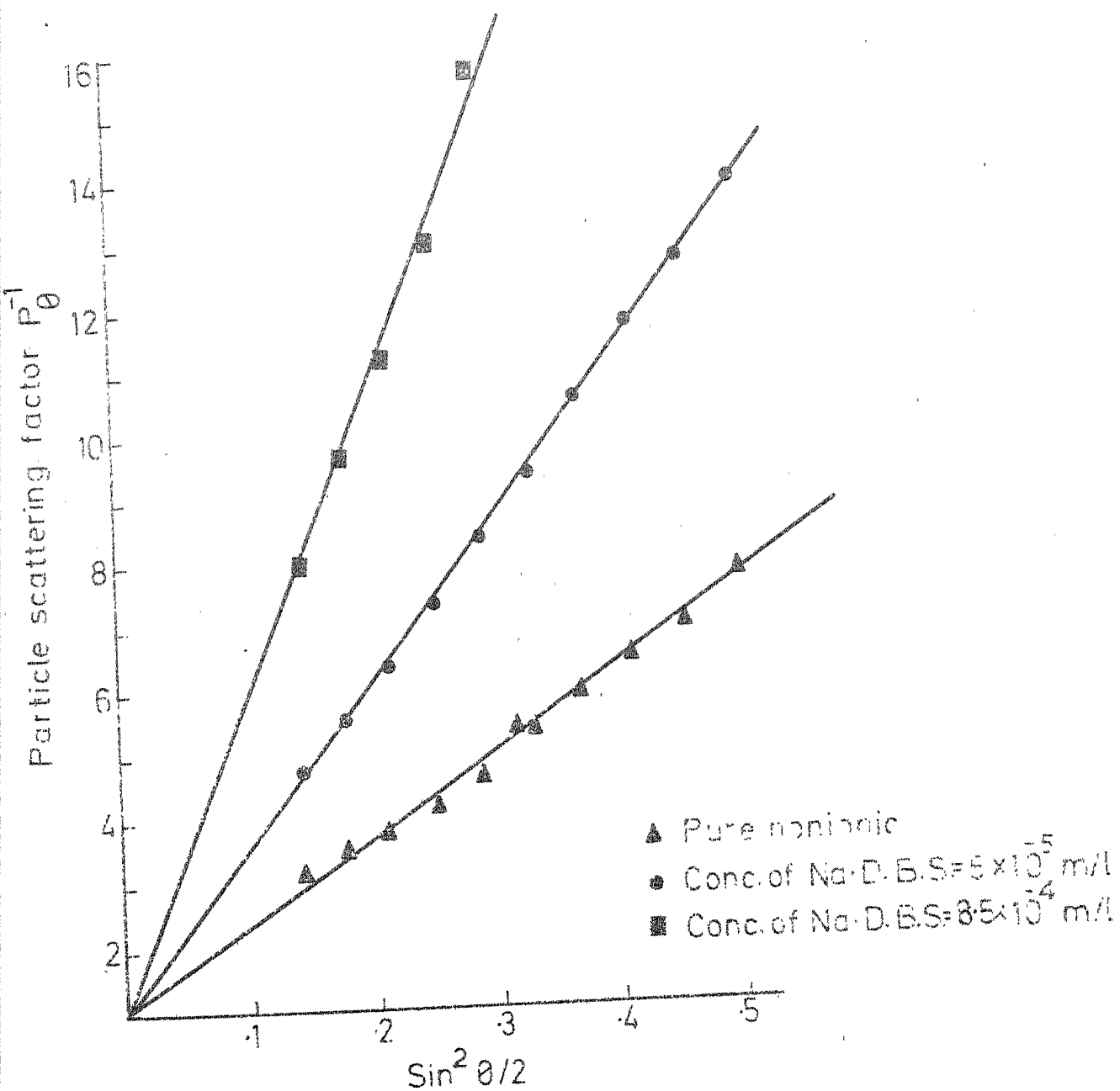


FIG. 5.9 EFFECT OF Na·D.B.S. ON THE PARTICLE SCATTERING FACTOR OF LOW MOL. WEIGHT NONIONIC MICELLE

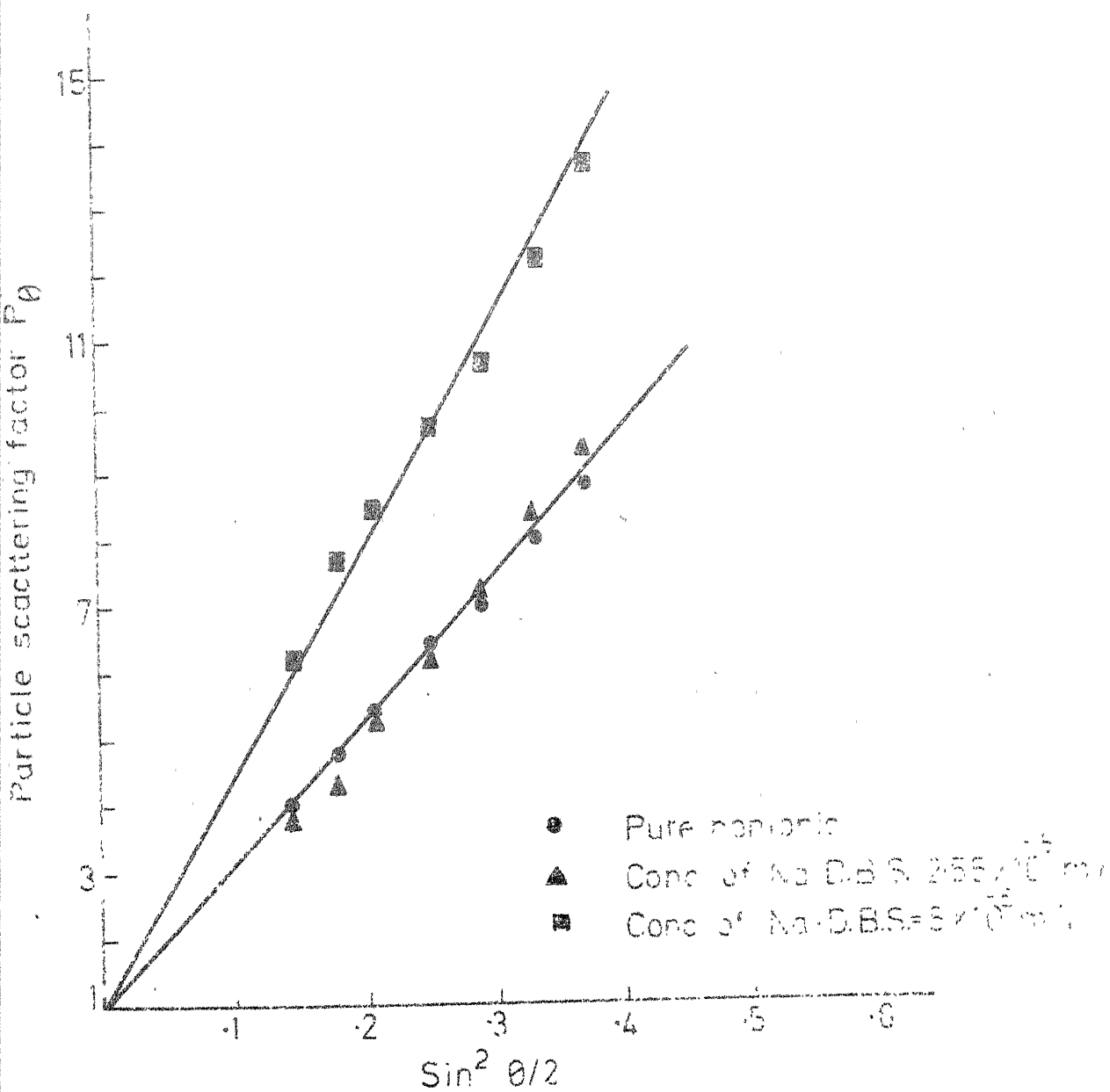


FIG.5.10 EFFECT OF Na-D.B.S. ON THE PARTICLE SCATTERING FACTOR OF HIGH MOL. WEIGHT NONIONIC MICELLE

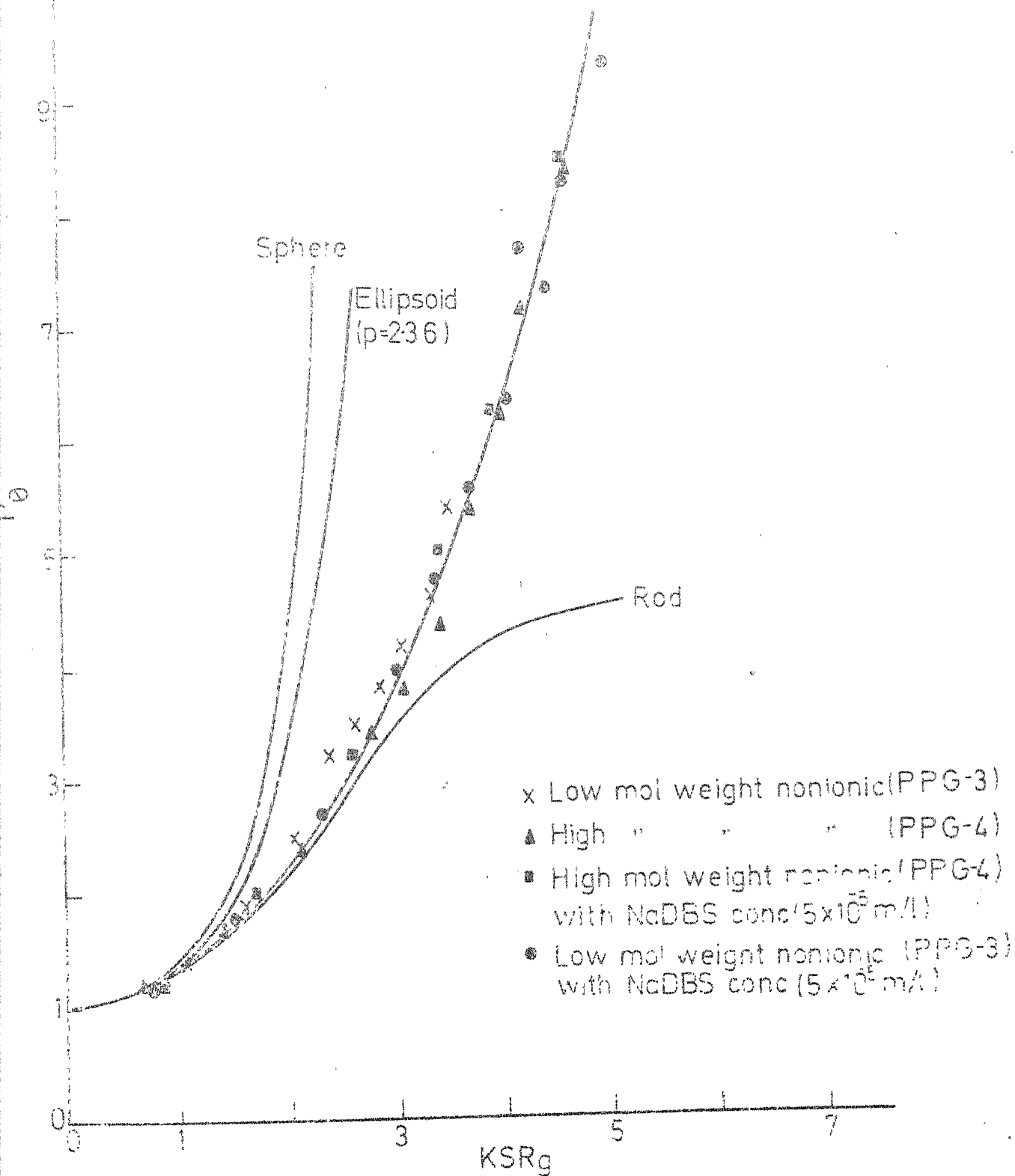


FIG-5.11 PARTICLE SCATTERING FACTOR OF MICELLE Vs  $KSR_g$

and incorporated into nonionic micelles. It also appears that there is no great change in the shape of micelles upon incorporation; Figs.(5.9) and (5.11) both bring out this point clearly. The  $P^{-1}(\theta)$  vs  $ksR_g$  plot for PPG-3, and NaDBS + PPG-3 are identical showing that essentially the same shape is maintained even after NaDBS incorporation into the mixed micelles.

Similar experiments on the system PPG-4 + NaDBS under condition identical to those of PPG-3 have also been done, and the results are reported in Figs. (5.7), (5.8), (5.10) and (5.11), and in Table 5.2. In the formation of mixed micelles PPG-4 behaves exactly as PPG-3 does in incorporating Na-DBS molecules. Upon addition of Na-DBS (always below its cmc) the molecular weight of PPG-4 micelle increases from  $3.3 \times 10^5$  to  $1.3 \times 10^6$  and the radius of gyration increases from  $2115 \text{ \AA}^0$  to  $2600 \text{ \AA}^0$  (Table 5.2). Thus it appears that PPG-4 is somewhat less effective in solubilizing Na-DBS and in increasing micelle size than PPG-3. Here again the inclusion of Na-DBS and formation of mixed micelles leads virtually to neither any net intermolecular interaction nor any change in shape of micelles.

We have also investigated the interaction of PPG-3 complexes with another collector, sodium oleate. The concentration of Na-oleate was below its cmc, and in the range  $10^{-5}$  to  $10^{-4}$  m/l,

Table 5.2

Molecular Weight, Radius of Gyration and Number of Monomers  
of Micelles

Sl. No.	System	Molecular Weight	Slope of $C=0$ line	Radius of Gyration $\langle R_G \rangle, \text{\AA}^0$	No. of Monomers
1.	PPG-3	$2.5 \times 10^5$	$5.2 \times 10^{-5}$	1627	1200
2.	PPG-4	$3.3 \times 10^5$	$6.8 \times 10^{-5}$	2115	1250
3.	Sodium dodecyle Benzene Sulfonate (Na-DBS)	$4.5 \times 10^4$	$1.75 \times 10^{-5}$	400	130
4.	PPG-4 + Na-DBS ( $2.5 \times 10^{-5}$ m/l)	$4.5 \times 10^5$	$4.9 \times 10^{-5}$	2115	Mixed System
5.	PPG-4 + Na-DBS ( $5 \times 10^{-5}$ m/l)	$1.25 \times 10^6$	$2.9 \times 10^{-5}$	2603	Mixed System
6.	PPG-3 + Na-DBS ( $5 \times 10^{-5}$ m/l)	$1.0 \times 10^6$	$2.6 \times 10^{-5}$	2300	Mixed System
7.	PPG-3 + Na-DBS ( $8.5 \times 10^{-4}$ m/l)	$5.0 \times 10^6$	$2.2 \times 10^{-5}$	4555	Mixed System
8.	PPG-4 + Na-01 ( $10^{-5}$ m/l)	$6.25 \times 10^6$	$0.46 \times 10^{-5}$	2407	Mixed System
9.	PPG-3 + Na-01 ( $10^{-5}$ m/l)	$7.7 \times 10^5$	$1.4 \times 10^{-5}$	1456	Mixed System
10.	PPG-4 + Na-01 ( $5 \times 10^{-5}$ m/l)	$2 \times 10^7$	-	-	Mixed System
11.	PPG-3 + Na-01 ( $5 \times 10^{-5}$ m/l)	$1.96 \times 10^7$	-	-	Mixed System
12.	PPG-4 + Na-01 ( $10^{-4}$ m/l)	$5 \times 10^7$	-	-	Mixed System
13.	PPG-3 + Na-01 ( $10^{-4}$ m/l)	$3.5 \times 10^7$	-	-	Mixed System



while those of frothers were above cmc as in the cases above. The Zimm plots for the system (PPG-3 + Na-Ol) are given in Figs. (5.12), (5.13) and (5.14), while those of (PPG-4 + NaOl) are in Figs. (5.15), (5.16) and (5.17). At low concentrations of Na-Ol ( $10^{-5}$  m/l) the Zimm plot looks reasonable, indicates small positive slope for the virial coefficient and suggests the formation of mixed micelles. The molecular weight of (PPG-3 + NaOl) and (PPG-4 + NaOl) are respectively  $7.7 \times 10^5$  and  $6.2 \times 10^6$  and the radii of gyration are  $1456 \text{ \AA}$  and  $2407 \text{ \AA}$  respectively. However, when greater amounts of Na-Ol were added to PPG-3 samples, the  $C = 0$  lines in the Zimm plots take on a positive curvature and at least in one case do not meet with the zero angle line at the y-axis. This discrepancy may arise possibly due to the likelihood of Na-Ol hydrolysing in solution as its concentration increases.

Powney and Jordan (42) have measured the degree of hydrolysis of Na-Ol as a function of concentration and have shown that at  $8 \times 10^{-5}$  m/l the degree of hydrolysis is minimum, increasing sharply below and above this concentration. It is particularly interesting that the hydrolysis is maximum in the micellar phase. Thus it is possible that complications due to hydrolysis arise in the mixed micelle system (PPG + NaOl) which make estimation of  $R_G$  values difficult, despite the low concentration of Na-Ol.

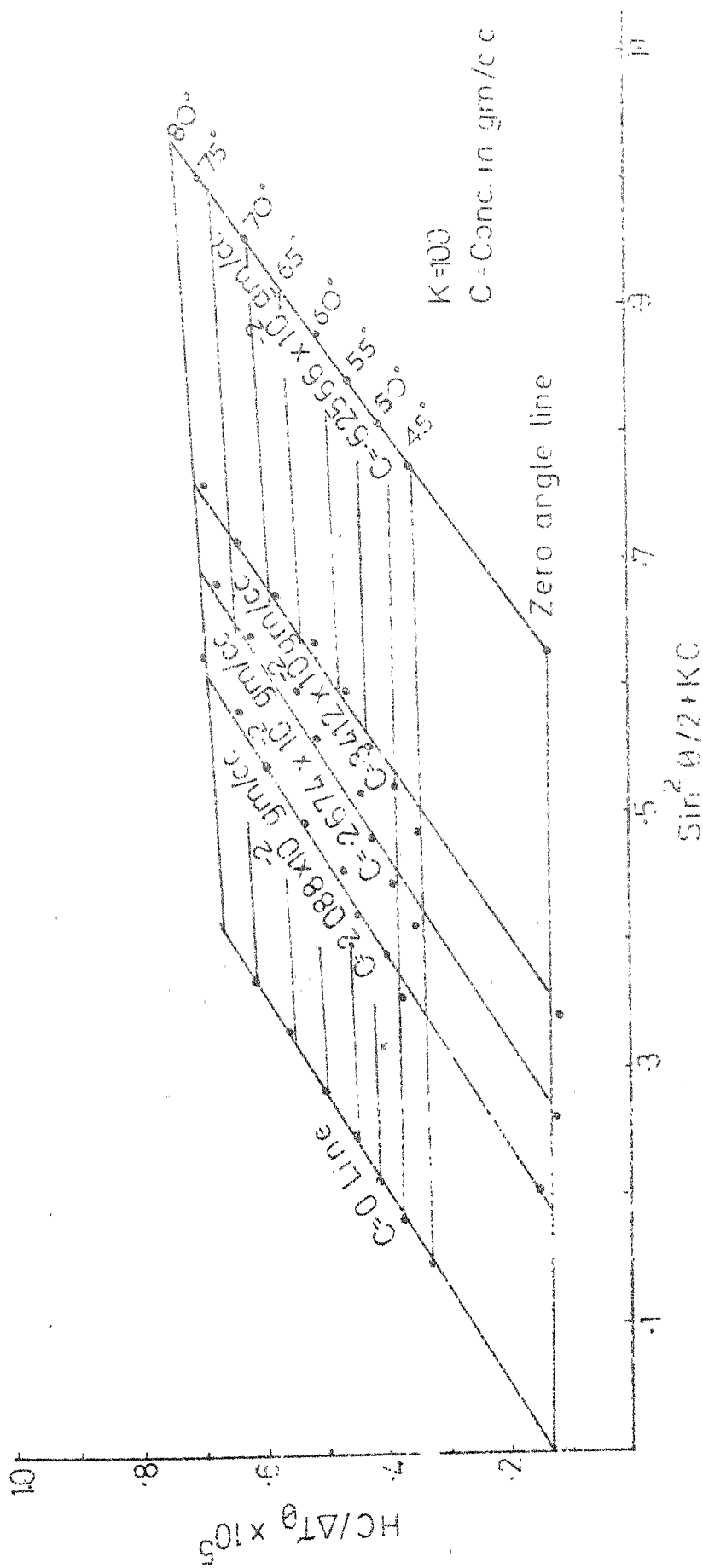


FIG. 5-12 ZIMM PLOT FOR LOW MOL. WEIGHT NONIONIC (PPG-3) MICELLE (CONC. OF SODIUM OLEATE =  $10^{-5} \text{ m/l}$ )

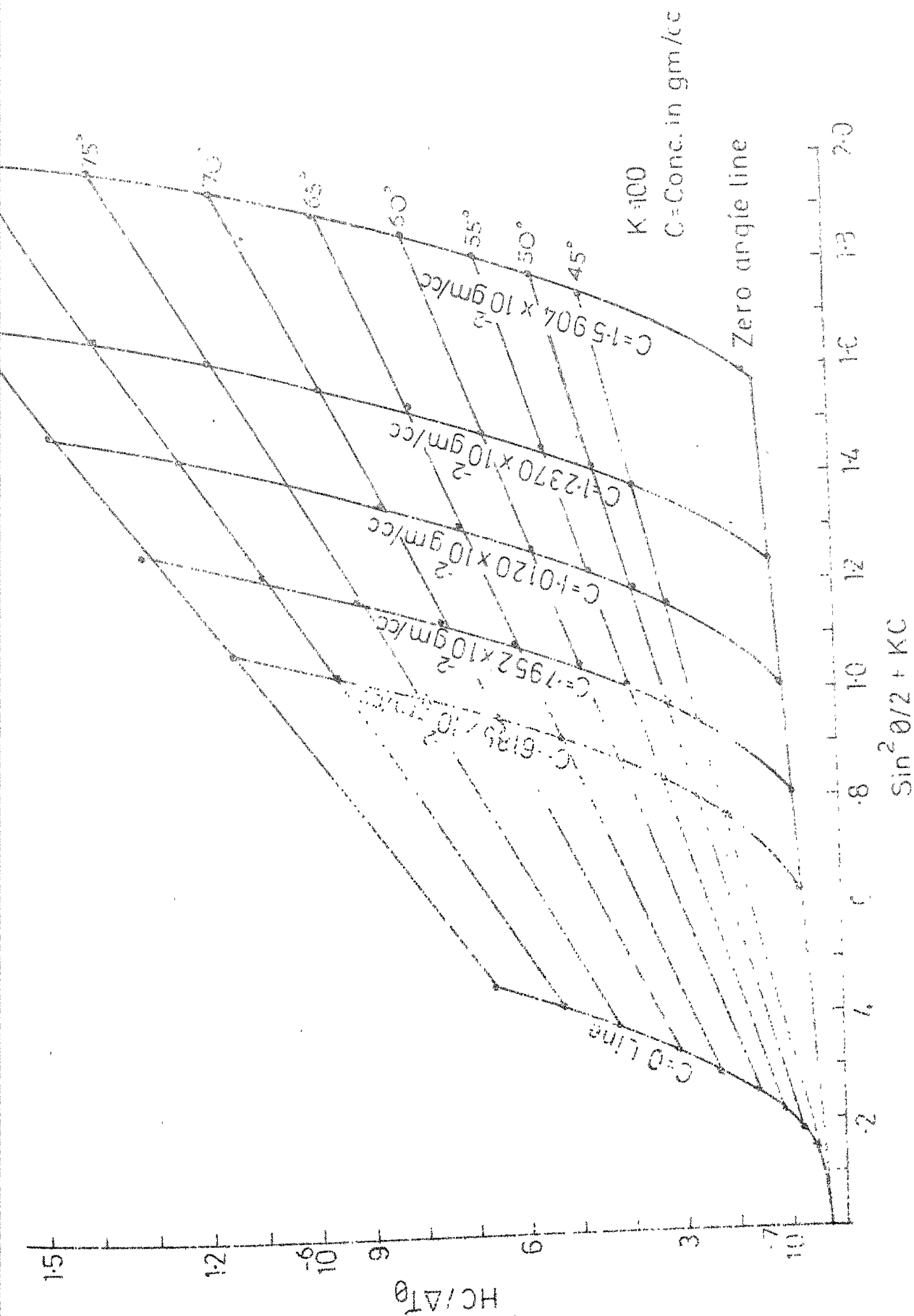


FIG. 5B ZIMM PLOT FOR LOW MOL. WEIGHT NONIONIC MICELLE IN PRESENCE  
 OF SODIUM OLEATE (CONC =  $5 \times 10^{-5}$  m/l)

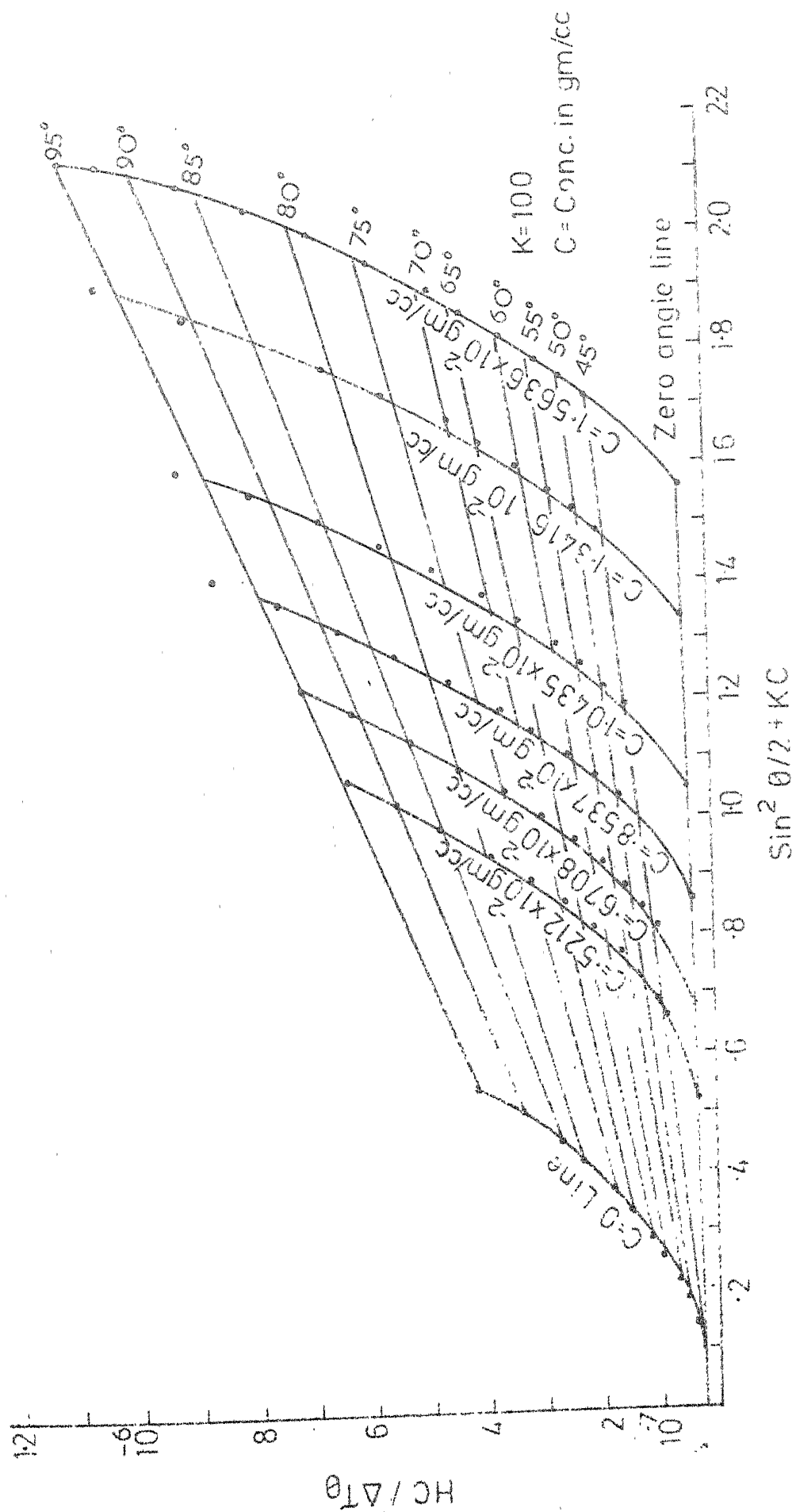


FIG. 5.14. ZIMM PLOT FOR LOW MOL. WEIGHT NONIONIC MICELLE IN PRESENCE  
 OF SODIUM OLEATE  $\text{CONC.} = 10^{-4} \text{ m/l}$

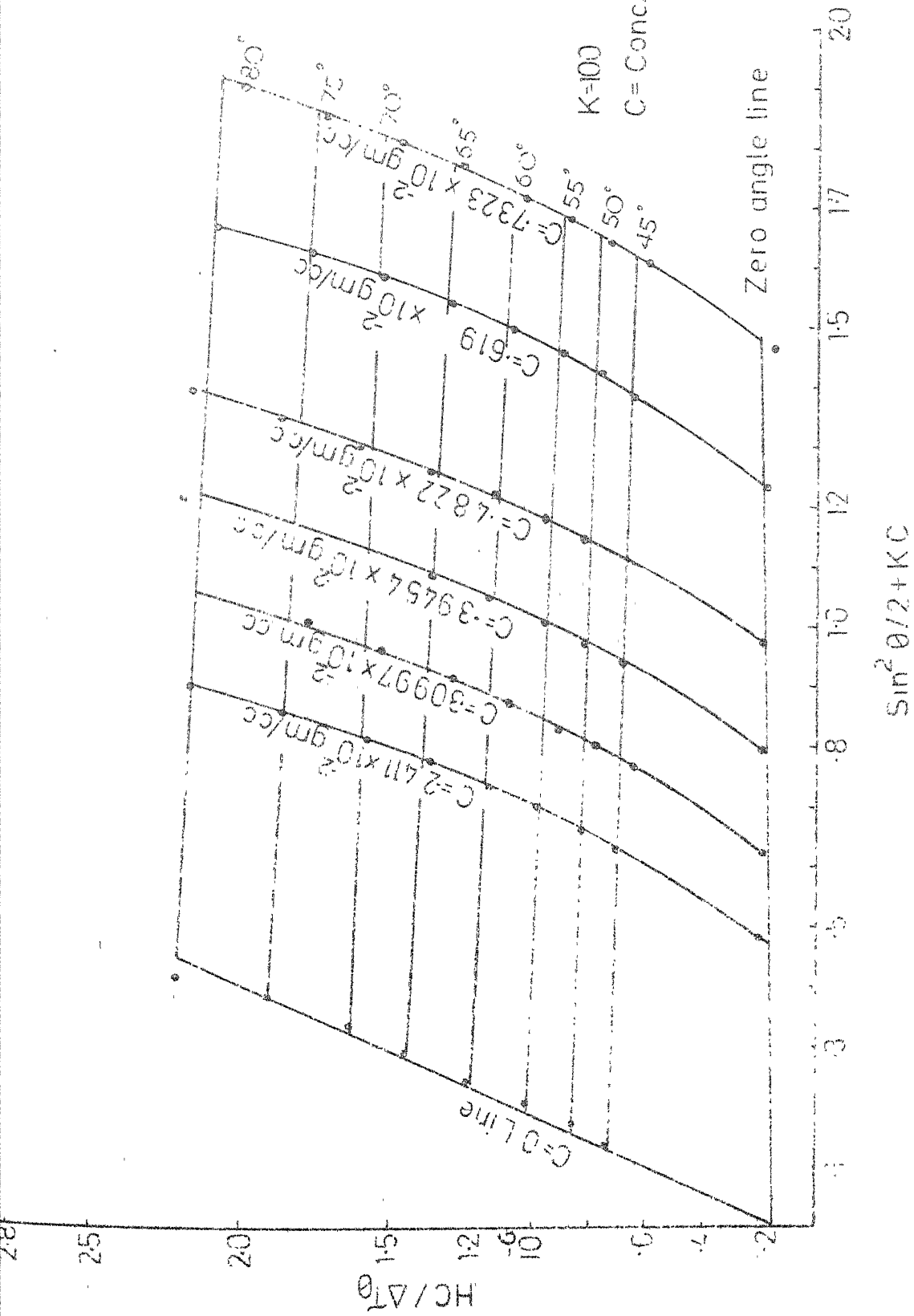


FIG. 515 ZIMM PLOT FOR HIGH MOLE WEIGHT NONIONIC (PPG-4) MICELLE IN PRESENCE OF  
 SODIUM OLLATE (CONC.  $= 10^{-5} \text{ m/l}$ )

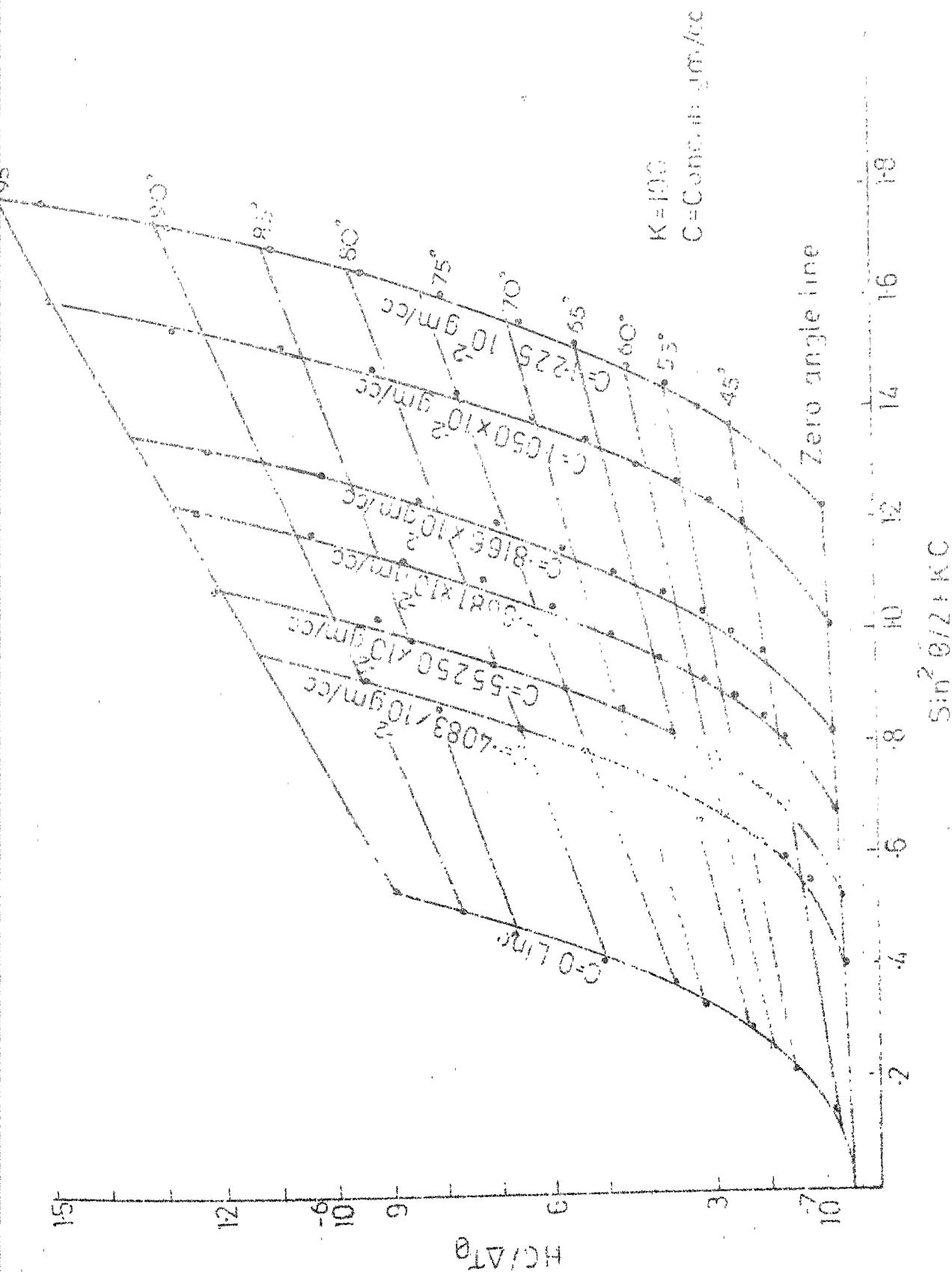


FIG. 5-15 ZIMM PLOT FOR HIGH MOL. WEIGHT NONIONIC MICELLE IN PRESENCE OF SOLUBLE SALT (CONC =  $5 \times 10^{-3}$  M)

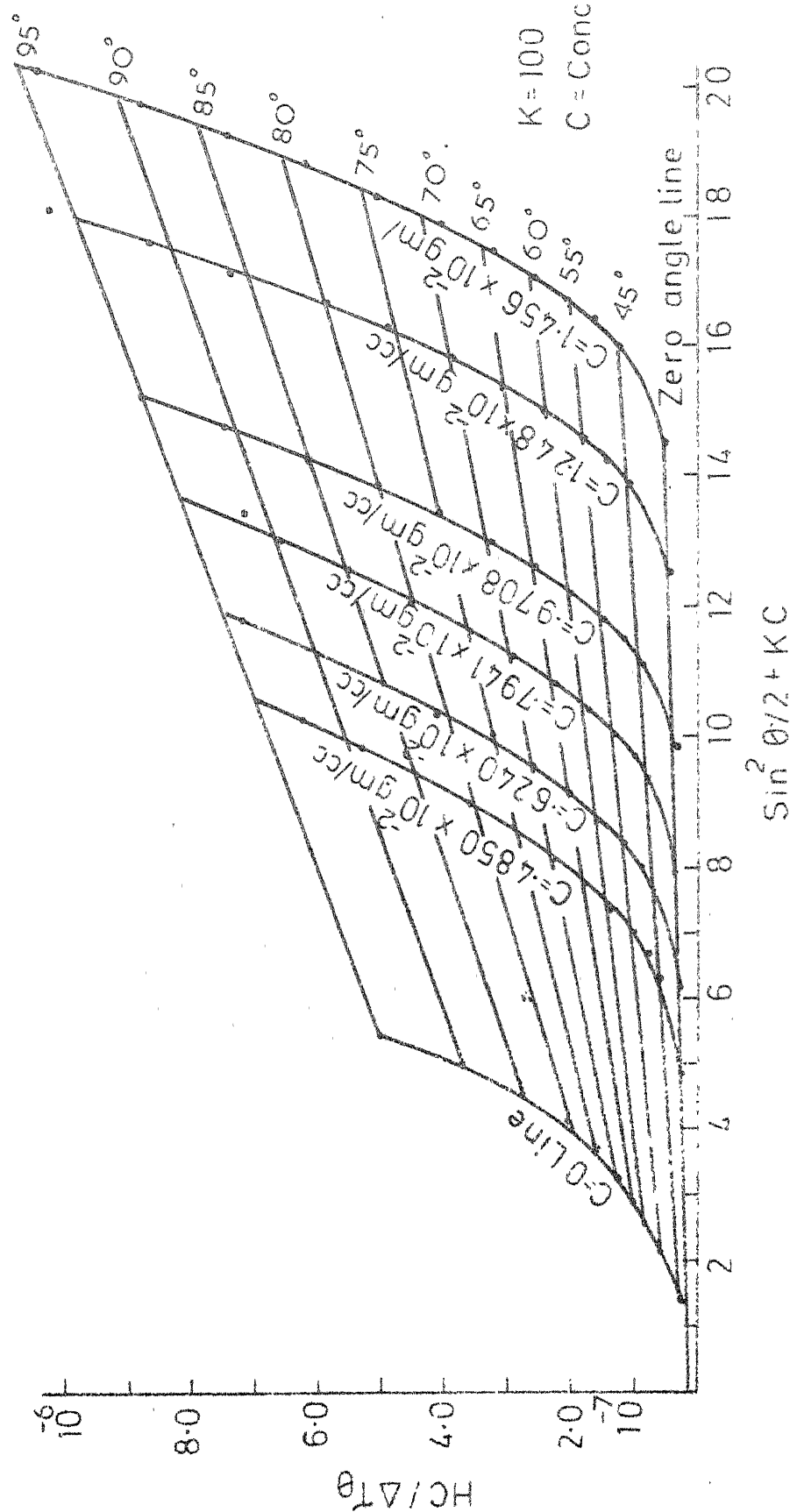
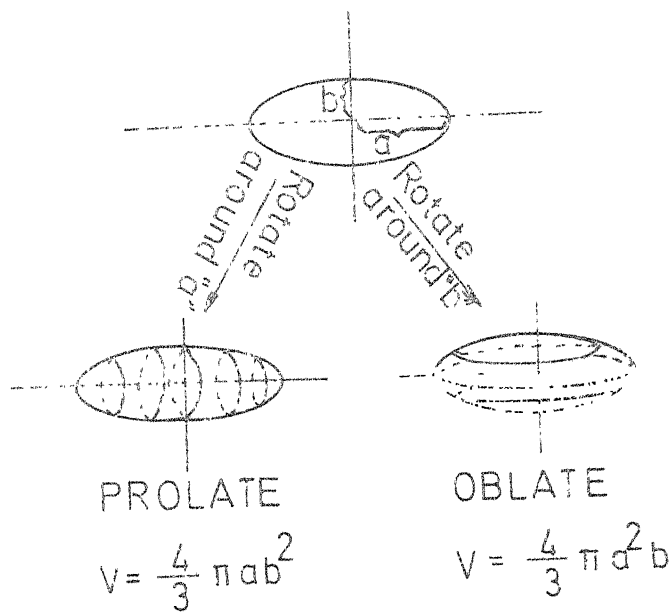
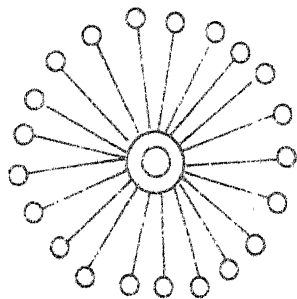


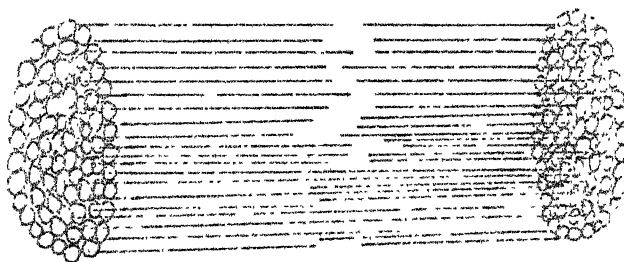
FIG.517 ZIMM PLOT FOR HIGH MOL. WEIGHT NONIONIC MICELLE IN PRESENCE OF SODIUM OLEATE (CONC. =  $10^{-4}$  m/l)



GENERATION OF PROLATE AND OBLATE ELLIPSOIDS



RADIAL OR "SAUSAGE" MODEL



LONGITUDINAL OR LOG BOOM MODEL

FIG. 5.18



We have shown, by using the light-scattering technique that (1) PPG aggregates to form micelles in aqueous system; (2) the aggregation number at  $35^{\circ}\text{C}$  is of the order of  $10^3$ ; (3) the shape of micelles has not been unequivocally established, but an unsymmetrical ellipsoid of revolution or rectangular McBain type box shape cannot be ruled out; (4) NaDBS is solubilized into, and gets incorporated in, PPG to form mixed micelles whose shapes are essentially the same as that of the pure nonionic micelles; (5) At low concentration, NaOl also gets solubilized in, and forms mixed micelles with PPG. At high concentrations, hydrolysis of Na-Ol within the mixed micelle renders the light-scattering data difficult to interpret in terms of radius of gyration and shape. However, it appears that the greater increase in molecular weight of PPG micelle seen upon the addition of sodium oleate as compared to Na-DBS can be interpreted as due to stronger interaction between sodium oleate and the nonionic molecule. The molecular weight of PPG-3 micelle increases from  $2.5 \times 10^5$  to  $1.0 \times 10^6$  upon addition of Na-DBS (concentration =  $5 \times 10^{-5}$  m/l) and from  $2.5 \times 10^5$  to  $1.96 \times 10^7$  upon addition of sodium oleate (Concentration =  $5 \times 10^{-5}$  m/l). Similar results were obtained for PPG-4 micelles.

## REFERENCES

1. Koch, A.L.  
Calculations on Turbidity of Mitochondria and Bacteria  
(1961), Biochimica Biophysica Acta, 51, 429-444.
2. Debye, P.  
Light-Scattering in Soap Solutions  
(1949), J. Phys. Chem., 53, 1-8.
3. Debye, P., and Anacker, E.W.  
Micelle Shape From Disymmetry Measurements  
(1951), J. Phys. Chem., 55, 644-655.
4. Mysels, K.J.  
Charge Effect in Light-Scattering by Colloidal Solutions  
(1954), J. Phys. Chem., 58, 303-307.
5. Mysels, K.J.  
Charge Effect in Light-Scattering by Colloidal Solutions  
(1955), J. Colloid Science, 10, 507-522.
6. Prins, W., and Hermans, J.J.  
Theory of Light-Scattering by Detergent Solutions  
(1956), Proc. Konn. Ned. Akad. Wetenschap, B 59, 162-170.
7. Prins, W., and Hermans, J.J.  
Light-Scattering by Solutions of Sodium Alkyl Sulfate  
(1956), Proc. Konn. Ned. Akad. Wetenschap, B 59, 298-311.
8. Princen, L.H., and Mysels, K.J.  
Light-Scattering by Ideal Colloidal Electrolyte  
(1957), J. Colloid Science, 12, 594-605.
9. Mysels, K.J., and Princen, L.H.  
Light-Scattering by Some Lauryl-Sulfate Solutions  
(1959), J. Phys. Chem., 63, 1696-1700.

10. Anacker, E.W.  
Light-Scattering by Solutions of Cetylpyridinium Chloride  
(1958), J. Phys. Chem., 62, 41-45.
11. Kushner, L.M., and Hubbard, W.D.  
Light Scattering and Micelle Structure in the System Sodium Dodecyl Sulfate- Sodium Chloride-Water  
(1955), J. Colloid Science, 10, 428-435.
12. Timasheff, S.N., and Coleman, B.D.  
The Extrapolation of Light-Scattering Data to Zero Concentration  
(1959), Arch. Biochem. Biophys., 83, 60-75.
13. McIntyre, D., and Gornick, F.  
Light-Scattering From Dilute Polymer Solutions  
(1964), Gordon and Breach Science, Publishers, (New York).
14. Mankowich, A.M.  
Micellar Molecular Weights of Selected Surface Active Agents  
(1954), J. Phys. Chem. 58, 1027-1030.
15. Sirianni, A.F., Cowle, J.M.G., and Puddington, I.E.  
The Number Av. and Mw of Some Nonionic Surface Active Agents  
(1962), Can. J. Chem., 40, 957-962.
16. Kushner, L.M., and Hubbard, W.D.  
Viscometric and Turbidimetric Measurements on Dilute Aqueous Solution of a Non-ionic Detergents  
(a) (1954), J. Phys. Chem., 58, 1163-1167.  
(b) (1957), J. Phys. Chem., 61, 371-372.
17. Schick, M.J., Atlas, S.M., and Eirich, E.R.  
Micellar Structure of Non-ionic Detergents  
(1962), J. Phys. Chem., 66, 1326-1333.
18. Attwood, D.  
The Effect of Electrolyte on the Micellar Properties of an Anionic-Nonionic Detergent in Aqueous Solutions  
(1964), Kolloid, Z.U.Z. Poly., 232, Heft 2, 788-792.
19. Nakagawa, T., Koriyama, K., and Inoue, H.  
Micellar Weights of Nonionic Surfactants in the Presence of n-Decane or n-Decanol  
(1960), J. Colloid Science, 15, 268-277.

20. Elworthy, P.H., and McDonald, C.  
Variation of the Micellar Structure of Some  
Synthetic Nonionic Detergents with Temperature  
(1964), Kolloid, Z.U.Z. Poly., 195, Heft 1, 16-27.
21. Attwood, D.  
A Light-Scattering Study of the Effect of Temperature  
on the Micellar Size and Shape of Nonionic Detergent  
in Aqueous Solutions  
(1968), J. Phys. Chem., 72, 339-345.
22. Corkill, J.M., Goodman, J.F., and Walker, T.  
Light-Scattering From Aqueous Solutions of Octyl  
Sulphanyl Alkonates  
(1967), Trans. Farad. Soc., 63, 759-767.
23. Elworthy, P.H., and Florence, A.T.  
Light-Scattering and Viscosity Studies on a Series of  
Synthetic Nonionic Detergents  
(1965), Kolloid, Z.U.Z. Poly., 204, 105-111.
24. Balmbra, R.R., Clunie, J.S., Corkill, J.M., and  
Goodman, J.F.  
Effect of Temperature on the Micelle Size of a  
Homogeneous Nonionic Detergent  
(1962), Trans. Farad. Soc., 58, 1661-1667.
25. Balmbra, R.R., Clunie, J.S., Corkill, J.M. and  
Goodman, J.F.  
Variation in the Micelle Size of Nonionic Detergents  
(1964), Trans. Farad. Soc., 60, 979-985.
26. Corkill, J.M., Goodman, J.F., and Ottowill, R.H.  
Micellization of Homogeneous Nonionic Detergents,  
(1961), Trans. Farad. Soc., 57, 1627-1636.
27. Corkill, J.M., and Herrmann, K.W.  
Solution Structure in Concentrated Nonionic  
Surfactant System  
(1963), J. Phys. Chem., 67, 934-937.
28. Elworthy, P.H., and Macfarlane, C.B.  
Micellar Structure of a Series of Synthetic Nonionic  
Detergents  
(1962), J. Chem. Soc., 534-541.
29. Elworthy, P.H., and Macfarlane, C.B.  
Micellar Structure of a Series of Synthetic Nonionic  
Detergents  
(1963), J. Chem. Soc., 907-914.

30. Becher, P., and Arai, H.  
Nonionic Surface Active Compounds. XI. Micellar Size, Shape and Hydration From Light-Scattering and Hydrodynamic Measurements  
(1968), J. Colloid. Interf. Sci., 27, 634-641.
31. Tokiwa, F., and Aigami, K.  
Light-Scattering and Electrophoretic Studies of Mixed Micelle of Ionic and Nonionic Surfactants  
(1970), Kolloid, Z.U.Z. Poly., 239(2), 687-691.
32. Schick, M.J.  
Physical Chemistry of Nonionic Detergents  
(1963), J. Am. Oil Chem. Soc., 40, 680-687.
33. Mankowich, A.M.  
Micellar Relationship of an Anionic-Nonionic Surfactant Mixture  
(1964), J. Am. Oil Chem. Soc., 41, 443-452.
34. Shinoda, K., Nakagawa, T., Tamamushi, B., and Isemura, T.  
Colloid Surfactants  
(1963), Academic Press, (New-York), 135-138.
35. Kuriyama, K., Inoue, H., and Nakagawa, T.  
Temperature Dependence of Micellar Weight of Nonionic Surfactant in the Presence of Various Additives  
(1962), Kolloid Z.U.Z. Poly., 183(2), 68-71.
36. Soloveva, T.S., Eromina, L.V., and Panich, R.M.  
Characteristics of Micelle Formation in Mixed Solution of Ionic and Nonionic Surfactants  
(1969), Colloid Journal of U.S.S.R., 31, 229-232.
37. Becher, P.  
Nonionic Surfactant (Schick, M.J., ed.), Vol. I.  
(1967), Marcel Dekker Inc., (New-York), 478-513.
38. Petres, J.J., and Dezetic, G.  
Light-Scattering by Large Ellipsoidal Particles  
(1975), J. Colloid, Interf. Sci., 50(2), 296-306.

39. Favro, L.D.  
Theory of the Rotational Brownian Motion of a  
Free Rigid Body  
(1960), Physical Review, 119, 53-62.
40. McBain, J.W., and Lee, W.W.  
Vapor Pressure Data and Phase Diagrams of Some  
Concentrated Soap-Water Systems  
(1943), Oil Soap Chicago, 20, 17-25.
41. Shah, D.O., and Hamlin, R.M.  
Structure of Water in Microemulsions  
(1971), Science, 171, 483-485.
42. Powney, J., and Jordon, D.O.  
The Hydrolysis of Soaps as Determined From Glass  
Electrode pH Measurements  
(1938), Trans. Farad. Soc., 34, 363-371.

at various concentration which give information about the micellar properties. However, most of these measurements have been done on single surfactant compounds (1-17), and not on mixed micellar system. Tokiwa (18,19) and Nakagawa (20) have described in detail NMR investigation on interaction between anionic and nonionic surfactants in aqueous solutions. where a mathematical analysis of the chemical shifts yielded several interesting parameters concerning the constitution of mixed micelle.

In any study of the interaction between nonionics, e.g. PPG, and collector e.g., Na-oleate, Na-DBS, or SDS, the concentration of the two species could be expected to be important in governing the nature, extent and mechanism of interaction. Such frother-collector interaction would therefore be a sensitive function of the molar ratio of collector to frother i.e., Na-DBS/PPG, which we shall denote as  $C$  henceforth. At low value of  $C$ , one expects solubilization of collector in the frother; if the frother concentration is above its cmc, such solubilization would amount to an incorporation of the collector in the frother micelle. Alternatively, if the value of  $C$  is high and if the collector molecules form micellar aggregates, incorporation of the frother in collector micelles is likely. In the intermediate range of  $C$  existence of mixed micelles are distinct possibilities. Indeed light-scattering experiments of

Chapter V show that such mixed micelles are formed, with the mol. weight of the mixed micelle increasing with C. Such mixed micelles incorporating two surfactants, one ionic and the other nonionic, have been reported in literature and studied in some detail. We are concerned here with the molecular aspects of such mixed micelle formed between PPG and Na-DBS for the following reasons.

While mixed micelles are formed between PPG and sodium oleate, we were not able to monitor any NMR chemical shift in this system. Similar observation was also made by Tokiwa (18) for the system sodium dodecyl sulphate (SDS) and nonionic ( $C_{12}$ POE). The problem apparently is one of having too many environmentally similar- $CH_2$  group protons which all resonate at approximately the same NMR frequency range. On the other hand, Na-DBS has benzene protons that not only resonate at considerably lower fields than the other protons, but also serve as a 'handle', since they are influenced, and in turn influence the chemical shift positions of the other protons in the mixture.

In a mixed micelle involving PPG and Na-DBS, it is likely that those protons of PPG that are packed facing the benzene ring will experience the ring current para magnetism and will be upfield shifted. Besides this, the number ratio of Na-DBS/PPG can also be easily monitored by integrating the



NMR spectrum. Tokiwa and Tsujii (18) have in fact failed to observe any chemical shift difference for the protons of the nonionics in presence of SDS, where as the effect of Na C<sub>8</sub>BS is pronounced.

## VI.2 EXPERIMENTAL:

The NMR spectra were run on a varian A 60 D spectrometer at the probe temperature of 39.5°C. Solutions of the surfactants were made in D<sub>2</sub>O, in order to eliminate the signals of water protons that would swamp the solute signals if H<sub>2</sub>O were the solvent. The concentration range used in NMR is necessarily much longer than in other experiments since the signals are weak; thus the concentrations of Na-DBS, and of PPG used were well above the cmc values. The NMR experiments were thus conducted in the post-micellar regions of the surfactants. The effects of Na-DBS on the PPG protons were studied by keeping the concentration of PPG constant ( $4 \times 10^{-2}$  g/ml), and varying the amount of Na-DBS; i.e. the molar ratio  $C = [\text{Na-DBS}]/[\text{PPG}]$ . The chemical shifts were measured in parts per million (ppm) with respect to the standard tetramethyl silane (TMS) which was inserted into the NMR tube, in a sealed capillary tube as an external reference. No bulk susceptibility corrections were made since the interest was in the relative shifts as a function of C. The positions of relevant protons were measured to an accuracy of  $\pm 0.2$  Hz.

Most of the spectra were run with 50 Hz sweepwidth in the regions of interest.

### VI.3 RESULTS AND DISCUSSION:

We describe in this chapter the interaction between PPG and the nonionic surfactant Na-DBS.

Upon the addition of increasing amounts of Na-DBS to aqueous solutions of PPG (degree of polymerization  $p = 3$  and also  $p = 4$ ) line broadening of the methylene and methine signals of the nonionics occurs, indicating an interaction wherein the environment of these protons is presumably somewhat more rigid. Besides this broadening, the  $\text{CH}_2$  and  $\text{CH}$  protons are also upfield shifted as a function of the molar ratio ( $C = \text{Na-DBS/PPG}$ ). (The results are illustrated in Fig. 6.1 and listed in Tables 6.1 and 6.2).

Table 6.1 summarizes the data of the NMR studies of mixtures of Na-DBS with the low mol. weight nonionic (PPG-3). The NMR spectrum of Na-DBS shows the aromatic  $\text{C}_6\text{H}_4$  protons in the region 420-470 Hz from TMS (in the A-60D spectrum), whereas the aliphatic protons appear as two broad signals at 46 and 68 Hz. Pure PPG-3 in aqueous solution shows the methyl proton at 70.6 Hz and the  $\text{OCH}$ ,  $\text{OCH}_2$  and  $\text{OCH}_3$  protons collectively near 200 Hz as a complex spectrum, with one sharp line at 204 Hz which presumably is the  $-\text{OCH}_3$  signal.

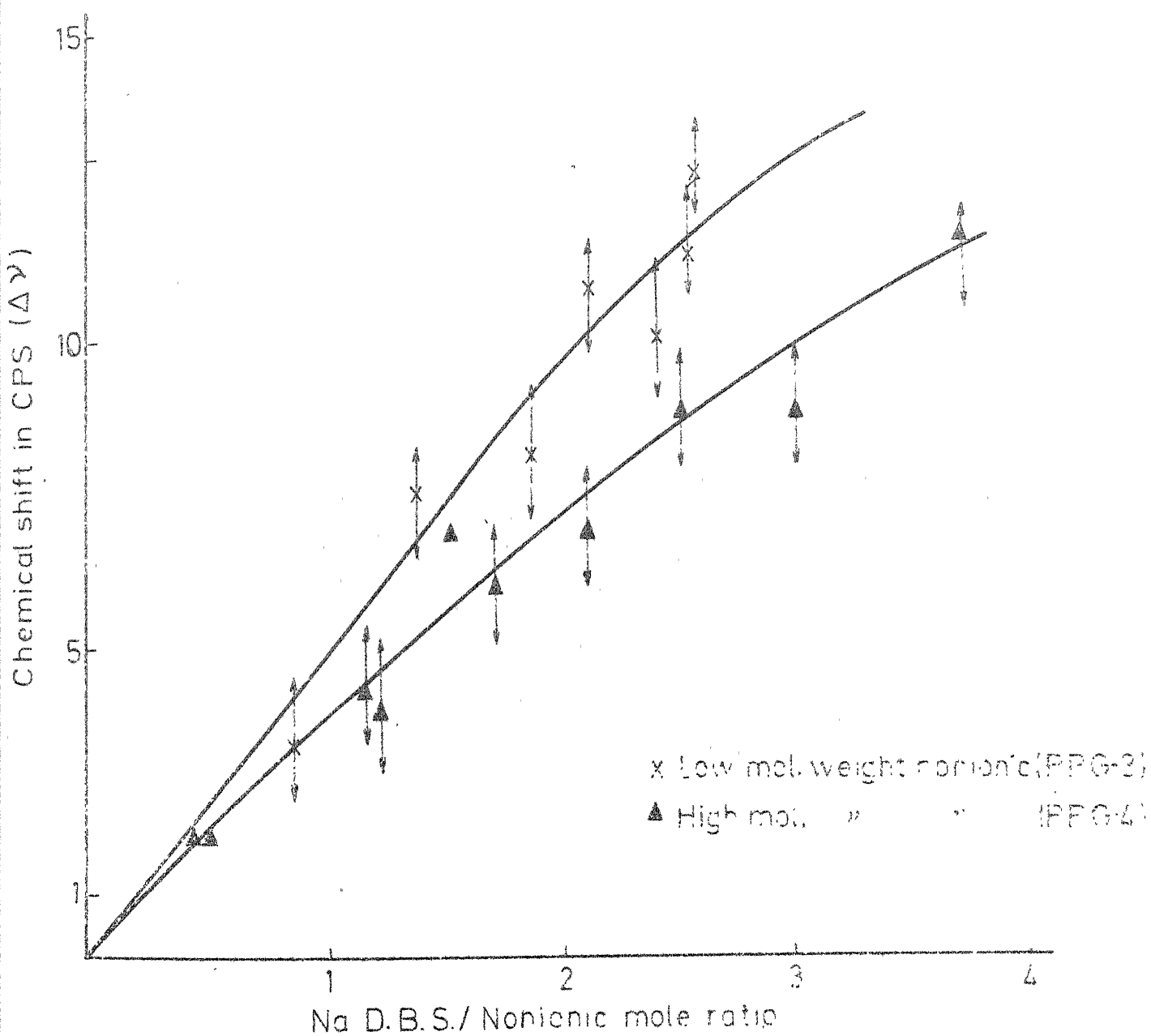


FIG 6.1 EFFECT OF Na D.B.S. ON CHEMICAL SHIFT OF PROPYLENE OXIDE PEAK OF NONIONIC SURFACTANT

NMR Spectral Features of Mixtures of Na-DBS and PPG-3.

Mole Ratio	Peak 1 in Hz 4 Protons	Peak 2 in Hz. 12 Protons	Peak 3 in Hz	$\frac{I \text{ Peak 1}}{I \text{ Peak 2}}$				
Sl.No.	$\frac{\text{Na-DBS}}{\text{PPG}} = C$	Benzene Peak (4 Protons) $\pm 1 \text{ Hz}$	Inte-gral Value	PPG(12 protons) $\text{OCH+OCH}_2 + \text{OCH}_3 \pm 0.2 \text{ Hz}$	Mix.of PPG-3 Me- and Na-DBS $\text{CH}_2 + \text{CH}_3 \pm .2 \text{ Hz}$	Inte-gral Value	Observed	Calculated $\frac{4}{12} \times C = 0.33 \text{ C}$
1.	Only PPG	-	-	204.0	42	70.6	31	-
2.	0.87	426,436, 445,462, 471	12	199.5	42	66.4	85	0.28
3.	1.36	424,434, 444,462, 469	13	195.4	38	63.0	103	0.38
4.	1.86	424,432, 443,461, 469	21	194.8	37	61.6	140	0.57
5.	2.4	424,434, 444,462, 469	21	192.8	40	60.0	170	0.5
6.	2.9	Broad peaks with last peak appearing at 462	19	191.4	24	58.2	187	0.56
7.	Only Na-DBS	423,431, 442,459, 467	17	-	-	46.0 68.0	102	-

Note: All measurements were done in a 60 MHz instrument, with  $S_{TNS} = 0$  Hz.

Table 6.2

## NMR Spectral Features of Mixtures of Na-DBS and PPG -4.

Sl.No.	Mole Ratio	$\frac{\text{NaDBS}}{\text{PPG}} = C$	Peak 1 in Hz	Peak 2 in Hz	Peak 3 in Hz	$\frac{\text{I Peak 1}}{\text{I Peak 2}}$	
			4 Protons	15 Protons		Observed	Calculated
			Benzene Peak 4 proton $\pm 1$ Hz	PPG, OCH, OCH <sub>2</sub> and OCH <sub>3</sub> $\pm 0.2$ Hz	Mix. of PPG-4 Me and Na-DBS CH <sub>2</sub> and CH <sub>3</sub>		$\frac{4}{15}^*C$ =0.267C
1.			-	202.2	71.0	-	-
2.	1.16		426,438, 447,463, 471	11 198.5	51 65.4	118 0.21	0.3
3.	1.48		427,437, 447,464, 471	20 195.0	64 63.0	163 0.31	0.39
4.	2.09		427,436, 447,463, 471	20 125.0	60 63.0	210 0.33	0.56
5.	2.47		427,436, 445,462, 470	23 193.0	50 61.4	205 0.46	0.66
6.	3.00		Broad peak 21 and the last one peak appears around 470	41 192.0	60.0	195 0.5	0.8

137

Note: All measurements were done in a 60 MHz instrument, with  $\delta_{\text{TMS}} \approx 0$  Hz.

We point out here that the concentration of PPG-3 and Na-DBS are much higher than their respective cmc values, and therefore we are looking at the signals of micelles in these cases. Upon the addition of Na-DBS to the solution of PPG-3 such that the molar ratio  $C$  equals 1.36 it can be seen that the PPG central protons are upfield shifted by about 8.5 Hz and the composite signal of PPG methyl, and the Na-DBS aliphatic protons appears at 63 Hz, corresponding to an upfield shift of about 7 Hz. The aromatic protons of Na-DBS undergo a very small almost negligible, downfield shift.

The  $C_6H_4$  protons of Na-DBS serve as a 'handle' to monitor Na-DBS independently, and the PPG protons that appear at the 200 Hz region serve as a 'handle' to monitor PPG independently and thus it is possible as a first approximation to estimate the amount of Na-DBS incorporated in the possible mixed micelle by measuring the relative integral intensities (NMR integration values) of the benzene peaks and the PPG peaks. If all the Na-DBS were incorporated in a mixed micelle, the intensities ratio,

$$I_0 / (I_{CH_2O} + I_{CHO} + I_{CH_3O})$$

would be expected to match the calculated ratio based on the actual  $C$  values of the mixtures. The calculated intensities values were arrived at from the expression  $4/12 \times C$ ,

Since there are 4 protons of Na-DBS in the aromatic region and 12 protons of PPG in the 200 Hz region; if the molar ratio of Na-DBS/PPG equals one the intensities ratio in that spectrum should be 4/12 i.e. 0.33. For all other C values the calculated intensities ratios would be given by 0.33 C.

These calculated values of  $I_0/(I_{\text{OCH}} + I_{\text{OCH}_2} + I_{\text{OCH}_3})$  are listed in the tables along with the observed ratios. In no case the observed ratio equals the calculated one. This disparity may be due to several reasons.

1. There may exist three independent micellar species: Na-DBS micelles, PPG-3 micelles and mixed micelles comprising both ionic and nonionic components. This does not seem likely to us because of the fact that our results here closely parallel those in the mixed micelle system of Tokiwa (10), and also no fine structure is observed in the 200 Hz signal; besides, other physical measurements suggest the likelihood of predominantly mixed micelles in a homogeneous fashion. If the three species were to exist with reasonable life times, the observed integration ratio should still account for all the Na-DBS and the PPG protons.

2. There is a likelihood that the homogeneous mixed micelles are formed but these are highly fluctuating and highly mobile species with no fixed composition during the time scale

of NMR measurement. This would account for the lowered observed values, and also the uniform upfield shift of PPG protons as Na-DBS is added. Essentially, the same results are obtained with the PPG-4 system also, as illustrated in Table 6.2.

Fig. 6.1 shows the variation of upfield shift of PPG protons upon the addition of Na-DBS. The shifts increase rapidly initially and level off to a saturation value ( $\Delta\mathcal{V}_s$ ) of about 16 Hz for the PPG-3, and about 14 Hz for the PPG-4 case, beyond a molar ratio of  $C = 4$ . It is worth while to compare our results with those obtained by Tokiwa and Tsujii(18) for the system Na  $C_8$ BS (Na-Octyl benzene surfonate) with non-polar derivatives of PEG (Polyethylene glycol). In their system each PEG molecule carries a  $C_{12}$  hydrocarbon chain so that their micelles could be expected to have a stable non-polar core. In comparison, our PPG micelle would be expected to have no deep core and therefore some what more fluid. Despite this difference, the trend of upfield shift and the values of  $\Delta\mathcal{V}_s$  in both the systems are very similar, suggesting the same kind of intermolecular associations.

Tokiwa and Tsujii (18) have used a statistical analysis to relate the upfield shift ( $\Delta\mathcal{V}$ ) produced in nonionic surfactants proton signals as a function of molar ratio  $C$ . They have considered a mixed micelle consisting of  $Q$  nonionic



molecules which can be divided into smaller sections each containing  $q$  nonionic molecules such that  $q \ll Q$ . If one molecule of ionic surfactant (Na-DBS) enters a given small section, it is assumed that this Na-DBS molecule will influence and cause upfield shift of all protons of nonionics (PPG). With this assumption, the differential upfield shift per micelle,  $d\delta_{mic}/dn$  is given by the probability expression:

$$\frac{d\delta_{mic}}{dn} = K P(n) \quad (6.1)$$

The probability function  $P(n)$  can be arrived at as follows.

The probability of finding a single Na-DBS molecule in a given small section is  $q/Q$ . If there are  $n$  Na-DBS molecules in a given micelle, the probability of finding  $m$  Na-DBS molecules in a small section of micelle and the remaining  $(n-m)$  outside the small section is given by,

$$(q/Q)^m (1-q/Q)^{n-m}$$

The probability of finding  $m$  arbitrary Na-DBS molecule in small section is given by,

$$\frac{n!}{m! (n-m)!} (q/Q)^m (1-q/Q)^{n-m} \quad (6.2)$$

Since there are  $n!/(m!(n-m)!)$  ways of selecting  $m$  Na-DBS molecule out of the total  $n$ . The probability of finding  $n$  Na-DBS molecules at all in the small section under consideration

is  $(1-q/Q)^n$ , since  $m = 0$ . Therefore the probability  $P(n)$  of finding small sections with no Na-DBS in the whole of micelle is given by,

$$P(n) = (1-q/Q)^n \quad (6.3)$$

Therefore,

$$\frac{d\Delta\psi_{mic}}{dn} = K(1-q/Q)^n \quad (6.4)$$

Integrating this equation, and applying the boundary conditions of  $\Delta\psi_{mic} = 0$  when  $n = 0$  and  $\Delta\psi_{mic} = \Delta\psi_s$  when  $n = \infty$  where  $\Delta\psi_s$  is saturation of the upfield shift, we get,

$$\Delta\psi_{mic} = \Delta\psi_s [1 - (1-q/Q)^n] \quad (6.5)$$

This equation holds for all micelles present in the solution, under the assumption the all molecules exists in the mixed micelle form. Therefore  $\Delta\psi_{mic}$  in the above equation will be the same as the observed upfield shift.

Since  $0 < (1-q/Q) < 1$ , one may write this as

$$1-q/Q = e^{-K} \quad \text{and} \quad \Delta\psi = \Delta\psi_s (1 - e^{-K'n})$$

where  $K' > 0$ ,  $n$  can be evaluated as  $n = L * M_i / N$  where  $L$  is the Avogadro Number,  $M_i$  = molar concentration of Na-DBS,  $N$  is the no. of micelles/cc of solution. If  $M_n$  is the molar concentration of PPG then  $n = L * M_n / C$  where  $C = M_i / M_n$ .

Therefore we get,

$$\Delta \psi = \Delta \psi_s \left[ 1 - \exp \left( - \frac{K' LM_n}{N} * C \right) \right] \quad (6.6)$$

or

$$\Delta \psi = \Delta \psi_s \left[ 1 - \exp \left( - \frac{q LM_n}{qN} * C \right) \right] \quad (6.7)$$

Since  $LM_n = qN = \text{no. of PPG molecule/cc.}$

$$\frac{q LM_n}{qN} = q \quad (6.8)$$

$$\Delta \psi = \Delta \psi_s (1 - e^{-qC}) \quad (6.9)$$

In order to determine  $\Delta \psi_s$  and  $q$  the following method is adopted, at any concentration  $C$ ,

$$\Delta \psi(C) = \Delta \psi_s (1 - e^{-qC}) \quad (6.10)$$

$$\Delta \psi(C+h) = \Delta \psi_s [1 - e^{-q(C+h)}] \quad (6.11)$$

where  $h$  is an arbitrary dummy constant. From these two equations one may write,

$$\Delta \psi(C+h) = e^{-qh} [\Delta \psi(C) + (1 - e^{-qh}) \Delta \psi_s] \quad (6.12)$$

A plot of  $\Delta \psi(C+h)$  vs.  $\Delta \psi(C)$  will then yield  $q$ . We have taken this approach for the determination of  $q$ , i.e. the no. of PPG molecules that are influenced by one Na-DBS molecule. These plots for the PPG-3 and PPG-4 cases are given in Fig. 6.2.

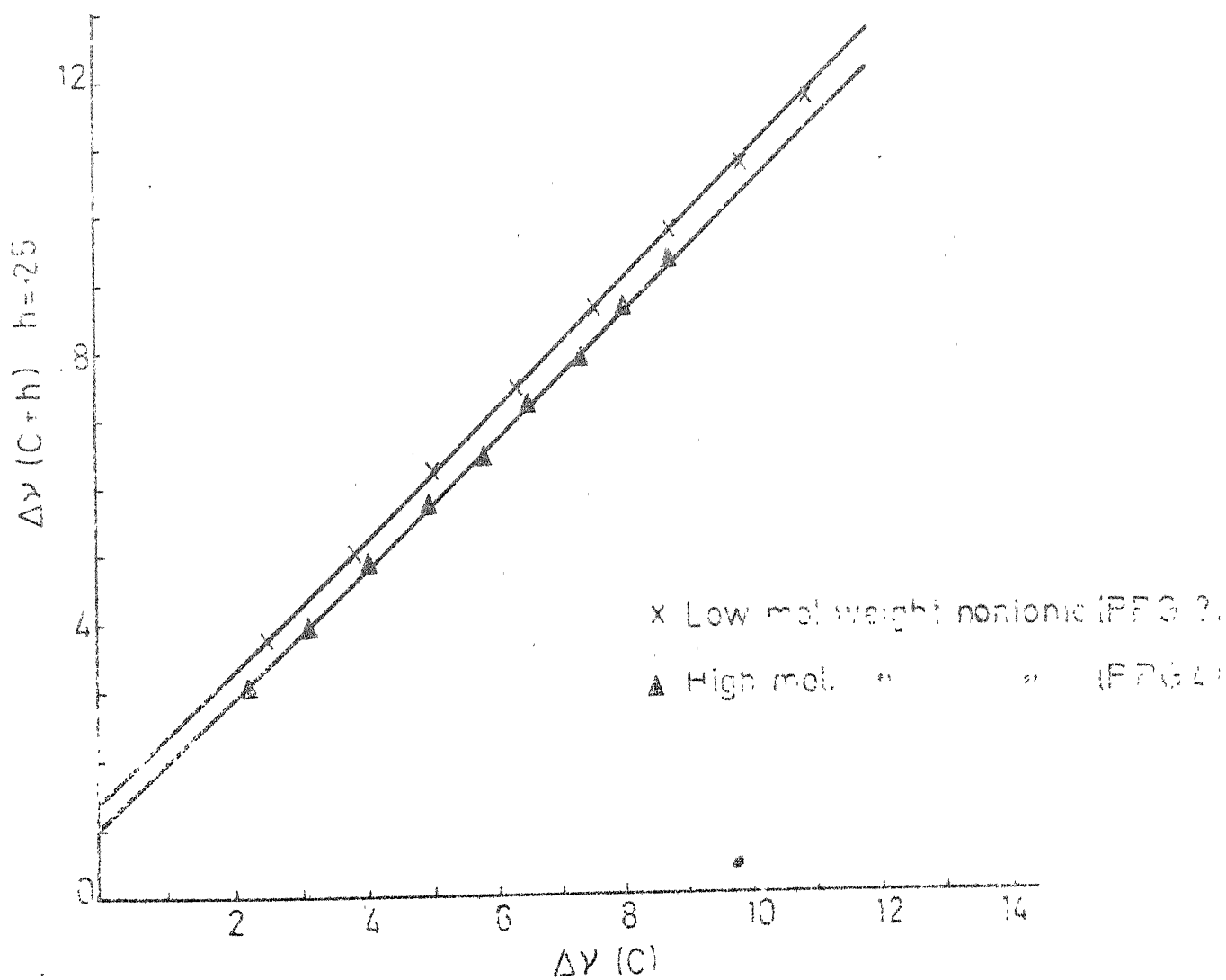


FIG. 6.2  $\Delta\gamma (C+h)$  Vs  $\Delta\gamma (C)$

The values of  $q$  obtained,  $q = .18$  for both the cases, is astonishingly small. In the case of the PEG surfactant carrying  $C_{12}$  hydrocarbon tail and Na  $C_8$ BS, Tokiwa and Tsujii (18) obtained the value of  $q=1.6$  for the Trimer nonionic and 1.2 for the tetramer nonionic surfactant.

The similarity of  $\Delta \nu_s$  values obtained by Tokiwa (18) and in our experiments leads us to believe that mixed micelle indeed occur predominantly in the system Na-DBS and PPG. The agreement of values between the systems ( $C_{12}$  PEG +  $C_8$ BS) and (Na-DBS + PPG) suggests that the mechanisms by which the upfield shift perturbation are caused are the same. However, while the saturation upfield shift in the Tokiwa system occurs already at a value  $C = 2$ , such a plateau is obtained in the PPG systems at  $C \geq 4$  (see Fig. 6.1). This might mean the mixed micelle in the present case is not as rigid, which is to be expected because PPG does not have a hydrocarbon core for stabilization. Support for this point of view also comes from the small value of  $q$  obtained in the present system. It would appear that in the present case there may be either a fast equilibrium process involving fluctuation of individual molecules in and out of the micelles; in other words, a highly mobile and fluid mixed micelle system can be suggested. A point to be noted here is the difference in length between the individual ionic and nonionic molecules. Each molecule of PPG-3 is approximately

no more than  $9\text{\AA}$ , PPG-4 no more than  $12\text{\AA}$ , whereas the length of Na-DBS molecules is roughly  $16\text{\AA}$ . This must be an important factor in generating such low  $q$  values. But the fact that  $q = .18$  is obtained, and upfield shifts are observed indicates that,

1. Mixed micelles are formed incorporating Na-DBS in PPG micelles,
2. Na-DBS molecules in the micelle influence the environment of the PPG molecules significantly.

It is important to reiterate the difference that exists between the Tokiwa system and the present system. In the former case, each nonionic molecule carries a long hydrocarbon tail which makes the formation of stable micelle easy. PPG samples however lack this hydrocarbon portion and therefore their micelles would be expected to be more mobile. The Tokiwa-Tsujii model of a palisade micelle is thus not applicable in our case and therefore to use the mathematical analysis of Tokiwa in the present system would lead only to limited information. One should therefore be cautious about the actual physical interpretation of parameters such as  $q$ , and their values.

An alternate, and equivalent point of view is to consider solubilization of one component in the other. If we take the approach of phase partition of the benzene moiety between a

hydrocarbon rich phase (Na-DBS micelles), and the sulfoxy-propylene phase, we can estimate the chemical potentials of the benzene part in these phases somewhat similar to what Takiwa and Tsujii (19) have done with mixed micelle systems using variants of  $C_8ES$  and  $C_{12}POE$ .

Assume a given Na-DBS molecule to be incorporated itself either in a pure micelle of Na-DBS itself (Phase II) or to enter a mixed micelle comprising PPG and Na-DBS (Phase I). It is only in phase I that a benzene ring of Na-DBS molecule will be able to influence the chemical shift position of the PPG protons. In this formalism, when  $C$  (mole ratio of Na-DBS to PPG) is small, the chemical potential of a given Na-DBS molecule in phases I and II can be expressed as,

$$\mu_I = \mu_I^C + RT \ln X_1 \quad (6.13)$$

$$\mu_{II} = \mu_{II}^0 + RT \ln X_2 \quad (6.14)$$

where  $X_1$  and  $X_2$  are mole fractions and  $\mu_I^C$  and  $\mu_{II}^0$  are the standard chemical potentials of Na-DBS in phases I and II respectively. Since at equilibrium  $\mu_I = \mu_{II}$ , we may write

$$\mu_I^0 - \mu_{II}^0 = RT \ln (X_{II}/X_I) \quad (6.15)$$

If we assume that at small  $C$ , the upfield chemical shift is proportional to  $X_1$  and also  $X_1 + X_2 = C$  then we have,

$$\Delta\gamma = k X_1 \quad (6.16)$$

$$\begin{aligned} \text{or } X_1 &= \Delta\gamma/k \\ \text{and } X_2 &= \frac{C - \Delta\gamma}{k} \end{aligned} \quad (6.17)$$

and further,

$$\mu_I^0 - \mu_{II}^0 = RT \ln \frac{k - \Delta\gamma/C}{\Delta\gamma/C} \quad (6.18)$$

where  $\Delta\gamma/C$  is the initial slope of the  $\Delta\gamma$  vs.  $C$  curve (Fig. 6.1). The constant  $k$  has been assumed to be 17 Hz from the  $\Delta\gamma$  vs.  $C$  initial curve for the mixture of Benzene and Polyethylene glycol (18). This is an assumption which is considered not too severe. However, it should be realized that the actual value of  $k$  determines to a large extent the value of  $\mu_I^0 - \mu_{II}^0$ . In the case of PPG-3, the initial slope  $\Delta\gamma/C$  is equal to 5 Hz (Fig. 6.1) and thus  $\mu_I^0 - \mu_{II}^0$  is estimated to be + 530 cal/mole. In the case of PPG-4, the initial slope is estimated to be 4 Hz and correspondingly  $\mu_I^0 - \mu_{II}^0$  is calculated as + 700 cal/mole at room temperature 300°K. These values are comparable with the thermal energy ( $RT$ ) of 600 cal/mole at room temperature and suggest no greater preference for a given Na-DBS molecule to be either exclusively in phase I or phase II. In other words mixed micelles of the detergent and collector appear quite likely and of a highly mobile nature. This is to be compared with the mixed micelle of the hydrocarbon tail-bearing  $C_{12}$  POE and Na- $C_8$ BS, where a



similar calculation (except phase II here corresponds to hydrocarbon core and phase I to polyoxyethylene shell of the mixed micelle) yield  $\mu_I^0 - \mu_{II}^0$  equals - 700 cal/mole showing slight preference for Na-C<sub>8</sub>BS to exist embedded in the mixed micelle. It is also noteworthy that in this mixed micelle, initial slope turns out to be 13.2 Hz, whereas in our PPG-NaDBS system the slope is much shallower (4.5 Hz) even though  $\Delta V_G$  values are about the same, pointing out a much more loosely packed and mobile mixed micelle in the latter case. The value of q in our system therefore is essentially a reflection of this loose and inefficient solubilization of the mixed micelle.

In summary, NMR measurement of mixture of Na-DBS and PPG indicates the formation of mixed micelles. The results are consistent with a highly fluid, perhaps fluctuating micelles of varying compositions. Experiments with longer chain PPG molecules will be of interest in further delineating the dynamics of such mixed micelle systems.

## REFERENCES

1. Eriksson, J.C.  
NMR Experiments on Solubilization in Soap Micelles  
(1963), Acta. Chem. Scand., 17, 1478-1481.
2. Eriksson, J.C., and Gillberg, G.  
NMR Studies of the Solubilization of Aromatic  
Compounds in Cetyltrimethyl Ammonium Bromide Solution  
(1966), Acta. Chem. Scand., 20, 2019-2027.
3. Clifford, J., and Pethica, B.A.  
NMR Chemical Shift of Water Protons in Solution of  
Sodium Alkyl Sulfates  
(1964), Trans. Farad. Soc., 60, 1483-1490.
4. Clifford, J., and Pethica, B.A.  
Spin Lattice Relaxation Time of Water Protons in  
Solutions of Sodium Alkyl Sulfates  
(1965), Trans. Farad. Soc., 61, 182-189.
5. Clifford, J.  
Spin Lattice Relaxation Time of Hydrocarbon Chain  
Protons in Solution of Sodium Alkyl Sulfates  
(1965), Trans. Farad. Soc., 61, 1276-1282.
6. Yan, J.F., and Palmer, M.B.  
A Nuclear Magnetic Resonance Method for Determination  
of Critical Micelle Concentration  
(1969), J. Colloid. Interf. Sci., 30, 177-181.
7. Haque, R.  
NMR Study of Micelle Formation in Sodium-Perfluoro-  
caprylate and Propionate  
(1968), J. Phys. Chem., 72, 3056-3058.
8. Bailey, R.E., and Cady, G.H.  
Nuclear Magnetic Resonance Studies of Hepta Fluorobutyric  
Acid Micelle Formation  
(1969), J. Phys. Chem., 73, 1612-1614.

9. Inoune, H., and Nakagawa, T.  
Shift of Nuclear Magnetic Resonance Signal  
Caused by Micelle Formation  
(1967), 4th International Congress on Surface  
Active Substance, Bruxelles, B IV, 11-16.
10. Odberd, L., Bengt, S., and Ingvar, D.  
The Association of Short Chain Alkanate as  
Studied by NMR Method  
(1972), J. Colloid. Interf. Sci., 41, 298-304.
11. Atinkson, R.E., Clint, G.E., and Walker, T.  
The Influence of Micelle Formation on the Internal  
Chemical Shift of the Aromatic Protons of Solution  
of a Cationic Surfactant  
(1974), J. Colloid. Interf. Sci., 46, 32-37.
12. Muller, N., and Johnson, T.W.  
Investigation of Micelle Structure by Fluorine  
Magnetic Resonance  
(1969), J. Phys. Chem., 73, 2042-2046.
13. Muller, N., and Birkhalm, R.H.  
Investigation of Micelle Structure by Fluorine  
Magnetic Resonance  
(1967), J. Phys. Chem., 71, 957-962.
14. Muller, N., and Birkhalm, R.H.  
Investigation of Micelle Structure by Fluorine  
Magnetic Resonance  
(1968), J. Phys. Chem., 72, 583-588.
15. Muller, N., and Platko, F.E.  
Investigation of Micelle Structure by Fluorine  
Magnetic Resonance  
(1971), J. Phys. Chem., 75, 547-553.
16. Muller, N., and Simsohn, H.  
Investigation of Micelle Structure by Fluorine  
Magnetic Resonance  
(1971), J. Phys. Chem., 75, 942-945.
17. Florence, A.T., and Parfitt, R.T.  
Micelle Formation by Some Phenothiazine Derivative 11  
(1971), J. Phys. Chem., 75, 3555-3560.

18. Tokiwa, F.  
NMR Study of Interaction Between Anionic and Nonionic  
Surfactant in Their Mixed Micelle  
(1971), J. Phys. Chem., 75, 3560-3565.
19. Tokiwa, F., and Tsujii, K.  
NMR Study of the Interaction Between Anionic and  
Nonionic Surfactant in Their Mixed Micelle  
(1972), J. Colloid Interf. Sci., 41, 343-349.
20. Inoue, H., and Nakagawa, T.  
Shift of NMR Signal Caused by Micelle Formation II  
Micelle Structure of Mixed Surfactants  
(1966), J. Phys. Chem., 70, 1108-1113.

## CHAPTER VII

### SUMMARY AND CONCLUSIONS

In this last chapter, the conclusions emerging out of the present investigation will be summarised.

Clear evidence has been obtained regarding interaction of collector and frother molecules at different interfaces in a flotation system, from a variety of techniques.

The flotation recovery of rutile and the collector (sodium oleate) adsorption density on the rutile surface are found to increase as functions of the concentration of the nonionic frothers (PPG). As the nonionic concentration approaches or exceeds its cmc, the above two parameters decrease, due to abstraction of collector ions from the bulk liquid phase to the mixed micelle.

Nonionic frothers (at concentrations slightly above  $10^{-3}$  M) are found to be adsorbed in presence of collector on rutile surface. Interestingly, there is no adsorption in the absence of collector, or if the collector concentration is too low. This seems to be a typical case of synergism between collector and frother molecules, each inducing adsorption of the other on the solid surface.

The beneficial effects of nonionic frothers in improving collector adsorption on rutile is also confirmed by the zeta-potential data. Increasing nonionic and sodium oleate concentrations make the negatively charged rutile particle even more negatively charged.

Similar synergistic effect is noticed in the liquid-gas interface in which not only frother molecules but also the collector molecules get adsorbed through mutual interaction. Somasundaran and Fuerstenau (1) had postulated earlier that the collector species are adsorbed both at the solid-liquid and the liquid-gas interfaces. The collector adsorbed at the liquid-gas interface, that is, at the interface of the gas bubble, facilitates reduction of the time necessary for the formation of the solid-gas interface, since the collector ions are now carried to the solid surface by the bubble. The amount of collector that could be transferred to the solid-gas interface from the bubble surface upon contact is significantly higher than that which could be transferred from the solid-liquid interface. Marcus and Sandvik (2) have suggested that under normal flotation conditions the adsorption of the surface-active collector on the solid surface is governed, to a large extent, by a transfer of the collector from the gas-liquid interface to the solid surfaces. Simultaneously, frother molecules are also transferred on to the solid surface to form a mixed film.

In studies of the flotation recovery of the mineral calcite using Na-DBS as the collector and PPS as the frothers, it was seen that the recovery increases steadily with the concentration of the nonionic both in the pre-micellar and post-micellar ranges. This is in contrast to the case of rutile, where the recovery drops when the frother concentration exceeds the cmc; and also in contrast to the situation when Na-Oleate is used as the collector rather than Na-DBS. This contrasting behaviour might be due to the possibility that the abstraction of Na-DBS ions from the bulk liquid phase to the mixed micelle phase is less efficient as compared to the case of Na-Oleate. Support for this comes from the conductance and hydrodynamic data reported in Chapters IV and V.

From the above observations, we can say that the conventional notion that collector is active at the solid liquid interface and frother at the liquid-gas interface only, is over-simplistic. In our opinion, much of the phenomenon of mineral particle-air bubble contact in a flotation system is due to mutual interaction and co-adsorption of collector and frother molecules at the different interfaces.

Evidences of collector-frother interaction in the bulk liquid phase (micellar) has been obtained by conductivity, light-scattering and nuclear magnetic resonance measurements.

Conductivity measurement of Na-DBS alone and in presence of nonionic (PPG-3 and PPG-4) at different concentration shows that when concentration of PPG is low, there is mixed micelle formation by the incorporation of PPG molecules in Na-DBS micelles. The observed decrease in conductance value of Na-DBS in the presence of the nonionics at their post-micellar concentration, has been explained in terms of the formation of mixed micelles which are essentially nonionic micelles with Na-DBS molecules incorporated in the host micelles.

Similar conductivity results have been obtained in the system: nonionics (PPG-3 and PPG-4)- sodium oleate, in the post micellar region, and a similar interpretation has been given as for the Na-DBS: nonionics system. In the pre-micellar region, conductance data for sodium oleate are somewhat difficult to interpret. This is on account of the possible hydrolysis of Na Oleate in water. Various kinds of dimers including sodium oleate-nonionic: are probably present.

Comparison of the conductance behaviours of the collectors Na-DBS and Na Oleate, in the presence of PPG, is revealing. The PPG-governed reduction in the conductance of Na-Oleate is greater than that of Na-DBS. This has been interpreted to mean that the interaction between Na Oleate



and PPG is somewhat more effective than that between Na-DBS and PPG. Support for this comes from hydrodynamic data mentioned below. This differential interaction may be of relevance in the synergism exhibited by the two frother: collector pairs in flotation recovery.

Light scattering studies of aqueous solutions of the frothers PPG have been undertaken and the results reveal that these nonionic surfactants readily form micelles. The radius of gyration of PPG-3 micelles was found to be 1627 Å, with an aggregation number of 1200 molecules in an average micelle at 35°C. PPG-4 also forms micelles with roughly the same aggregation number and the radius of gyration of these PPG-4 micelles was determined to be 2155 Å. The shapes of these micelles were tentatively suggested to be unsymmetrical ellipsoids of revolution, or 3-dimensional McBain-type boxes.

Introduction of Na-DBS to aqueous PPG has the effect of increasing the molecular weight and, to some extent, the radius of gyration of the micelles. Na-DBS is suggested to get incorporated in PPG forming mixed micelles. The shapes of the mixed micelles do not differ from those of pure PPG micelles.

Na-Oleate also gets solubilized in PPG micelles in a manner similar to Na-DBS, and mixed micelles of similar shape form with increased molecular weight. However, at high

concentrations of Na-Oleate, complications arise due to hydrolysis of the oleate, making meaningful interpretation of data difficult.

The quantitative increase in the molecular weights of nonionic micelles upon addition of anionics is more in the case of sodium oleate as compared to Na-DBS (sodium dodecyl benzene sulfonate) suggesting that Na-Oleate interacts more efficiently, an inference that is in consonance with earlier results of conductance measurements.

Nuclear magnetic resonance measurements of mixtures of Na-DBS and PPG (nonionics) are consistent with the view that mixed micelles form. The changes in the chemical shift values and the integration values of the polypropylene protons, and of the collector (Na-DBS) have been interpreted in terms of mixed micelle formation with the simultaneous presence of highly fluid mixed micelles of varying composition.

Here, it is worth mentioning that, while mixed micelles are formed between PPG (nonionics), and collectors such as sodium oleate and SDS, these are not conveniently monitored by NMR chemical shift measurements. The problem apparently is one of having too many environmentally similar  $-CH_2$  groups which all resonate at approximately the same NMR frequency range. On the other hand, Na-DBS has benzene protons that not only resonate at considerably lower fields

than the other protons, but also serve as a 'handle', since they are influenced, and in turn influence the chemical shift positions of the other protons in the mixture.

In the end, it would be worthwhile to highlight the achievements in the present series of investigation and to point out the scope of future research on the subject.

Collector and frother molecules have been shown to aggregate in bulk solutions of pre-micellar concentration. It would be difficult to establish the number of molecules participating in the loosely bound aggregate. (Osmometric and related experiments may be useful in this regard). However, it is entirely conceivable that these aggregates of a very small number of collector or frother molecules may be adsorbed on the various interfaces in the flotation system. This postulate needs detailed investigation. One should also investigate the interesting transport phenomenon regarding transfer of additional collector and frother molecules from the bubble to the solid interface during the establishment of the three-phase contact in a flotation system.

Micellar interaction between the collector and the frother molecules is of significance in flotation systems since some frother chemicals are used in post-micellar concentrations. Mixed micelles are formed in the bulk

phase, and therefore formation of similar mixed hemi-micelles on the solid surface may also be postulated. NMR studies clearly provide the spectroscopic evidence of interaction. However, such evidences have so far been restricted to those systems which contain molecules with fluorine atoms, aromatic rings etc. or tagged with free radicals. Similar evidences for conventionally used collectors and frothers, not containing such special groups would be particularly welcome.

The investigation on mixed micellar interaction is relevant to the flotation studies for another vital reason. There is strong parallelism between the two phenomena viz., (1) synergistic co-adsorption of the collector and frother molecules on the solid surface (mixed 'hemi-micellisation') and (2) mixed micellisation in the bulk phase. In both the cases, ionic repulsion between the collector hydrophilic heads is decreased due to incorporation of the nonionic molecules in the mixed aggregate. As a consequence, there is greater association of surfactant molecules, disruption of water structure and augmentation of hydrophobic zones in both the systems, viz., solid surface as well as the bulk aqueous phase. In the earlier case, mineral particles are rendered more floatable. The nature and energetics of interaction between the collector and frother molecules on the solid surface can be often inferred from the bulk micellar studies. Thus, the link between the interfacial and bulk interaction studies is provided.

Adsorption and zeta potential measurements reported in the earlier chapters provide evidences of interaction on the solid surface. To study the energetics of collector-frother interaction through calorimetric measurement would be a fascinating piece of work. Enthalpies of dilution in collector-frother-water systems would provide thermodynamic information for pre-micellar and mixed micellar interactions. More relevant (in the context of mineral processing technology) and parallel information may be obtained through measurements of heats of adsorption of collector and frother on the mineral surfaces. Adoption of micro-calorimetric and tracer techniques (with labelled chemicals) would be useful in this regard.

#### REFERENCES

1. Somasundaran, P., and Fuerstenau, D.W.  
On Incipient Flotation Conditions  
(1968), Trans. Soc. Min. Engrs., 241, 102-104.
2. Marcus, D., and Sandvik, K.L.  
Adsorption of Anion on Quartz Through Bubble  
Interaction  
(1968), Trans. Inst. Mining and Metallurgy (Section C),  
77, C 61-64.

## APPENDIX

### EXPERIMENTAL DATA

Table I

Surface Tension Value of Sodium Oleate Solutions

Temperature =  $27 \pm 1^{\circ}\text{C}$ 

Sl.No.	Concentration of Sodium oleate solutions Moles/lit.	Surface Tension Values dynes/cm
1.	$9.068 \times 10^{-7}$	62.3
2.	$1.2 \times 10^{-6}$	60.0
3.	$1.87 \times 10^{-6}$	58.5
4.	$2.0 \times 10^{-6}$	56.5
5.	$2.81 \times 10^{-6}$	55.2
6.	$3.0 \times 10^{-6}$	53.5
7.	$4.68 \times 10^{-6}$	51.0
8.	$5.62 \times 10^{-6}$	47.5
9.	$7.6 \times 10^{-6}$	46.5
10.	$1.52 \times 10^{-5}$	42.1
11.	$1.97 \times 10^{-5}$	41.0
12.	$7.6 \times 10^{-5}$	37.5
13.	$1.52 \times 10^{-4}$	34.5
14.	$7.6 \times 10^{-4}$	27.3
15.	$9.85 \times 10^{-4}$	26.7
16.	$1.52 \times 10^{-3}$	25.7
17.	$3.8 \times 10^{-3}$	25.8

Table II

Surface Tension Value for Pure Low Molecular Weight

Nonionic (PPG-3)

Temperature =  $27 \pm 1^{\circ}\text{C}$ 

Sl.No.	Concentration of nonionic Mols/lit.	Surface Tension Values Dynes/cm
1.	$1.85 \times 10^{-6}$	67.5
2.	$2.5 \times 10^{-6}$	65.0
3.	$3.7 \times 10^{-6}$	64.0
4.	$5.0 \times 10^{-6}$	62.5
5.	$7.5 \times 10^{-6}$	61.2
6.	$9.23 \times 10^{-6}$	61.0
7.	$1.0 \times 10^{-5}$	60.6
8.	$1.85 \times 10^{-5}$	59.4
9.	$2.3 \times 10^{-5}$	55.1
10.	$2.5 \times 10^{-5}$	56.2
11.	$4.6 \times 10^{-5}$	57.5



Table III

Surface Tension Value for Pure High Molecular Weight  
Nonionic (PPG-4)

Temperature =  $27 \pm 1^{\circ}\text{C}$

Sl.No.	Concentration of Nonionic Moles/lit.	Surface Tension Values Dynes/cm.
1.	$2.30 \times 10^{-6}$	71.4
2.	$4.60 \times 10^{-6}$	69.5
3.	$5.0 \times 10^{-6}$	68.0
4.	$7.5 \times 10^{-6}$	67.0
5.	$1.15 \times 10^{-5}$	64.0
6.	$1.5 \times 10^{-5}$	61.0
7.	$2.0 \times 10^{-5}$	57.5
8.	$2.30 \times 10^{-5}$	55.5
9.	$2.38 \times 10^{-5}$	56.4
10.	$4.76 \times 10^{-5}$	58.5
11.	$7.14 \times 10^{-5}$	57.5
12.	$9.21 \times 10^{-5}$	58.4

Table IV

Effect of Nonionic on Surface Tension of Sodium Oleate

Temperature =  $27 \pm 1^\circ\text{C}$ 

Sl.No.	Concentration of Nonionic (PPG-4) = $1.39 \times 10^{-5}$ moles/lit.		Concentration of Nonionic (PPG-3) = $1.3 \times 10^{-5}$ moles/lit.	
	Concentration of Sodium Oleate Moles/lit.	Surface Tension Values Dynes/cm.	Concentration of Sodium Oleate Moles/lit.	Surface Tension Values Dynes/cm.
1.	$1.97 \times 10^{-5}$	37.9	$5.0 \times 10^{-6}$	39.7
2.	$9.85 \times 10^{-5}$	36.1	$1.0 \times 10^{-6}$	36.7
3.	$1.97 \times 10^{-4}$	33.0	$2.0 \times 10^{-5}$	34.5
4.	$3.94 \times 10^{-4}$	30.8	$3.0 \times 10^{-5}$	32.7
5.	$9.85 \times 10^{-4}$	26.5	$1.0 \times 10^{-4}$	27.3
6.	-	-	$3.12 \times 10^{-4}$	26.0

Table V

Effect of Sodium Oleate on Surface Tension Values of Nonionics

Temperature =  $27 \pm 1^\circ\text{C}$ 

S.N.	PPG-4 Concentration of Sodium Oleate = $1.97 \times 10^{-6}$ moles/lit.		PPG-3 Concentration of Sodium Oleate = $2.0 \times 10^{-6}$ moles/lit.	
	Concentration of Nonionic (Moles/lit.)	Surface Tension Values Dynes/cm.	Concentration of Nonionic Moles/lit.	Surface Tension Values Dynes/cm.
1.	$4.60 \times 10^{-6}$	64.0	$2.0 \times 10^{-6}$	58.5
2.	$6.94 \times 10^{-6}$	59.1	$3.24 \times 10^{-6}$	50.0
3.	$1.39 \times 10^{-5}$	48.1	$4.0 \times 10^{-6}$	46.9
4.	$2.79 \times 10^{-5}$	48.3	$5.0 \times 10^{-6}$	44.5
5.	$4.19 \times 10^{-5}$	49.0	$6.0 \times 10^{-6}$	43.6
6.	-	-	$1.29 \times 10^{-5}$	39.6
7.	-	-	$2.59 \times 10^{-5}$	40.5
8.	-	-	$3.24 \times 10^{-5}$	41.0

Table VI

Effect of Collector Concentration on Flotation Recovery  
of Calcite

Collector = Na-DBS

No Frother

pH =  $7 \pm .05$

Conditioning Time = 5 min.

Flotation Time = 1.5 min.

Sl.No.	Collector Concentration Moles/lit.	Flotation Recovery
1.	$2.5 \times 10^{-5}$	Nil
2.	$2.77 \times 10^{-5}$	Nil
3.	$4.63 \times 10^{-5}$	12.0%
4.	$6.48 \times 10^{-5}$	26.0%
5.	$9.28 \times 10^{-5}$	34.3%
6.	$1.39 \times 10^{-4}$	71.3%
7.	$1.85 \times 10^{-4}$	92.4%
8.	$2.3 \times 10^{-4}$	96.0%

Table VII

Effect of Collector Concentration on Flotation Recovery  
of Calcite

Frother Concentration =  $1.026 \times 10^{-4}$  m/l

<u>Sl.No.</u>	<u>Collector Concentration</u>	<u>Flotation Recovery</u>
1.	$2.45 \times 10^{-5}$ m/l	18.3%
2.	$4.90 \times 10^{-5}$ m/l	21.6%
3.	$1.22 \times 10^{-4}$ m/l	56.4%
4.	$1.47 \times 10^{-4}$ m/l	75.8%
5.	$1.71 \times 10^{-4}$ m/l	95.2%

Table VIII

Effect of Collector Concentration on Flotation Recovery  
of Calcite

Frother Concentration =  $5.14 \times 10^{-5}$  m/l

<u>Sl.No.</u>	<u>Collector Concentration</u>	<u>Flotation Recovery</u>
1.	$2.45 \times 10^{-5}$ m/l	3.0%
2.	$4.90 \times 10^{-5}$ m/l	12.6%
3.	$1.22 \times 10^{-4}$ m/l	46.4%
4.	$1.71 \times 10^{-4}$ m/l	74.7%
5.	$1.96 \times 10^{-4}$ m/l	83.3%
6.	$2.45 \times 10^{-4}$ m/l	91.0%

Table IX

Effect of Collector Concentration on Flotation Recovery  
of Calcite

Collector = Na-DBS

Frother = Tripropylene glycol

monomethyl ether (PFG-3)

Concentration of Frother =  $2.78 \times 10^{-4}$  m/l

Sl.No.	Collector Concentration Moles/lit.	Flotation Recovery
1.	$1.82 \times 10^{-5}$	6.0%
2.	$5.46 \times 10^{-5}$	24.4%
3.	$7.28 \times 10^{-5}$	35.2%
4.	$9.10 \times 10^{-5}$	47.5%
5.	$1.27 \times 10^{-4}$	61.8%
6.	$1.82 \times 10^{-4}$	79.7%
7.	$2.73 \times 10^{-4}$	94.4%
8.	$3.64 \times 10^{-4}$	100.0%

Table X

Effect of Nonionic (PPG-3) on Flotation Recovery of Calcite

Concentration of Collector

(Na-DBS) =  $7.45 \times 10^{-5}$  m/l.pH =  $7 \pm 0.05$ 

Conditioning Time = 5 min.

Flotation Time = 1.5 min.

Sl.No.	Concentration of nonionic Moles/lit.	Flotation Recovery
1.	$5.0 \times 10^{-5}$	25%
2.	$5.14 \times 10^{-5}$	26%
3.	$1.00 \times 10^{-4}$	47%
4.	$1.02 \times 10^{-4}$	38%
5.	$2.5 \times 10^{-4}$	49%
6.	$2.57 \times 10^{-4}$	49%
7.	$5.0 \times 10^{-4}$	54%
8.	$5.14 \times 10^{-4}$	43%
9.	$7.5 \times 10^{-4}$	51%
10.	$7.7 \times 10^{-4}$	55%
11.	$1.0 \times 10^{-3}$	53%
12.	$1.02 \times 10^{-3}$	47%

Table XI

Effect of Nonionic (PPG-3) on Flotation Recovery of  
Calcite

Concentration of Collector

(Na-DBS) =  $1.02 \times 10^{-4}$  moles/lit.

pH =  $7 \pm 0.05$

Conditioning Time = 5 min.

Flotation Time = 1.5 min.

---

Sl.No.	Concentration of Nonionic Moles/lit.	Flotation Recovery
<hr/>		
1.	$5.56 \times 10^{-5}$	55.6%
2.	$1.10 \times 10^{-4}$	62.7%
3.	$2.78 \times 10^{-4}$	69.0%
4.	$5.56 \times 10^{-4}$	72.0%
5.	$8.34 \times 10^{-4}$	70.0%
6.	$1.11 \times 10^{-3}$	72.0%

---



Table XII

Effect of Nonionic (PPG-4) on the Contact Angle in the  
System Rutile-Sodium Oleate-AIR

S.N.	Concentration of sodium oleate moles/lit.	Contact Angle Values Concentration of nonionic moles/lit.			
		No nonionic	$4 \times 10^{-4}$	$10^{-4}$	$10^{-3}$
1.	$1.9 \times 10^{-6}$	$58^\circ$	-	-	$58^\circ$
2.	$3.8 \times 10^{-6}$	$60^\circ$	$60^\circ$	$59^\circ$	$61^\circ$
3.	$7.6 \times 10^{-6}$	$62^\circ$	$62^\circ$	$59^\circ$	$64^\circ$
4.	$1.15 \times 10^{-5}$	$64^\circ$	$63^\circ$	$60^\circ$	$65^\circ$
5.	$1.9 \times 10^{-5}$	$68^\circ$	$65^\circ$	$64^\circ$	$63^\circ$
6.	$2.4 \times 10^{-5}$	$67^\circ$	-	-	-
7.	$3.0 \times 10^{-5}$	$74^\circ$	-	-	-
8.	$3.4 \times 10^{-5}$	$72^\circ$	$73^\circ$	-	-
9.	$3.7 \times 10^{-5}$	$74^\circ$	$74^\circ$	$75^\circ$	$72^\circ$
10.	$5.6 \times 10^{-5}$	$75^\circ$	-	-	-
11.	$1.15 \times 10^{-4}$	$73^\circ$	$72^\circ$	-	-
12.	$1.4 \times 10^{-4}$	$70^\circ$	-	-	-
13.	$1.9 \times 10^{-4}$	$65^\circ$	$64^\circ$	-	-
14.	$3.8 \times 10^{-4}$	$68^\circ$	$63^\circ$	-	-

Table XIII

Adsorption of Sodium Oleate on Rutile (Direct Adsorption Method)

S.N.	No Nonionic Present	
	Concentration of sodium oleate moles/lit $\times 10^{+5}$	Adsorption moles/cm <sup>2</sup> $\times 10^{+10}$
1.	23.8	1.59
2.	29.7	2.24
3.	35.7	2.36
4.	59.5	3.34
5.	81.25	3.34
6.	119.0	5.2

Table XIV

Effect of Nonionic (PPG-3) on Adsorption of Sodium  
Oleate on Rutile (Direct Adsorption Method)  
at Constant Concentration of Sodium Oleate

S. No.	Concentration of Sodium oleate = $29.75 \times 10^{-5}$ moles/lit.		Concentration of sodium oleate = $59.5 \times 10^{-5}$ moles/lit.	
	Concentration of nonionic moles/lit.	Adsorption in moles/cm <sup>2</sup>	Concentration of nonionic moles/lit.	Adsorption in moles/cm <sup>2</sup>
1.	$4.89 \times 10^{-5}$	$2.69 \times 10^{-10}$	$1.95 \times 10^{-5}$	$3.52 \times 10^{-10}$
2.	$7.82 \times 10^{-5}$	$2.78 \times 10^{-10}$	$4.89 \times 10^{-5}$	$3.65 \times 10^{-10}$
3.	$9.78 \times 10^{-5}$	$3.42 \times 10^{-10}$	$9.78 \times 10^{-5}$	$4.47 \times 10^{-10}$
4.	Nonionic	$2.24 \times 10^{-10}$	Nonionic	$3.34 \times 10^{-10}$

Table XV

Effect of Nonionic (PPG-4) on Adsorption of Sodium Oleate on Rutile (Direct Adsorption Method) at Constant Concentration of Sodium Oleate

S.N.	Concentration of Sodium oleate = $29.75 \times 10^{-5}$ moles/lit.		Concentration of sodium oleate = $59.5 \times 10^{-5}$ moles/lit.	
	Concentration of nonionic moles/lit.	Adsorption in moles/cm <sup>2</sup>	Concentration of nonionic moles/lit.	Adsorption in moles/cm <sup>2</sup>
1.	$5.75 \times 10^{-5}$	$2.25 \times 10^{-10}$	$5.75 \times 10^{-5}$	$3.71 \times 10^{-10}$
2.	$1.43 \times 10^{-4}$	$2.45 \times 10^{-10}$	$1.43 \times 10^{-4}$	$3.79 \times 10^{-10}$
3.	$2.87 \times 10^{-4}$	$2.72 \times 10^{-10}$	$2.87 \times 10^{-4}$	$4.18 \times 10^{-10}$
4.	No nonionic	$2.24 \times 10^{-10}$	No nonionic	$3.34 \times 10^{-10}$

Table XVI

Specific Conductivity Data for Sodium Dodecyle Benzene  
Sulfonate (Na-DBS) Alone and in Presence of Nonionic  
(PPG-4) Surfactant

S.N.	Solution of Na-DBS Alone		Concentration of Nonionic $10^{-5}$ moles/lit.	
	Concentration of Na-DBS Moles/lit. $\times 10^{+3}$	Specific Conduc- tance $\times 10^{+5}$ $\text{cm}^{-1}$ mhos.	Concentration of Na-DBS $\times 10^{+3}$ moles/lit.	Specific Conductance $\times 10^{+5}$ $\text{cm}^{-1}$ mhos.
1.	4.13	72.22	3.97	72.22
2.	3.54	62.91	3.40	63.41
3.	3.09	55.72	2.98	56.52
4.	2.75	52.00	2.65	51.32
5.	2.47	47.56	2.38	46.43
6.	2.06	40.41	2.17	43.10
7.	1.90	37.50	1.98	39.30
8.	1.77	35.14	1.83	37.14
9.	1.65	33.05	1.70	34.52
10.	1.55	30.95	1.59	32.64
11.	1.45	29.10	1.49	30.71
12.	1.37	27.66	1.40	28.89

Table XVI Continued

Concentration of Nonionic						
S.N.	10 <sup>-4</sup> moles/lit.		10 <sup>-3</sup> moles/lit.		10 <sup>-2</sup> moles/lit.	
	Concentration of Na-DBS x 10 <sup>+3</sup> moles/lit.	Specific Conductance x 10 <sup>+5</sup> mhos cm <sup>-1</sup>	Concentration of Na-DBS x 10 <sup>+3</sup> moles/lit.	Specific conductance x 10 <sup>+5</sup> mhos	Concentration of Na-DBS x 10 <sup>+3</sup> moles/lit.	Specific Conductance x 10 <sup>+5</sup> mhos cm <sup>-1</sup>
1.	4.08	77.23	4.09	69.65	5.206	88.64
2.	3.50	68.40	3.50	63.94	4.46	78.0
3.	3.06	60.94	3.06	57.35	3.94	69.65
4.	2.72	54.93	2.72	52.35	3.47	63.41
5.	2.45	50.65	2.45	47.56	3.12	57.35
6.	2.04	42.86	2.23	43.82	2.84	52.70
7.	1.88	39.80	2.05	40.62	2.60	49.37
8.	1.75	37.50	1.88	37.68	2.40	45.88
9.	1.63	35.30	1.75	35.45	2.23	42.86
10.	1.53	33.30	1.64	33.34	2.08	40.62
11.	1.44	31.20	1.53	31.45	1.95	38.24
12.	1.36	29.55	1.44	29.55	1.56	31.44

Table XVII

Specific Conductance Value of Na-DBS Solution in Presence  
of Nonionic (PPG-3) Surfactant

S.N.	Concentration of nonionic = $10^{-5}$ moles/lit.		Concentration of nonionic = $10^{-4}$ moles/lit.	
	Concentration of Na-DBS moles/lit $\times 10^{+3}$	Specific Conductance mhos $\times 10^{+5}$ $\text{cm}^{-1}$	Concentration of Na-DBS moles/lit. $\times 10^{+3}$	Specific Conductance mhos $\times 10^{+5}$ $\text{cm}^{-1}$
1.	4.25	73.58	3.97	72.22
2.	3.64	66.10	3.40	63.41
3.	3.19	59.09	2.98	55.52
4.	2.83	53.79	2.65	51.32
5.	2.55	49.06	2.382	46.71
6.	2.32	44.83	2.17	42.86
7.	2.13	41.45	1.98	40.00
8.	1.96	38.42	1.83	37.14
9.	1.82	36.28	1.70	34.51
10.	1.60	32.23	1.49	30.47
11.	1.50	30.47	1.40	28.63
12.	1.41	28.68	1.32	27.08

Table XVII Contd...

S.N.	Concentration of nonionic = $10^{-3}$ moles/lit.		Concentration of nonionic = $10^{-2}$ moles/lit.	
	Concen- tration of Na-DBS moles/lit. $\times 10^{-3}$	Specific conductance mhos $\times 10^{+5}$ $\text{cm}^{-1}$	Concentra- tion of Na-DBS moles/lit $\times 10^{+3}$	Specific conductance mhos $\times 10^{+5}$ $\text{cm}^{-1}$
1.	3.79	68.42	3.96	70.27
2.	3.25	60.00	3.40	61.42
3.	2.84	53.79	2.98	55.32
4.	2.53	48.75	2.65	50.00
5.	2.27	43.82	2.38	45.35
6.	2.07	40.63	2.17	41.71
7.	1.90	37.68	1.98	39.00
8.	1.75	35.14	1.83	36.28
9.	1.62	32.77	1.70	34.06
10.	1.42	29.10	1.49	30.00
11.	1.34	27.27	1.40	28.16
12.	1.26	25.83	1.32	26.62



Table XVIII

HC/ $\Delta\tau_\theta$  Values of Low Molecular Weight Nonionic (PPG-3)  
Micelle

$$\frac{dn}{dc} = 1.34 \times 10^{-2} \text{ cc/gm.}$$

S.No.	Angle	HC/ $\Delta\tau_\theta$ Values moles/gm $\times 10^5$					
		Concentration of nonionic gm/cc $\times 10^2$					
		1.9877	1.5466	1.1595	0.8696	0.6957	0.5795
1.	45°	0.99	1.079	1.11	1.18	1.32	1.35
2.	50°	1.11	1.19	1.22	1.28	1.43	1.50
3.	55°	1.23	1.33	1.33	1.43	1.56	1.58
4.	60°	1.35	1.45	1.47	1.55	1.70	1.77
5.	65°	1.52	1.65	1.66	1.77	1.95	1.99
6.	70°	1.69	1.83	1.86	1.98	2.18	2.22
7.	75°	1.88	2.04	2.03	2.17	2.37	2.43
8.	80°	2.07	2.24	2.24	2.39	2.65	2.69
9.	85°	2.26	2.45	2.46	2.63	2.90	3.04
10.	90°	2.52	2.74	2.72	2.93	3.24	3.40
11.	95°	2.80	3.05	3.01	3.29	3.69	3.91
12.	100°	3.08	3.36	3.42	3.58	4.06	4.32
13.	105°	3.29	3.59	3.58	3.73	4.20	4.54
14.	110°	3.58	3.93	3.86	4.06	4.71	5.05
15.	115°	3.84	4.23	4.27	4.47	5.11	5.55
16.	120°	4.15	4.65	4.83	5.06	5.93	6.40
17.	125°	4.55	5.15	5.06	5.18	6.37	7.10
18.	130°	4.88	5.43	5.17	5.47	6.87	7.46
19.	135°	5.29	5.89	5.62	5.69	8.49	10.1

Table XIX

$HC/\Delta\tau_\theta$  Values of High Molecular Weight Nonionic (PFG-4)

Micelle

$$\frac{dn}{dc} = 1.48 \times 10^{-2} \text{ cc/gm.}$$

S.N.	Angle	$HC/\Delta\tau_\theta$ Values Molcs/gm $\times 10^5$				
		Concentration of nonionic gm/cc $\times 10^2$				
		1.4102	1.1538	0.9066	0.7051	0.5288
1.	45°	0.88	0.960	1.00	1.02	1.05
2.	50°	1.04	1.10	1.16	1.22	1.22
3.	55°	1.21	1.28	1.36	1.42	1.48
4.	60°	1.37	1.48	1.55	1.61	1.69
5.	65°	1.55	1.69	1.78	1.83	1.96
6.	70°	1.83	1.98	2.07	2.19	2.30
7.	75°	2.11	2.25	2.38	2.52	2.64
8.	80°	2.35	2.52	2.75	2.81	3.19
9.	85°	2.56	2.90	3.14	3.32	3.75
10.	90°	2.89	3.22	3.50	3.74	4.22
11.	95°	3.32	3.65	4.03	4.32	5.01
12.	100°	3.78	4.14	4.60	4.98	5.95
13.	105°	4.05	4.43	4.94	5.19	6.16
14.	110°	4.47	4.82	5.42	5.64	6.58
15.	115°	4.87	5.30	5.88	6.27	7.22
16.	120°	5.29	5.83	6.57	6.84	8.40
17.	125°	5.78	6.37	6.79	7.25	8.58
18.	130°	5.89	6.52	7.03	7.11	8.56
19.	135°	6.55	7.17	7.59	7.72	9.39

Table XX

HC/ $\Delta\tau_\theta$  Value of Sodium Dodecyl Benzene Sulfonate (Na-DBS)

Micelle

$$\frac{dn}{dc} = 1.36 \times 10^{-2} \text{ cc/gm}$$

S.No.	Angle	HC/ $\Delta\tau_\theta$ Values moles/gm $\times 10^4$				
		Concentration of Na-DBS gm/cc $\times 10^2$				
		2.2951	1.7850	1.3387	0.8925	0.5950
1.	45°	0.131	0.140	0.184	0.200	0.239
2.	50°	0.151	0.158	0.201	0.220	0.256
3.	55°	0.170	0.177	0.223	0.222	0.253
4.	60°	0.187	0.195	0.235	0.239	0.279
5.	65°	0.195	0.202	0.236	0.240	0.277
6.	70°	0.203	0.210	0.240	0.247	0.282
7.	75°	0.207	0.219	0.245	0.256	0.296
8.	80°	0.217	0.224	0.248	0.256	0.290
9.	85°	0.218	0.224	0.247	0.262	0.294
10.	90°	0.223	0.230	0.257	0.260	0.297
11.	95°	0.227	0.234	0.262	0.265	0.304
12.	100°	0.233	0.240	0.266	0.274	0.316
13.	105°	0.238	0.249	0.276	0.303	0.354
14.	110°	0.250	0.252	0.286	0.304	0.373
15.	115°	0.254	0.257	0.304	0.315	0.373
16.	120°	0.263	0.274	0.309	0.329	0.421
17.	125°	0.266	0.278	0.313	0.337	0.432
18.	130°	0.277	0.278	0.322	0.351	0.445
19.	135°	0.280	0.294	0.331	0.361	0.495

Table XXI

Effect of Na-DBS (Concentration  $2.55 \times 10^{-5}$  moles/lit)  
On  $HC/\Delta\tau_\theta$  Values of High Molecular Weight Non-  
ionic (PPG-4) Micelles

$$\frac{dn}{dc} = 1.34 \times 10^2 \text{ cc/gm}$$

S.No.	Angle	$HC/\Delta\tau_\theta$ Values moles/gm $\times 10^5$					
		Concentration of Nonionic gm/cc $\times 10^2$					
		1.3637	1.1717	.9113	.7457	.5858	.4546
1.	45°	0.89	0.89	0.89	0.90	0.90	0.94
2.	50°	1.05	1.07	1.06	1.08	1.13	1.19
3.	55°	1.21	1.23	1.21	1.22	1.27	1.46
4.	60°	1.36	1.45	1.40	1.47	1.61	1.73
5.	65°	1.54	1.60	1.56	1.62	1.73	2.13
6.	70°	1.63	1.73	1.72	1.79	2.09	2.40
7.	75°	1.71	1.90	1.87	1.94	2.26	2.43
8.	80°	1.90	2.19	2.11	2.2	2.34	2.60
9.	85°	2.04	2.26	2.26	2.5	2.61	2.78
10.	90°	2.19	2.52	2.49	2.75	2.82	3.19
11.	95°	2.32	2.73	2.73	3.03	3.12	3.59
12.	100°	2.39	2.84	2.84	3.03	3.15	3.37
13.	105°	2.58	3.11	3.01	3.24	3.36	3.65
14.	110°	2.66	3.21	3.19	3.30	3.34	3.59
15.	115°	2.59	3.15	2.86	2.89	2.87	2.85
16.	120°	2.69	3.15	2.86	2.69	3.23	3.00
17.	125°	2.72	3.28	3.04	2.97	3.64	3.29
18.	130°	2.63	3.07	2.75	2.56	2.70	2.23
19.	135°	2.60	2.98	2.59	2.30	2.69	2.53

Table XXII

Effect of Na-DBS (Concentration =  $5 \times 10^{-5}$  moles/lit.) on  
 $HC/\Delta\tau_{\theta}$  Values of High Molecular Weight Nonionic  
 (PPG-4) Micelle

$$\frac{dn}{dc} = 1.28 \times 10^{-2} \text{ cc/gm.}$$

S.No.	Angle	$HC/\Delta\tau_{\theta}$ Values moles/gm $\times 10^5$					
		Nonionic Concentration gm/cc $\times 10^2$					
		1.066	0.9137	0.7106	0.5814	0.4568	0.3553
1.	45°	0.63	0.63	0.65	0.67	0.67	0.77
2.	50°	0.67	0.66	0.67	0.67	0.70	0.72
3.	55°	0.73	0.72	0.73	0.73	0.72	0.79
4.	60°	0.79	0.79	0.76	0.78	0.78	0.83
5.	65°	0.80	0.87	0.86	0.87	0.86	0.95
6.	70°	0.96	0.93	0.92	0.93	0.92	1.01
7.	75°	1.02	1.01	0.99	1.00	0.96	1.07
8.	80°	1.12	1.12	1.10	1.00	1.04	1.20
9.	85°	1.25	1.25	1.24	1.23	1.10	1.39
10.	90°	1.36	1.34	1.33	1.30	1.25	1.50
11.	95°	1.43	1.41	1.40	1.34	1.20	1.53
12.	100°	1.43	1.45	1.41	1.32	1.21	1.5
13.	105°	1.45	1.54	1.50	1.38	1.28	1.59
14.	110°	1.64	1.60	1.64	1.51	1.46	1.81
15.	115°	1.87	1.83	1.77	1.64	1.53	1.93
16.	120°	2.01	1.98	1.95	1.76	1.66	2.25
17.	125°	2.06	2.10	2.15	1.83	1.76	2.33
18.	130°	2.10	2.15	1.97	1.83	1.65	2.36
19.	135°	2.23	2.2	2.00	1.86	1.70	2.41

Table XXIII

Effect of Na-DBS (Concentration =  $5 \times 10^{-5}$  moles/lit) on  
 $HC/\Delta\tau_\theta$  Values of Low Molecular Weight (PPG-3)  
 Nonionic Micelle

$$\frac{dn}{dc} = 1.1 \times 10^{-2} \text{ cc/gm}$$

S.No.	Angle	$HC/\Delta\tau_\theta$ Values Moles/gm $\times 10^5$					
		Concentration of Nonionic gm/cc $\times 10^2$					
		1.2123	1.0391	0.0082	0.6612	0.5195	0.4041
1.	45°	0.40	0.40	0.44	0.44	0.48	0.49
2.	50°	0.46	0.46	0.49	0.52	0.50	0.54
3.	55°	0.53	0.53	0.56	0.58	0.63	0.60
4.	60°	0.59	0.60	0.63	0.65	0.67	0.70
5.	65°	0.67	0.67	0.72	0.74	0.77	0.78
6.	70°	0.75	0.75	0.80	0.82	0.84	0.87
7.	75°	0.83	0.84	0.91	0.91	0.96	1.00
8.	80°	0.92	0.94	1.02	1.04	1.11	1.12
9.	85°	1.03	1.04	1.12	1.19	1.23	1.31
10.	90°	1.13	1.15	1.26	1.27	1.36	1.46
11.	95°	1.23	1.25	1.38	1.41	1.49	1.62
12.	100°	1.33	1.33	1.47	1.54	1.63	1.73
13.	105°	1.44	1.46	1.60	1.74	1.78	2.02
14.	110°	1.54	1.55	1.74	1.81	1.87	2.01
15.	115°	1.62	1.64	1.85	1.86	2.11	2.27
16.	120°	1.81	1.89	2.16	2.25	2.41	2.74
17.	125°	1.91	2.02	2.24	2.59	2.56	2.92
18.	130°	1.94	2.02	2.27	2.34	2.62	2.82
19.	135°	1.87	2.14	2.22	2.29	2.33	2.62

Table XXIV

Effect of Na-DBS (Concentration =  $8.5 \times 10^{-4}$  moles/lit.) on  
 $HC/\Delta\tau_\theta$  Values of Low Molecular Weight Nonionic (PPG-3)  
 Micelle

$$\frac{dn}{dc} = 1.30 \times 10^{-2} \text{ cc/gm.}$$

S.No.	Angle	$HC/\Delta\tau_\theta$ Values moles/gm $\times 10^5$					
		Concentration of Nonionic gm/cc $\times 10^2$					
		1.6710	1.4322	1.1140	0.8355	0.6266	0.4557
1.	45°	0.33	0.32	0.31	0.31	0.31	0.30
2.	50°	0.42	0.40	0.37	0.36	0.37	0.37
3.	55°	0.49	0.45	0.44	0.46	0.45	0.44
4.	60°	0.57	0.57	0.53	0.55	0.54	0.54
5.	65°	0.67	0.66	0.62	0.65	0.66	0.63
6.	70°	0.78	0.75	0.73	0.76	0.76	0.73
7.	75°	0.89	0.86	0.82	0.84	0.84	0.82
8.	80°	1.01	0.97	0.94	0.96	0.97	0.95
9.	85°	1.13	1.10	1.05	1.07	1.11	1.02
10.	90°	1.22	1.20	1.15	1.17	1.18	1.13
11.	95°	1.35	1.35	1.32	1.36	1.33	1.34
12.	100°	1.50	1.53	1.40	1.57	1.60	1.50
13.	105°	1.62	1.65	1.60	1.72	1.76	1.71
14.	110°	1.75	1.82	1.71	1.83	1.90	1.85
15.	115°	1.87	1.94	1.85	1.96	2.02	2.02
16.	120°	2.01	2.00	2.01	2.10	2.22	2.24
17.	125°	2.07	2.26	2.10	2.19	2.30	2.33
18.	130°	2.16	2.26	2.16	2.36	2.40	2.30
19.	135°	2.21	2.40	2.27	2.49	2.44	2.49

Table XXV

Particle Scattering Factor ( $P^{-1}_0$ ) Values of Low Molecular Weight Nonionic (PPG-3) Micelle

Sl.No.	Angle	$P^{-1}_0$ Values (Particle Scattering Factor)		
		Pure PPG-3 System	In Presence of Na-DBS Concentration of Na-DBS moles/lit.	
			$5 \times 10^{-5}$	$0.5 \times 10^{-4}$
1.	45°	3.25	4.80	8.00
2.	50°	3.50	9.60	9.72
3.	55°	3.87	6.40	11.25
4.	60°	4.20	7.40	13.00
5.	65°	4.65	8.40	15.75
6.	70°	5.40	9.40	18.00
7.	75°	5.95	10.60	21.00
8.	80°	6.55	11.60	23.50
9.	85°	7.05	12.00	25.20
10.	90°	7.80	14.00	28.25



Table XXVI  
Particle Scattering Factor ( $P^{-1}\theta$ ) Values of High Molecular  
Weight Nonionic (PPG-4) Micelle

Sl.No.	Angle	$P^{-1}\theta$ Values (Particle Scattering Factor)		
		Pure PPG-4 System	In Presence of Na-DBS Concentration of Na-DBS moles/lit.	
			$2.55 \times 10^{-5}$	$5 \times 10^{-5}$
1.	$45^\circ$	3.80	4.00	6.25
2.	$50^\circ$	4.40	4.81	7.75
3.	$55^\circ$	5.40	5.45	8.51
4.	$60^\circ$	6.26	6.36	9.75
5.	$65^\circ$	7.20	7.09	10.75
6.	$70^\circ$	8.40	8.00	12.25
7.	$75^\circ$	9.46	8.82	13.75

Table XXVII

Effect of Sodium Oleate (Concentration =  $10^{-5}$  moles/lit.)  
 On  $HC/\Delta\tau_{\theta}$  Values of Low Molecular Weight Nonionic  
 (PPG-3) Micelle

$$\frac{dn}{dc} = 1.21 \times 10^{-2} \text{ cc/gm.}$$

S.N.	Angle	$HC/\Delta\tau_{\theta}$ Values moles/gm $\times 10^5$				
		Concentration of Nonionic gm/cc $\times 10^2$				
		0.6256	0.5362	0.3412	0.2674	0.2088
1.	45°	0.36	0.42	0.35	0.36	0.39
2.	50°	0.41	0.46	0.39	0.38	0.41
3.	55°	0.46	0.51	0.44	0.42	0.46
4.	60°	0.50	0.55	0.47	0.44	0.47
5.	65°	0.58	0.64	0.52	0.52	0.54
6.	70°	0.64	0.69	0.59	0.55	0.60
7.	75°	0.72	0.79	0.65	0.62	0.64
8.	80°	0.77	0.83	0.70	0.67	0.70
9.	85°	0.85	0.94	0.76	0.75	0.81
10.	90°	0.89	0.97	0.79	0.78	0.81
11.	95°	0.95	1.04	0.83	0.83	0.85
12.	100°	1.00	1.10	0.90	0.88	0.91
13.	105°	1.06	1.16	0.95	0.91	0.96
14.	110°	1.10	1.24	0.99	0.96	1.03
15.	115°	1.21	1.32	1.04	1.06	1.05
16.	120°	1.24	1.40	1.13	1.15	1.11
17.	125°	1.30	1.44	1.13	1.07	1.06
18.	130°	1.33	1.46	1.16	1.09	1.20
19.	135°	1.33	1.48	1.21	1.13	1.19

Table XXVIII

Effect of Sodium Oleate (Concentration =  $5 \times 10^{-5}$  moles/lit.)  
On  $HC/\Delta\tau_\theta$  Values of Low Molecular Weight Nonionic  
(PPG-3) Micelle

$$\frac{dn}{dc} = 1.19 \times 10^{-2} \text{ cc/gm.}$$

S.N.	Angle	$HC/\Delta\tau_\theta$ Values Moles/gm. $\times 10^6$					
		Concentration of Nonionic gm/cc $\times 10^2$					
		1.8555	1.5904	1.123	1.012	0.725	0.6167
1.	45°	0.52	0.48	0.38	0.31	0.26	0.20
2.	50°	0.62	0.57	0.45	0.38	0.32	0.25
3.	55°	0.74	0.68	0.55	0.47	0.39	0.3
4.	60°	0.86	0.82	0.66	0.58	0.49	0.41
5.	65°	1.02	0.99	0.81	0.72	0.61	0.52
6.	70°	1.21	1.13	0.97	0.87	0.76	0.64
7.	75°	1.43	1.40	1.18	1.04	0.92	0.78
8.	80°	1.68	1.64	1.38	1.23	1.09	0.95
9.	85°	1.94	1.90	1.63	1.47	1.31	1.13
10.	90°	2.21	2.20	1.90	1.71	1.51	1.37
11.	95°	2.53	2.54	2.19	1.99	1.76	1.54
12.	100°	2.86	2.89	2.53	2.27	2.01	1.79
13.	105°	3.17	3.27	2.86	2.57	2.28	2.03
14.	110°	3.47	3.66	3.17	2.89	2.56	2.23
15.	115°	3.91	4.05	3.55	3.19	2.87	2.56
16.	120°	4.30	4.48	3.98	3.56	3.19	2.86
17.	125°	4.66	4.93	4.42	4.07	3.68	3.20
18.	130°	5.19	5.72	5.03	4.73	4.06	3.90
19.	135°	5.77	6.34	5.66	5.18	4.59	4.34

Table XXIX

Effect of Sodium Oleate (Concentration =  $10^{-4}$  moles/lit.)  
On  $HC/\Delta\tau_{\theta}$  Values of Low Molecular Weight Nonionic  
(PPG-3)

$$\frac{dn}{dc} = 1.2 \times 10^{-2} \text{ cc/gm.}$$

S.N.	Angle	$HC/\Delta\tau_{\theta}$ Values moles/gm $\times 10^6$					
		Concentration of Nonionic gm/cc $\times 10^2$					
		1.5636	1.3416	1.0435	0.6537	0.6708	0.5212
1.	45°	0.21	0.19	0.14	0.12	0.09	0.07
2.	50°	0.25	0.23	0.18	0.15	0.12	0.09
3.	55°	0.29	0.27	0.22	0.19	0.15	0.12
4.	60°	0.35	0.33	0.26	0.24	0.19	0.16
5.	65°	0.42	0.40	0.33	0.30	0.24	0.20
6.	70°	0.48	0.45	0.39	0.36	0.29	0.25
7.	75°	0.58	0.57	0.46	0.45	0.36	0.32
8.	80°	0.69	0.67	0.57	0.54	0.44	0.39
9.	85°	0.80	0.79	0.68	0.65	0.52	0.47
10.	90°	0.92	0.91	0.80	0.75	0.62	0.55
11.	95°	1.05	1.00	0.93	0.87	0.71	0.64
12.	100°	1.21	1.25	1.00	1.02	0.83	0.75
13.	105°	1.36	1.38	1.21	1.15	0.96	0.84
14.	110°	1.56	1.61	1.41	1.34	1.10	0.96
15.	115°	1.71	1.76	1.61	1.50	1.25	1.10
16.	120°	1.95	2.01	1.80	1.68	1.40	1.27
17.	125°	2.18	2.22	2.04	1.91	1.59	1.47
18.	130°	2.43	2.55	2.34	2.37	1.87	1.78
19.	135°	2.80	3.10	2.89	3.05	2.20	2.36

Table XXX

Effect of Sodium Oleate (Concentration =  $10^{-5}$  moles/lit.)On  $HC/\Delta\tau_\theta$  Values of High Molecular Weight Nonionic  
(PPG-4) Micelle

$$\frac{dn}{dc} = 1.31 \times 10^{-2} \text{ cc/gm.}$$

S.N.	Angle	$HC/\Delta\tau_\theta$ Values moles/gm $\times 10^6$					
		Concentration of Nonionic gm/cc $\times 10^2$					
		0.7323	0.6199	0.4822	0.3945	0.3099	0.2111
1.	45°	0.60	0.65	0.69	0.68	0.63	0.71
2.	50°	0.74	0.77	0.81	0.82	0.77	0.83
3.	55°	0.87	0.91	0.95	0.97	0.90	0.95
4.	60°	1.03	1.08	1.14	1.16	1.03	1.15
5.	65°	1.25	1.31	1.38	1.36	1.28	1.35
6.	70°	1.47	1.54	1.62	1.61	1.52	1.59
7.	75°	1.73	1.78	1.89	1.87	1.76	1.85
8.	80°	2.01	2.10	2.18	2.21	2.07	2.16
9.	85°	2.34	2.45	2.54	2.52	2.36	2.42
10.	90°	2.64	2.77	2.87	2.85	2.70	2.78
11.	95°	3.00	3.14	3.21	3.28	3.07	3.20
12.	100°	3.41	3.58	3.70	3.67	3.38	3.53
13.	105°	3.78	3.98	4.11	4.16	3.77	3.95
14.	110°	4.20	4.42	4.49	4.48	4.26	4.41
15.	115°	4.62	4.86	4.95	4.95	4.73	4.88
16.	120°	5.10	5.48	5.58	5.46	5.19	5.35
17.	125°	5.55	5.97	6.35	6.11	5.83	5.77
18.	130°	6.08	6.68	6.79	6.81	6.12	6.56
19.	135°	6.81	7.36	7.27	7.76	6.91	7.22

Table XXXI

Effect of Sodium Oleate (Concentration =  $5 \times 10^{-5}$  moles/lit.)On  $HC/\Delta\tau_{\theta}$  Values of High Molecular Weight Nonionic  
(PPG-4) Micelle

$$\frac{dn}{dc} = 1.28 \times 10^{-2} \text{ cc/gm.}$$

S.N.	Angle	$HC/\Delta\tau_{\theta}$ Values moles/gm $\times 10^6$					
		Concentration of Nonionic gm/cc $\times 10^2$					
		1.225	1.050	0.9166	0.6681	0.5250	0.403
1.	45°	0.27	0.25	0.21	0.16	0.15	0.12
2.	50°	0.32	0.30	0.26	0.20	0.19	0.17
3.	55°	0.38	0.36	0.32	0.25	0.24	0.21
4.	60°	0.46	0.44	0.39	0.31	0.30	0.27
5.	65°	0.55	0.53	0.48	0.39	0.37	0.35
6.	70°	0.66	0.63	0.50	0.48	0.46	0.44
7.	75°	0.81	0.77	0.70	0.59	0.57	0.54
8.	80°	0.95	0.93	0.85	0.72	0.71	0.65
9.	85°	1.11	1.08	1.02	0.87	0.86	0.81
10.	90°	1.29	1.28	1.22	1.04	1.02	0.94
11.	95°	1.52	1.50	1.46	1.24	1.21	1.13
12.	100°	1.73	1.74	1.70	1.45	1.41	1.34
13.	105°	2.02	2.02	1.94	1.69	1.65	1.56
14.	110°	2.29	2.29	2.26	1.93	1.89	1.76
15.	115°	2.55	2.60	2.54	2.20	2.13	2.11
16.	120°	2.85	2.91	2.95	2.52	2.45	2.20
17.	125°	3.19	3.31	3.40	2.95	2.80	2.69
18.	130°	3.63	3.76	3.91	3.31	3.31	3.05
19.	135°	4.16	4.44	4.77	4.40	3.63	4.20

Table XXXII

Effect of Sodium Oleate (Concentration =  $10^{-4}$  moles/lit.)  
On  $HC/\Delta\tau_{\theta}$  Values of High Molecular Weight Nonionic  
(PPG-4) Micelle

$$\frac{dn}{dc} = 1.25 \times 10^{-2} \text{ cc/gm.}$$

S.N.	Angle	$HC/\Delta\tau_{\theta}$ Values moles/gm $\times 10^6$					
		Concentration of Nonionic gm/cc $\times 10^2$					
		1.456	1.248	0.9700	0.7941	0.6210	0.4050
1.	45°	0.12	0.11	0.08	0.07	0.06	0.05
2.	50°	0.16	0.14	0.11	0.10	0.08	0.07
3.	55°	0.20	0.18	0.15	0.13	0.11	0.10
4.	60°	0.26	0.24	0.19	0.17	0.15	0.13
5.	65°	0.32	0.31	0.25	0.22	0.20	0.18
6.	70°	0.40	0.38	0.32	0.29	0.26	0.23
7.	75°	0.51	0.48	0.41	0.36	0.32	0.27
8.	80°	0.62	0.59	0.51	0.45	0.41	0.36
9.	85°	0.75	0.74	0.62	0.55	0.50	0.44
10.	90°	0.89	0.87	0.75	0.66	0.60	0.51
11.	95°	1.05	1.03	0.89	0.78	0.72	0.61
12.	100°	1.23	1.21	1.04	0.91	0.84	0.72
13.	105°	1.39	1.38	1.22	1.07	1.00	0.88
14.	110°	1.75	1.63	1.41	1.21	1.09	0.95
15.	115°	1.80	1.83	1.59	1.38	1.19	1.06
16.	120°	2.04	2.15	1.91	1.62	1.40	1.15
17.	125°	2.33	2.58	2.35	1.92	1.59	1.34
18.	130°	2.76	3.30	2.92	2.29	2.01	1.73
19.	135°	3.64	4.01	4.77	3.69	2.80	2.31

A 4552

Date Slip A 4552

This book is to be returned on the  
date last stamped.


CD 6.72.9

ME-1975-P-BAN-COL